

1 **Editor Decision: Reconsider after major revisions** (08 Jun 2017) by Eric Wolff

2

3 Comments to the Author:

4

5 Thank you for the considerable changes you have made to the paper. These have certainly improved  
6 it. I apologise for the delay in obtaining reviews on this version. As you will see, I sent the new  
7 version to two reviewers - one was the same as for the previous version, the other was a new  
8 reviewer. Both reviewers agree that your paper is valuable and should eventually be published.  
9 However, although they go into different levels of detail, both still have significant issues on two  
10 aspects of your paper: the analytical uncertainty you quote, and the use of SD data for the IPD. You  
11 need to address their detailed comments as well as these two major issues.

12

13 I would like to particularly emphasise the need to either alter or explain better the uncertainty  
14 calculation. Your paper has been seen by 3 reviewers, all of them VERY familiar with measurements  
15 of methane in ice and with the sources of error in such measurements. Despite your explanations all  
16 3 of them (and me as editor) still don't understand how it is possible, when you have a strongly  
17 varying blank, to arrive at such a small uncertainty. As one reviewer says, you need either to come up  
18 with a convincing discussion of this, or resist the temptation to claim a very low uncertainty.

19

20 I would also like to expand further rev 1's comment about the blank. They correctly point out that, if  
21 you draw 4 samples from the range 5-15 ppb, the SE of the mean ( $SD/2$ ) is indeed around 2 ppb. This  
22 implies that the intraday uncertainty is no less than the inter-day uncertainty. The uncertainty on  
23 each sample is controlled by the blank of that sample, not by the uncertainty of the daily average so  
24 you should not be dividing by  $\text{root}(4)$  to obtain it. It seems impossible that the uncertainty on a  
25 measurement can actually be less than the standard deviation of the blank measurements, which  
26 presumably is 4 ppb.

27

28 I look forward to seeing a revised manuscript.

29

30

1 *We appreciate the editor for thoughtful comments and patient guidance. Agreeing with both*  
2 *reviewers, we added more details on analytical method, and we re-defined data uncertainty including*  
3 *the uncertainties due to corrections for daily systematic offset (e1) and the other effects (e2). The*  
4 *uncertainty of daily systematic offset (e1) was estimated from results of bubble-free ice with a*  
5 *standard air (now we use “bubble-free ice” instead of “blank ice” because the ice was used only for*  
6 *e1 estimation). As we used the average of four “bubble-free ice” results for the daily systematic offset,*  
7 *the best estimation of the daily e1 is the standard error of the mean for the day. The e2 includes*  
8 *uncertainty from solubility correction and inhomogeneous CH<sub>4</sub> distribution in ice. We estimated the*  
9 *e2 with intra-day duplicates from the same depths. Because a daily systematic uncertainty was*  
10 *applied to all the samples for the day, any intra-day distribution of CH<sub>4</sub> from the same depth should*  
11 *indicate e2. The total uncertainty of individual ice is now calculated by  $((e1)^2 + (e2)^2)^{1/2} = (1.9^2 +$   
12  $3.3^2)^{1/2} = 3.8$  ppb. Because we used the average of a duplicate ice samples for the same depth, the  
13 *data uncertainty for data plot and IPD calculations is  $3.8/2^{1/2} = 2.7$  ppb. The details are described in*  
14 *our response to the reviewers’ comments.**

15 *We revised solubility correction method. Instead of calculating Henry’s law and applying a correction*  
16 *factor of 1.0058, we estimated solubility effect from the results of direct measurement of CH<sub>4</sub> mixing*  
17 *ratio of air remained in refrozen meltwater. Mean difference between before and after revising the*  
18 *solubility correction is less than 1.0 ppb, while intra-day scattering among the four bubble-free ice*  
19 *samples remains unchanged (average SEM = 1.9 ppb). We also clearly stated the data rejection*  
20 *scheme, and carefully reviewed our data set. Due to changes in correction method, two data points*  
21 *previously rejected are now included in data set, while five data points were newly rejected.*  
22 *Regarding IPDs, we present a combined IPD by using IPD-1 for 9.0 – 10.0 ka and IPD-2 for 10.0 – 11.5*  
23 *ka, because IPD-2 is better constrained in this period as the reviewer recommended. However, it does*  
24 *not change the major findings of our manuscript.*

25 *Finally, we included the important information in Supplements into main text and the other contents*  
26 *that are not essential were removed. The English was improved as the reviewer suggested.*

27 *Below our responses are written in red italics, and the point-to-point revisions are in Times New*  
28 *Roman, where the words of the original manuscript version are black, [the changes of the first major](#)*  
29 *[revisions are shown in blue](#) and [those of the second major revisions appears in green.](#)*

30

**Anonymous Reviewer #1: Suggestions for revision or reasons for rejection (will be published if the paper is accepted for final publication)**

Hello,

The manuscript improved considerably, however, major aspects of the analysis are presented in a confusing or even misleading way. I have no doubt that the author group can iron this out and that this manuscript will eventually be suitable for publication in CP.

Cheers

1

2

Thanks a lot to the authors for their considerable revisions of the original manuscript. In my view,

3

the new version is a great improvement. The structure gained clarity and the refined focus on the

4

time scale makes the entire paper appear more concise. Again, this manuscript might require some

5

language editing or input by the native speaker of the author list. On top of the good development, I

6

recommend major revisions on several aspects of the new manuscript. These include i) the

7

description of the analytical system and its uncertainties, ii) the use of IPD-1 and IPD-2, iii) Section

8

3.3, Comparison with late Holocene variability, iv) conclusions, v) Supplements.

9

10 **i) the description of the analytical system and its uncertainties**

11

I find the part on the analytical uncertainty of the methods section extremely hard to follow and

12

even after careful re-reading, I am not sure what data were used to calculate the stated averages,

13

pooled standard deviations etc. The authors have chosen to publish the data paper before their new

14

method is published in a separate publication. In my point of view, this requires a sufficient

15

description of method and uncertainty if it is claimed that the new method is superior to existing

16

methods, even if a dedicated publication follows. It seems to me that the authors should increase

17

their resistance to the temptation to choose statistical methods that understate the uncertainty of

18

their analytical system, as this leaves the reader rather suspicious.

19

→ We agree that our description of analytical method and uncertainty was not sufficient. Now

20

we elaborated more description on analytical method, especially on correction methods.

21

Our new estimation of analytical uncertainty for each individual ice is 3.8 ppb and 2.7 ppb

22

for the mean of duplicates used in the data plot and IPD calculation. Details on revised

23

analytical uncertainty are found in our responses to the following comments. To improve

24

our description of the analytical method, we added sentences below:

25

→ “Different solubilities of each air component cause preferential dissolution during

26

melting procedure. gas species cause preferential dissolution of a gas having higher solubility

27

than others, and consequently it makes the mixing ratio of extracted air different from that

28

trapped originally within the ice (solubility effect hear after). As the solubility of CH<sub>4</sub> is

29

higher than the other major components of air – nitrogen (N<sub>2</sub>), oxygen (O<sub>2</sub>), Argon (Ar), the

1 ~~solubility effect lowers and needs to be corrected properly.~~ the CH<sub>4</sub> mole fraction of the  
2 extracted air is lower than originally enclosed air (solubility effect). The original CH<sub>4</sub> mole  
3 fraction of air enclosed in ice sample is estimated from residual gas fraction and CH<sub>4</sub> mixing  
4 ratio in air remained in refrozen meltwater (retrapped air). Residual gas fraction is a measure  
5 of how much air is retrapped during refreeze, which is defined as ratio of amount (pressure)  
6 of air extracted from the 2<sup>nd</sup> gas extraction to the 1<sup>st</sup> extraction. The 2<sup>nd</sup> gas extraction was  
7 carried out by an additional melting-refreezing process after the 1<sup>st</sup> extraction and evacuation  
8 of the sample cup. Residual gas fraction was measured during the 10 experimental days.  
9 Mean residual gas fraction is  $1.05 \pm 0.13\%$  ( $1\sigma$ ,  $n=60$ ) for SDMA ice samples and  $0.38 \pm$   
10  $0.08\%$  ( $1\sigma$ ,  $n=40$ ) for bubble-free ice. The test with ice samples from Styx glacier, Antarctica  
11 revealed that CH<sub>4</sub> mixing ratio in retrapped air is enriched 3.11 times ( $n=12$ ) for glacial ice  
12 and 2.98 times ( $n=7$ ) for bubble-free ice. Then the solubility effect is corrected by using a  
13 simple mass balance calculation.”

14 → “Daily systematic offset correction was applied to account for the daily-varying system  
15 condition. To do this, we measured four bubble-free ice samples every day with SDMA ice  
16 samples. The experimental procedures for the bubble-free ice were identical to the SDMA ice.  
17 After the sample flasks are evacuated, standard air is injected into the flasks containing  
18 bubble-free ice, so that it returns similar amount of air into the sample loop to typical size of  
19 SDMA ice when the extracted air inside the bubble-free ice flasks is expanded. The solubility  
20 correction for the bubble-free ice was done by the same formula as SDMA ice samples, but  
21 using different CH<sub>4</sub> mixing ratio (see above) and residual gas fraction. After corrected for  
22 solubility effect, the daily systematic offset is calculated by difference between CH<sub>4</sub> mixing  
23 ratio of the injected standard air and results from the four flasks containing bubble-free ice.  
24 The daily systematic offset fluctuates from 5 to 15 ppb during SDMA measurements, and is  
25 subtracted from the samples corrected for gas solubility effect, including bubble-free ice and  
26 SDMA samples. This is one of the major difference with OSU wet extraction system, where  
27 the daily systematic offset was interpolated from the results of blank tests carried out between  
28 several days (Mitchell et al., 2011).

29 The bubble-free ~~blank~~ ice was made by chilling the degassed ultrapure water (resistivity >  
30  $18.2 \text{ M}\Omega\cdot\text{cm}$  at  $25^\circ\text{C}$ ) slowly from the bottom in a closed stainless steel chamber. From gas  
31 extraction test using our bubble-free ice without injecting standard air, we observed that no  
32 significant pressure increase at the pressure gauge with a detection limit of 0.01 Torr  
33 (corresponding to less than 0.03% of sample air pressure in the extraction line) after melting-  
34 refreezing the bubble-free ice.”

35  
36 Please make sure it is well described how you achieve the values you present and what data they

1 were calculated from. For example on page 42, line 6-7 of the document including the tracked  
2 changes, you state a standard error of the mean (SEM) of  $2.0 \pm 1.0$  ppb. To my understanding, the  
3 SEM is the uncertainty measure, it has no uncertainty itself. What has been calculated here? In  
4 general, SEM's may be used as measure of uncertainty when a sufficient number of samples have  
5 been measured. In this manuscript, the authors seem to apply SEM to sample sizes of  $n=2$ . If the  
6 authors have a good reason to use SEM for  $n=2$ , they should clearly state why and account for the  
7 obvious lack of sample size (student's t). I feel very strongly that using SEM on  $n=2$  is not OK and  
8 needs changing in every uncertainty calculation (e.g. p. 42, L10). Presenting a formula may help  
9 clarify what has been calculated. An understandable and ethically correct uncertainty demonstration  
10 will provide more credibility to the technical aspects of this manuscript than unrealistically small  
11 values. If the system is a new game changer, it should be possible to show outstanding performance  
12 using appropriate statistical methods.

13 → To derive a more comprehensive and conservative error estimation, we address two types  
14 of uncertainty sources: uncertainty of systematic offset ( $e_1$ ) and other causes ( $e_2$ ). The daily  
15 systematic offset uncertainty ( $e_1$ ) is estimated as standard error of the mean (SEM) of four  
16 flasks containing bubble-free ice and standard air (Now we use "bubble-free ice" instead of  
17 "blank ice" because we use the "bubble-free ice" only to estimate daily systematic offset  
18 and its uncertainty ( $e_1$ )). Here we use SEM ( $n=4$ ) because the daily systematic offset is  
19 calculated from the mean of the four bubble-free ice samples. The average of daily  $e_1$  was  
20 1.9 ppb. To estimate the  $e_2$ , (e.g., uncertainty from variable degree of solubility equilibrium  
21 of  $\text{CH}_4$  and inhomogeneous  $\text{CH}_4$  distribution in ice at the same depth), we used results from  
22 duplicates. Because any duplicates from same depths were analyzed on the same days, the  
23 differences in duplicate ice measurements should reflect uncertainty other than  $e_1$ . Thus,  
24 the  $e_2$  was determined by pooled standard deviation (PSD) of ice duplicates of all depths.  
25 PSD of SNU data set is 3.3 ppb. Taking in to account the above two uncertainty terms ( $e_1$   
26 and  $e_2$ ), we state a revised analytical uncertainty of 3.8 ppb ( $((e_1)^2 + (e_2)^2)^{1/2}$ ) for individual  
27 ice measurement. With regard to the data used in graphs and IPD reconstruction, we used  
28 the mean values of duplicates with uncertainty of 2.7 ppb ( $3.8/(2^{1/2})$ ). Based on this  
29 argument, we added the paragraph below:

30 → "Here we consider two types of uncertainty sources: uncertainty in (1) estimating daily  
31 systematic offset and (2) other causes. The former indicates uncertainty of the daily  
32 systematic offset ( $e_1$ ). As the daily systematic offset is calculated from the mean of the four  
33 flasks with bubble-free ice and standard air, scattering of the bubble-free ice samples can  
34 induce uncertainty in the systematic offset correction. The daily  $e_1$  is estimated with standard

1 error of the mean (SEM, n=4), because the daily systematic offset is calculated from the  
2 mean of the four bubble-free ice samples. The average of daily e1 is 1.9 ppb. The latter (e2)  
3 includes uncertainty due to solubility correction and inhomogeneous distribution of CH<sub>4</sub>.  
4 Given our solubility correction uses the mean value of residual gas fraction and the ratio at  
5 which CH<sub>4</sub> enriches in retrapped air, different solubility effect and/or inhomogeneous CH<sub>4</sub>  
6 distribution in individual ice causes offset between adjacent duplicate ice samples analysed  
7 on the same day. As the duplicates from same depths were measured on the same day, we  
8 estimated the e2 with pooled standard deviation (PSD) between duplicate measurements from  
9 entire depths, which yields 3.3 ppb. Taking the e1 and e2 into account together, the final  
10 uncertainty of individual measurement is given as 3.8 ppb by error propagation. The  
11 uncertainty for the mean of duplicate results is obtained by dividing the individual  
12 uncertainty by square root of 2, yielding 2.7 ppb.”

13 This manuscript version has a lot of emphasis on the use of bubble-free blank ice to determine the  
14 system blank. The authors state that based on their method to produce the blank ice, they can  
15 exclude that CH<sub>4</sub> is introduced with the blank ice. From personal experiences, I wouldn't trust that  
16 statement. Dedicated blank ice tests including several labs showed that while it is easily possible to  
17 produce bubble free ice, there is no such thing as gas-free blank ice. The gas content of the blank ice  
18 varied both between the labs and between the batches produced in each lab. All labs used deionised  
19 water and pumped on the water for 90 minutes and froze large crystals bottom up... While blank ice  
20 allows for a valuable tests, great care has to be taken in the use and interpretation of the results.

21 → From our test using bubble-free ice samples without injecting any standard, we found that  
22 the pressure of the extracted air is below the detection limit (0.01 Torr) of our system.  
23 Compared to the air pressure of the typical SDMA ice samples is ~30 Torr when expanded  
24 into the vacuum line, air content in bubble-free ice is less than 0.03% of the SDMA ice. We  
25 added this information on our method section.

26  
27 Based on 4 daily blank ice analyses, the authors state an intra-day SEM of 2.0±1.0 ppb and a  
28 variation of the inter-day mean between 5 and 15 ppb. I think the authors intention to present these  
29 data is to show that even if the inter-day variation is as large as 15 ppb, the daily blank can be  
30 quantified with low uncertainty (SEM 2.0±1.0 ppb) and a correction can therefore be accurately  
31 determined. I find this hard to understand. If I chose 4 random values between 5 and 15 (as  
32 representative for the large variability of the inter-day blank) and calculate the SEM for these 4  
33 values, the SEM is <2.5. The authors state that the blank estimate of OSU has a high uncertainty of  
34 10% due to the small peak size, but don't seem to think this is a problem when quantifying the blank

1 ice contribution with higher relative uncertainties. Please clarify.

2 I would think that introducing a known amount of air with a known CH<sub>4</sub> mixing ratio into the melt  
3 chambers and to analyse that air in the same way as an ice core sample could provide a useful  
4 measure of analytical error. This could be done in a dry chamber and over melt water to test for  
5 differences. Such experiments could be useful to determine the **accuracy of the measurements**.

6 → Here we disagree with the Reviewer in including uncertainty induced from inter-day blank  
7 fluctuations because we measured the systematic offset daily. This is one of main difference  
8 from OSU method. If we estimate the systematic offset once in several days, it should  
9 introduce a certain amount of uncertainty in interpolating the inter-day blank.

10

11 The authors use table R1 to show the reproducibility of the analytical system. I find this is a very  
12 useful way to state the potential uncertainty/reproducibility of the system and would suggest to  
13 improve the clarity and possibly give this more weight in the formulation of the uncertainty estimate.  
14 On p. 42 L. 12, the authors refer to the data in table R1 and state, that the differences between the  
15 averages from the 1st and the 2nd measurement pair is on average 1.9 ppb. Even though this is nice,  
16 it ignores the uncertainty of each single measurement as well as the differences within each sample  
17 pair. Again, the authors do not clearly state how the uncertainty in R1 is calculated for 1st and 2nd  
18 measurement, is it SEM again for  $n=2$  or  $1\sigma$ ? The authors provide one depth interval for all for  
19 samples in table R1, where the depth is sometimes stated to the mm. Are really all four samples  
20 from the same mm depth? In my view, this table should include all 4 measurements per depth level.  
21 You can then add columns for  $1\sigma$  or SEM for all four, and calculate the pooled standard deviation  
22 (PSD) of the whole lot afterwards as total uncertainty estimate for **measurement precision**. I am not  
23 sure if this is what the authors describe on p. 42, L. 13 (PSD of 1.4 ppb)? Did you calculate the PSD  
24 based on 4 individual measurements per depth or based on the averages from 1st and 2nd  
25 measurements? If this is the “final” uncertainty that the authors intend to state for their analytical  
26 system, they should clearly say so in a dedicated sentence, not hidden in a sentence and  
27 furthermore in brackets.

28 → Now we include all the four measurements in Table R1. The uncertainties in Table R1  
29 indicates 1 standard deviation between duplicates. PSD from quadruplicate measurements  
30 is 3.0 ppb. The PSD among the four individual ice measurements is similar to the PSD of  
31 duplicate measurements of the SNU data ( $e_2 = 3.3$  ppb). The PSD among the mean of  
32 duplicate analyses of the 1st and 2nd measurements is 1.1 ppb. The good agreement among  
33 the duplicate means indicates good reproducibility. The better PSD obtained from the mean  
34 of duplicates than from the four individual measurements could be attributed to casual

underestimation due to insufficient number of replicate pairs, as well as to non-Gaussian distribution of individual measurement that might results better agreement when averaged 2 to 4 replicates, even though the error of each data point is larger. There is no evidence that each duplicate analysis (consist of 3 injections) is Gaussian, and even if the duplicates individually follow Gaussian distribution, the final results (mean of duplicates) are not necessarily Gaussian (e.g., Anderson, 2011). We added below paragraph and Table:

→ “We made additional measurements using adjacent samples (depth difference of 10 cm) at randomly selected 8 depth intervals to examine reproducibility and long-term stability of our system. The second measurements of duplicates were performed 8 to 80 days after the first analysis. Table 1 displays quadruplicate results at each depth. PSD between the mean of duplicate analyses of the first and second measurements on different days yields 1.1 ppb. The good agreement between duplicate means indicates good reproducibility of our system. In the meanwhile, PSD of the quadruplicate measurements is 3.0 ppb, which is similar to PSD of duplicate samples for the entire data set (3.3 ppb).”

→ Table 1 is as below:

Depth (m)	1 <sup>st</sup> measurements					2 <sup>nd</sup> measurements				
	Dup.1 (ppb)	Dup.2 (ppb)	Mean (ppb)	1sigma (ppb)	Date (dd/mm/yy)	Dup.1 (ppb)	Dup.2 (ppb)	Mean (ppb)	1sigma (ppb)	Date (dd/mm/yy)
523.150	634.8	634.7	634.7	0.1	27-1-14	637.5	634.3	635.9	1.6	24-2-14
530.950	669.0	665.8	667.4	1.6	03-2-14	669.4	670.7	670.0	0.7	24-2-14
558.295	682.5	678.2	680.3	2.2	14-3-14	687.5	678.3	682.9	4.6	02-4-14
559.850	689.8	680.3	685.0	4.7	03-2-14	683.8	690.0	686.9	3.1	26-3-14
561.150	687.8	689.2	688.5	0.7	14-3-14	684.0	690.4	687.2	3.2	02-4-14
562.407	687.2	685.5	686.4	0.8	26-3-14	689.4	686.4	687.9	1.5	02-4-14
575.913	679.2	679.2	679.2	0.0	07-2-14	686.7	678.9	682.8	3.9	28-3-14

P. 42, L 30: You mention the difference OSU-SNU of 3ppb and present a hypothesis on what might have caused this offset. However, this dilemma shows that an analytical uncertainty of 1.4 ppb cannot include the entire uncertainty to the NOAA scale. It would be great to see this resolved, i.e. precision and accuracy, or at least clearly discussed if unresolvable.

→ The uncertainty of standard air affects accuracy of measurements, not analytical precision. According to the results of calibration of the standard air that was carried out at NOAA shows PSD of about 0.4 ppb, while the repeatability of NOAA04 scale has been reported as < 1.5 ppb for ambient air mole fractions (~1700 ppb) (Dlugokencky et al., 2005). As described



1 above, our new uncertainty model yields average offset between OSU and SNU data set of  
2 ~0.1 ppb, which lies within the precision of our working standard.

3  
4 On p. 42 L. 34, the authors state that their new Siple Dome data have the third highest temporal  
5 resolution. However, they don't say how high it is, as they do for the others. Please quantify,  
6 otherwise your statement of 3rd highest is meaningless.

7 → The mean temporal resolution of our Siple Dome composite record is ~26 years, while those  
8 of WAIS discrete and continuous data is ~20 and ~2 years, respectively. The sentence was  
9 changed as below:

10 → “Our new Siple Dome CH<sub>4</sub> composite data have mean temporal resolution of ~26 years. The  
11 WAIS Divide continuous CH<sub>4</sub> records shows much higher resolution (~2 years), but does not  
12 cover the entire early Holocene period (Rhodes et al., 2015).”

#### 14 ii) Use of IPD-1 and IPD-2

15 The authors calculate IPD's based on NEEM discrete and Siple discrete (IPD-1) and NEEM discrete  
16 and WAIS continuous (IPD-1). Unfortunately, the authors do not describe how the uncertainty  
17 envelope is calculated. Furthermore, you do not state the temporal resolution of the Siple data, as  
18 compared to the WAIS continuous (p. 42, L. 34).

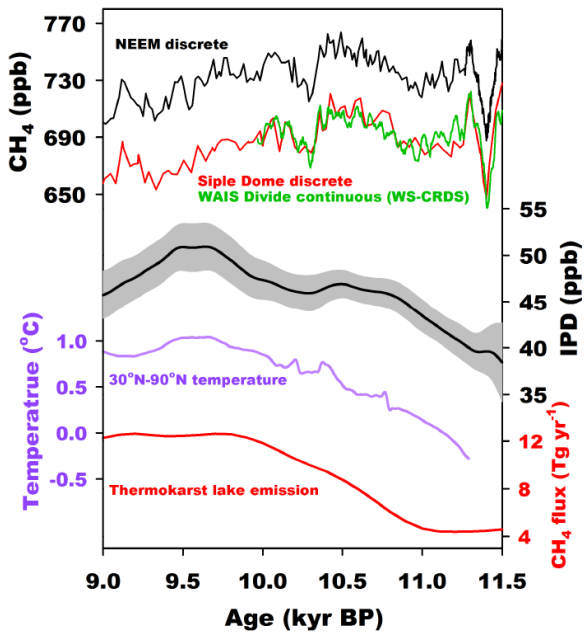
19 → The error range of IPD was calculated from synchronization uncertainty and CH<sub>4</sub>  
20 measurement uncertainty. The Monte Carlo-based synchronization routine produces 20 sets  
21 of age offset at each of the tie points that were resampled every 30 years. The age offsets  
22 were linearly interpolated and added to the initial synchronization ages, creating 20 sets of  
23 synchronized age scales. The standard deviation of the 20 IPD records calculated from the  
24 20 synchronized age scales is taken as synchronization uncertainty. The CH<sub>4</sub> measurement  
25 uncertainty was estimated with the stated uncertainty of each data set (4.3 ppb for NEEM  
26 discrete / 2.7 ppb for SDMA / 1.5 ppb for WAIS continuous, 1 sigma). To check the  
27 sensitivity of the uncertainties, we carried out Monte Carlo simulations. We produced 1000  
28 different sets of IPD, which vary randomly with Gaussian propagation in their ages and CH<sub>4</sub>  
29 concentration uncertainties. Each IPD was annually interpolated and smoothed by a 1/1000  
30 year<sup>-1</sup> low-pass filter. The standard deviation of the 1000 smoothed IPDs was taken as the  
31 uncertainty envelop of IPD. In Figure R1 and R2, the uncertainties were reported as 95%  
32 confidence interval by multiplying 1.96 to standard deviation. We also added the mean  
33 temporal resolution of each data set. The paragraph was updated as below:

34 → “Temporal uncertainty (synchronizing error) was determined for each point as 1 standard

~~deviation of 20 replicates and CH<sub>4</sub> uncertainty includes analytical error of the both records-~~  
The uncertainty range of IPD was calculated from synchronization uncertainty and CH<sub>4</sub> data uncertainty. To estimate synchronization uncertainty, we created 20 IPDs from the 20 sets of maximum correlation time series, and the standard deviation of the 20 records was taken as synchronization uncertainty for each of the data points. The CH<sub>4</sub> data uncertainty was estimated with the stated uncertainty of each data set (4.3 ppb for NEEM ~~discrete and/ 2.7 ppb 1.4 ppb~~ for SDMA / 1.5 ppb for WAIS continuous, 1 sigma). To check the sensitivity of the uncertainties, we carried out Monte Carlo simulations. We produced 1000 different sets of IPD, which vary randomly with Gaussian propagation in their ages and CH<sub>4</sub> concentration uncertainties. Each IPD was annually interpolated and smoothed by a 1/1000 year<sup>-1</sup> low-pass filter. The cutoff frequency of 1000 years was chosen to examine multi-centennial to millennial scale change, because ~~Since the IPD calculation is very sensitive to high frequency variability of CH<sub>4</sub> records from both poles. To report 95% confidence interval, we multiplied the standard deviation by 1.96 and enveloped the IPD.,-and it is difficult to reconstruct reliable IPD in short time scales, all IPD records in this study were filtered by a 1000 year low pass window to discuss multi-centennial to millennial scale change.~~

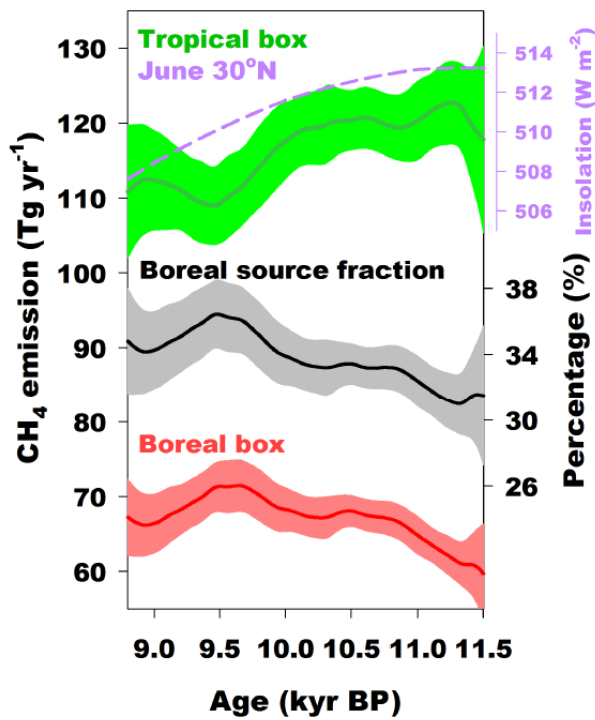
There are a few periods between 11.4 and 10.5 ka where WAIS and Siple are different by ~20 ppb, which produces the different IPD shapes. While WAIS continuous includes several 100 data points (mean resolution of 2 years), I manually count ~15 in the Siple record in Figure 3. Moreover, both the WAIS and NEEM records share several features, that are not resolved at all in the Siple record. It seems to me, that focussing your IPD interpretation on IPD reconstructions that are best constraint makes most sense. I understand the temptation to focus your analysis on the new data. However, I would strongly recommend to shift IPD-2 from Supplements into the main figure and to use IPD-2 for interpretation between 11.5 and 10.0 ka. This will still leave you with the IPD increase until 9.5 ka, but is better constraint and has less artefacts. In the box model, this would create rather stable emissions from tropics until 10.0 and a decrease thereafter. To me, this would seem the best IPD reconstruction possible.

→ We agree with the Reviewer and we create a combined IPD using IPD-1 for 10.0 – 9.0 ka and IPD-2 for the rest of the studied interval (Fig. R1). The new IPD composite maintains major findings of our manuscript, but shows less fluctuation for 11.5 – 10.0 ka period. Figure R2 presents revised box model results using combined IPD. It does not change our findings, showing a gradual strengthening of boreal sources while tropical emission was reduced along with insolation in northern hemisphere. We also changed colors of Greenland- and Antarctic CH<sub>4</sub> records in Figure R1 and R3 for better readability.



1  
2  
3  
4  
5  
6

**Figure R1.** Inter-polar difference (IPD) reconstructions. Top: high resolution CH<sub>4</sub> records from Greenland and Antarctica, synchronized to NEEM gas age scale by Monte Carlo procedure. Middle: Millennial-scale IPD composite derived from IPD-1 and IPD-2. Shaded area indicates 95% significance interval. Bottom: Proxy-based temperature reconstruction for northern mid to high latitude and boreal CH<sub>4</sub> emission from northern thermokarst lakes.



7  
8  
9

**Figure R2.** Revised 3-box model results from the combined IPD and its 95% significance interval.

### iii) Section 3.3, Comparison with late Holocene variability

This section feels completely unattached to the rest of the manuscript. The figures are described but any quantification is hard to follow. The section title is meaningless and confusing.

→ Actually, the Section 3.3 was added following comment of one of the previous reviewers for the first open discussion. However, we agree with the reviewer that this section is not in line with the main text, and therefore we deleted this section.

### iv) Conclusions

Please quantify your statements and avoid generalisations, such as high resolution (how high), agree well with previous measurements (how well), four CH<sub>4</sub> minima (how big are anomalies, how long in duration), first reporting of IPD increase from 11.5 to 9.9 (how much increase), elevated emissions from NH extra-tropics (how much did emissions from NH extra tropics increase), RMS amplitude smaller (how much) and what does this even mean in conclusions?

→ To avoid ambiguity, we revised the conclusion paragraph as below:

→ ~~In this study w~~We reconstructed a new high resolution CH<sub>4</sub> record during the early Holocene from Siple Dome ice core, Antarctica, to study millennial CH<sub>4</sub> variability and its natural controls under Holocene interglacial condition. The new Siple Dome record agrees well with previous records measured at OSU within analytical uncertainty, showing a mean difference of 0.1 ppb. By combining the two data sets, we present a SDMA CH<sub>4</sub> composite record covering from ~7.7 to 11.6 ka. ~~the early Holocene CH<sub>4</sub> time-series in high resolution to discuss natural processes that control the millennial scale CH<sub>4</sub> variations in the past atmosphere. Since the new SDMA data agree well with previous measurements at OSU, we made SDMA CH<sub>4</sub> composite data covering ~7.7 to 11.6 ka. We observed~~ Our results show a series of the ~~four~~ millennial scale CH<sub>4</sub> minima having 10–20 ppb of amplitude with 300–400 years duration. It is found that these CH<sub>4</sub> minima were accompanied with Greenland cooling, changes in ITCZ position and reduced Asian and Indian monsoon intensities. The observed evidences suggest that low latitude hydro climate changes were closely related to millennial scale CH<sub>4</sub> minima. and the evidence suggests that the low latitude source changes were the major causes of the early Holocene CH<sub>4</sub> minima. Further, this study presented the millennial scale change of IPD, which was calculated from high resolution discrete data set of NEEM and SDMA, and a continuous record of WAIS Divide. Here we reported that the IPD increased by ~13 ppb ~~increase~~ from the onset of the Holocene to ~~~9.9 ka~~ ~9.5 ka following the temperature rise in NH extra-tropical regions. The three-box model demonstrates that ~~elevated emission from NH extratropics and reduction of tropical sources~~ NH extratropical emissions elevated by ~11 Tg yr<sup>-1</sup>, while tropical emission was reduced by ~9 Tg yr<sup>-1</sup>,

1 ~~resulting the increased contribution of the NH extra-tropical sources by ~5%. Finally, we~~  
2 ~~observed that RMS amplitude of earlier part of the late Holocene is smaller than that of the~~  
3 ~~early Holocene, which may be attributed to different orbital paramet~~ However, the North  
4 ~~Atlantic induced changes in low latitude hydrology cannot fully explain the CH<sub>4</sub> minimum at~~  
5 ~~~10.2 ka. High resolution IPD and 3 box source distribution model results indicate that~~  
6 ~~fraction of boreal sources increased by 5 % during the early Holocene, which indicates that~~  
7 ~~fraction of boreal sources increased from ~10.7 ka and remained high until ~9.3 ka. To~~  
8 ~~summarize, the millennial scale variability of CH<sub>4</sub> during the early Holocene was primarily~~  
9 ~~controlled by low latitude climatic and surface hydrological conditions, while relative boreal~~  
10 ~~source contribution increased during 10.7-9.3 ka by newly developed high latitude sources~~  
11 ~~following terrestrial deglaciation. Further, our observations imply that ~20-40 ppb of CH<sub>4</sub>~~  
12 ~~change could be induced naturally by low latitude hydroclimate changes.”~~

#### 14 v) Supplements

15 I would like to encourage the authors to shift all these important information on analytical  
16 reproducibility, gas age uncertainty, IPD-2, age model effect on previous gas age scale and box model  
17 data in the main text. Figures can be reduced size, e.g. one column etc, but including those  
18 information will increase value of paper! I don't recall being frequently referred to supplements in  
19 the main text. Having a lot to read every day, I would probably never get to read supplements that  
20 aren't constantly advertised in the main paper, unless this is the most critical paper for my current  
21 work.

22 → Here we moved part of the supplements into main text, because some of them are essential  
23 for the discussion of this manuscript. We included information on chronology and gas age  
24 uncertainty in the main text. The IPD-2 and corresponding box model data were deleted  
25 because this information is already included in our new IPD. However, description of the  
26 results from the Styx glacier ice core was not included in the main text, because comparison  
27 of data set measured in different period and from different ice core may not be directly  
28 related to data interpretation.

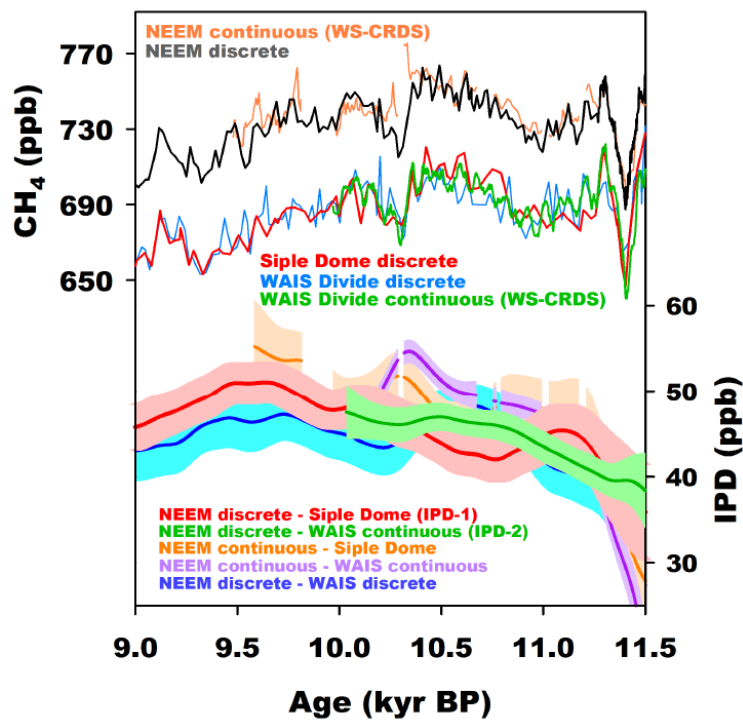


**Figure R3.** Various IPD scenarios during the early Holocene. Top: High resolution CH<sub>4</sub> records available covering the early Holocene. Bottom: Different IPDs derived from various pairs of data set.

### General comments

P36 L11: human influence was substantially smaller

→ The sentence was modified as below:

→ “In contrast, the early Holocene was a period when human influence ~~should have been was~~ substantially smaller, ~~so that it allows~~ allowing us to elucidate the natural controls under interglacial conditions more clearly.”

P37 L1: is geological CH<sub>4</sub> really the 2nd most important natural source? Not sure if most recent 14C-CH<sub>4</sub> tells the same story. The authors might want to consider to tone this statement down a bit.

→ According to synthesis of IPCC 5<sup>th</sup> report, geological sources (including oceans) are the largest natural emission except for natural wetlands, but the range of minimum and maximum estimations in literatures is largely overlapped with freshwater sources. We modified the sentence as below:

→ “Other, more minor sources include Ggeological CH<sub>4</sub> released from mud volcanoes and gas seepages through faults ~~is the second most important natural source~~ (e.g., Etiope et al., 2008 and references therein), pyrogenic sources such as wildfire and biomass burning (Andreae

1 [and Merlet, 2001; Ferretti et al., 2005; Hao and Ward, 1993](#)), and microbial digestion by wild  
2 [animals and termites \(e.g., Sanderson, 1996\).](#)”

3 P37 L4: The CH<sub>4</sub> flux from the ocean to the atmosphere

4 → We changed the sentence as below:

5 → “The ~~oceanic~~-CH<sub>4</sub> flux [from the ocean to the atmosphere](#) is considered as too small to create  
6 a significant change in global budget compared to the other sources ([e.g., Rhee et al., 2009](#)).”

7 P37 L7: not to forget CH<sub>4</sub> itself

8 → The sentence was modified as below:

9 → “The major sink of atmospheric CH<sub>4</sub> is photochemical reactions (oxidation) with the  
10 hydroxyl radical (OH), which is mainly controlled by atmospheric temperature, humidity,  
11 and ~~concentration~~ [the mixing ratio](#) of [CH<sub>4</sub> itself](#) and non-methane volatile organic compound  
12 (NMVOC) (e.g., Levine et al., 2011 and references therein).”

13 P37 L15: ...during the past climate changes... could you be more specific on time scales?

14 → The cited references are dealing with CH<sub>4</sub> sink contribution on glacial-interglacial (LGM-PI)  
15 time scales. The sentence was changed as below:

16 → “However, recent model studies suggested ~~the dominant role of source changes rather than~~  
17 ~~sink in controlling atmospheric CH<sub>4</sub> during the past climate changes that CH<sub>4</sub> changes~~  
18 [between glacial- and interglacial conditions were driven mostly by source changes, rather](#)  
19 [than sink changes](#) (Weber et al., 2010; Levine et al., 2011).”

20 P37 L15-16: This sentence should be in the section that describes the box model method

21 → We removed this sentence because the box model does account for sink term.

22 P37 L18: polar firn and ice

23 → We modified following the comment, but also reworded thoroughly.

24 → “Since [direct monitoring of CH<sub>4</sub> mixing ratio in modern atmosphere](#) ~~the direct CH<sub>4</sub>-~~  
25 ~~monitoring of modern air samples~~ only covers the late 20<sup>th</sup> and early 21<sup>st</sup> centuries  
26 (Dlugokencky et al., 1994, 2011), [polar firn and ice is the unique archive that preserves the](#)  
27 [ancient atmosphere for the research of fossil air older than 20<sup>th</sup> century.](#) ~~investigation further~~  
28 ~~back in time requires the unique archive of polar firn and ice that preserves the ancient-~~  
29 ~~atmospheric air.”~~

30 P37 L20: cite Louergue 2008

31 → We cited Louergue et al. (2008) in the sentence.

32 P37 L29: Greenland temperature change

33 → The sentence was modified as below:

34 → “[The resemblance between water stable isotopes records from Greenland ice cores, a proxy](#)

1 for Greenland temperature ~~climate~~-change, and global CH<sub>4</sub> mixing ratio on millennial time  
2 scales is also well known. ~~has been largely reported.~~”

3 P37 L30: ...around Greenland is linked to the...

4 → This was changed as below:

5 → “This implies that local temperature change around Greenland is linked to ~~could affect the~~  
6 major CH<sub>4</sub> sources in low latitudes (e.g., Brook et al., 1996; Chappellaz et al., 1993; Huber et  
7 al., 2006; EPICA Community Members, 2006; Grachev et al., 2007, 2009).”

8 P37 L32: with abrupt Northern Hemispheric warming during DO...

9 → We deleted the paragraph.

10 P38 L8-11: Please develop this sentence, I cannot follow the line of argumentation

11 → We removed the sentence.

12 P38 L25: cover only a part...

13 → We removed the sentence.

14 P38 L34: To my knowledge, there is no plural for “ice”, “ices” doesn’t exist. Please correct here and  
15 everywhere else.

16 → Done.

17 P38 L37: On the other hand...

18 → Here we thought “in principle” is better than “on the other hand”.

19 → “~~In the other hand~~In principle, stable isotope ratios of CH<sub>4</sub> help us to distinguish the types of  
20 sources – biogenic, pyrogenic, and geologic.”

21 P39 L20: record from the early Holocene and investigate...

22 → The sentence was modified as follows:

23 → “Therefore, in this study we present a new high-resolution CH<sub>4</sub> record ~~from during the early~~  
24 Holocene ~~and to~~ investigate natural control mechanisms under interglacial condition.”

25 P40 L30: starts below 400 m and continues to the bottom of the core at 1004 m

26 → The sentence was changed as below:

27 → “~~Since~~The brittle zone of SDMA ice starts below 400 m ~~depth~~ and continues to the bottom  
28 of the core at 1004 m (Gow and Meese, 2007) and samples from this region are more likely  
29 to be fractured. ~~that makes some part of ices fractured and/or cracked internally.~~”

30 P41 L3: SEM of n=2???

31 → As we re-defined the analytical uncertainty, the sentence was modified as below:

32 → “All samples were duplicated, so that our final CH<sub>4</sub> data were presented by averaging the  
33 results of duplicate analysis from the same depth. ~~and the~~The analytical uncertainty of each  
34 data point is estimated by the uncertainty of individual ice measurement divided by square  
35 root of 2 (see below). ~~standard error of the mean of duplicate pairs.~~”



1 P41 L25-27: How do you expand the gas into the GC and ensure 100% sample transfer into the GC?

2 Do you flush the headspace with He? Could this He create a blank that varies with He cylinder?

3 → No He flush is used in our method. The sample gas in flask is expanded into evacuated  
4 vacuum line and sample loop of GC. We added this into the sentence to clarify it:

5 → “The extracted air in the headspace was expanded into the evacuated vacuum line and sample  
6 loop of a gas chromatograph (GC) equipped with a flame ionization detector (FID) to  
7 measure CH<sub>4</sub> mixing ratio. After detecting the CH<sub>4</sub> peak in the GC chromatogram (retention  
8 time of ~1.6 minutes), the vacuum line and sample loop is evacuated again prior to the next  
9 injection.”

10 P42 L6-7: SEM of 2.0±1.0ppb... please explain your calculations

11 → This value was calculated from average of the daily SEM of four bubble-free ice samples,  
12 indicating the uncertainty of the daily systematic offset correction ( $e_1$ ). Therefore, we  
13 added below paragraph to explain it:

14 → “Here we consider two types of uncertainty sources: uncertainty in (1) estimating daily  
15 systematic offset and (2) other causes. The former indicates uncertainty of the daily  
16 systematic offset ( $e_1$ ). As the daily systematic offset is calculated from the mean of the four  
17 flasks with bubble-free ice and standard air, scattering of the bubble-free ice samples can  
18 induce uncertainty in the systematic offset correction. The daily  $e_1$  is estimated with standard  
19 error of the mean (SEM,  $n=4$ ), because the daily systematic offset is calculated from the  
20 mean of the four bubble-free ice samples. The average of daily  $e_1$  is 1.9 ppb. The latter ( $e_2$ )  
21 includes uncertainty due to solubility correction and inhomogeneous distribution of CH<sub>4</sub>.  
22 Given our solubility correction uses the mean value of residual gas fraction and the ratio at  
23 which CH<sub>4</sub> enriches in retrapped air, different solubility effect and/or inhomogeneous CH<sub>4</sub>  
24 distribution in individual ice causes offset between adjacent duplicate ice samples analysed  
25 on the same day. As the duplicates from same depths were measured on the same day, we  
26 estimated the  $e_2$  with pooled standard deviation (PSD) between duplicate measurements from  
27 entire depths, which yields 3.3 ppb. Taking the  $e_1$  and  $e_2$  into account together, the final  
28 uncertainty of individual measurement is given as 3.8 ppb by error propagation. The  
29 uncertainty for the mean of duplicate results is obtained by dividing the individual  
30 uncertainty by square root of 2, yielding 2.7 ppb.”

31 P42 L10: SEM of  $n=2$ ???

32 → In the previous version, we meant SEM between duplicate measurements ( $n=2$ ). However,  
33 we re-defined the analytical uncertainty and decided not to use SEM of  $n=2$  for representing  
34 individual data uncertainty. Revised analytical uncertainty for individual ice measurement is  
35 3.8 ppb, and uncertainty for the mean of duplicate measurements is 2.7 ppb. Please refer to

1 our response to general comment on analytical uncertainty.

2 P42 L12: Everything will agree well if you average often enough. Please develop transparent and  
3 unbiased approach.

4 → We re-defined our analytical uncertainty by including uncertainty of systematic offset and  
5 solubility correction. This yields final uncertainty of 3.8 ppb for individual ice measurement.  
6 But as we made duplicate measurements for all samples and took the mean of the  
7 duplicates, uncertainty of our data set should be  $3.8/2^{1/2} = 2.7$  ppb. Please refer to our  
8 responses above.

9 P42 L13: If this is your final uncertainty estimate, please state this in a clear and dedicated sentence.

10 → As the reviewer pointed out in general comment, we revised the analytical uncertainty  
11 estimate. Please refer to our response to general comment on determining analytical  
12 uncertainty.

13 P42 L17: You might want to consider leaving the “M” at the beginning of the sentence.

14 → Modified.

15 P42 L34: Please quantify the temporal resolution of your Siple Dome data

16 → We stated temporal resolution of our Siple Dome data and re-worded the sentence as  
17 below:

18 → “Our new SDMA Siple Dome CH<sub>4</sub> composite data have mean temporal resolution of ~26  
19 years. The WAIS Divide continuous CH<sub>4</sub> records show much higher resolution (~2 years),  
20 but does not cover the entire early Holocene period (Rhodes et al., 2015). ~~is the currently~~  
21 ~~third highest temporal resolution of Antarctic CH<sub>4</sub> records~~ record is the one of the high-  
22 ~~resolution data set covering the early Holocene after the WAIS Divide continuous (~2 years,~~  
23 ~~Rhodes et al., 2015) and discrete (~20 years, WAIS Divide members, 2015) records. from~~  
24 ~~11.6 to 8.5 ka, apart from the WAIS Divide records (Rhodes et al., 2015; WAIS Divide~~  
25 ~~members, 2015).~~”

26 P44 L31: from Asian and Amazon wetlands

27 → We changed the words.

28 → “Sperlich et al. (2015) also suggested ~~found~~ that a sharp CH<sub>4</sub> peak at Greenland Interstadial  
29 21.2 (~85 ka) was ~~caused~~ ~~occurred~~ by emission from Asian and Amazon ~~South American~~  
30 wetlands.”

31 P47 L29: Another argument to use NEEM discrete is that these data were measured at OSU as well.

32 No?

33 → The reviewer is right. We added this rationale in the paragraph as below:

34 → “Regarding the Greenland side, we use NEEM discrete records because not only there are  
35 discrepancies between continuous- and discrete data in some intervals, but also NEEM

1 discrete records were measured by similar wet extraction technique at OSU (Chappellaz et al.,  
2 2013). ~~we use NEEM discrete records because there are discrepancies between continuous~~  
3 ~~and discrete data in some intervals, but also because the NEEM continuous record is not~~  
4 ~~exactly “continuous”. Hence, here we regard the NEEM discrete, Siple Dome discrete, and~~  
5 ~~WAIS Divide continuous data as more reliable ones than the others to reconstruct IPD during~~  
6 ~~the early Holocene. In this study, the IPD was calculated by using our Siple Dome CH<sub>4</sub>~~  
7 ~~record and a NEEM high-resolution discrete CH<sub>4</sub> record (Chappellaz et al., 2013).”~~

8 P48 L9: Please provide a transparent description of how you calculate 1.4 ppb.

9 → Please refer to our response to general comment above.

10 P48 L13: “regarded as more accurate”, not exactly a scientific term. Haven’t the uncertainties of 1.4  
11 ppb and 1.5 ppb just been stated for Siple and WAIS, respectively, in the previous sentence? I  
12 strongly recommend to re-think the presented uncertainty model. Accuracy is part of the  
13 uncertainty but doesn’t seem to be considered in the uncertainties presented in this manuscript. If  
14 ice core specific accuracy problems infiltrate IPD analysis, how reliable is the magnitude of IPD  
15 reconstructions?

16 → Now the analytical uncertainties of SDMA and WAIS continuous records are 2.7 and 1.5 ppb,  
17 respectively. We calibrated WAIS continuous data against to SDMA data because  
18 continuous data require to be calibrated against discrete measurements, but also SDMA  
19 records show good agreement with OSU measurements. Given that NEEM discrete data  
20 were measured in OSU by using similar method as well, by doing this we can rule out any  
21 discrepancy between IPD-1 and IPD-2 due to different measurement techniques used. The  
22 sentence was changes as below:

23 → “Before IPD calculation, WAIS continuous data were calibrated to SDMA data instead of  
24 WAIS discrete record, given the discrete measurements generally have better accuracy than  
25 continuous ones.”

26 P48 L17: Describe the calculation of the envelope

27 → Please refer to our response to general comment above.

28 P49 L3: State lifetime and transport time you assume in model

29 → We used lifetime of 18.7, 8.1, and 26.8 years for N, T, and S box, respectively, and transport  
30 time of 9 months following Chappellaz et al. (1997). We added these information in the text:

31 → “Following Chappellaz et al. (1997), we assume the lifetime of 18.7, 8.1, and 26.8 years in N,  
32 T, and S-box, respectively, and transport time of 9 months.”

33 P49 L7: 15 Tg

34 → We changed the lower case “t” into the capital “T”.

1 P49 L8: IPD-2, 134 to 115 Tg, I don't see anything >125 Tg in Figure S3. I am confused with some of  
2 the quantifications in the following text, often, the stated numbers don't seem to match the values in  
3 the figures.

4 → As the Reviewer suggested above, we presented a combined IPD (Fig. R1) and newly  
5 calculated box-model result (Fig. R2). As we replaced the discussion on IPD-2 with that for  
6 combined IPD, we changed the numbers correspondingly.

7 P49 L9: What trend? I can't see a trend in Fig. S3.

8 → The Reviewer is right, we revised the paragraph thoroughly with a combined IPD.

9 P49 L12: Where are these numbers from? Fig S3? Fig 4?

10 → The former Fig. 4 is now Fig. 8. We modified the sentence as below and added "Fig. 8" in the  
11 sentence:

12 → "The T-box emission is reduced from ~118 Tg yr<sup>-1</sup> to ~109 Tg yr<sup>-1</sup>, and the N-box source  
13 strength increases from ~60 Tg yr<sup>-1</sup> to ~71 Tg yr<sup>-1</sup> during the 11.5 – 9.5 ka interval (Fig. 8).  
14 The tropical emission was elevated by ~98 Tg yr<sup>-1</sup> from the onset of the Holocene to its  
15 maximum at 10.6 ka, followed by ~15 Tg yr<sup>-1</sup> reduction to ~111 Tg yr<sup>-1</sup> at 9.5 ka. Tropical  
16 emission decrease is also observed in IPD-2 from 134 to 115 Tg yr<sup>-1</sup> during the 11.5–10.0 ka,  
17 but this change is not significant in 95% confidence range (Fig. S3 and Table S2)."

18 P49 L12: The minima at 10.7 ka is only a feature in IPD-1, not in IPD-2. Again, this is misleading, as  
19 IPD-1 is based on much lower temporal resolution. Please use IPD-2 where possible.

20 → We agree with the Reviewer, and we presented a combined IPD using IPD-2 for younger  
21 period and IPD-1 for the rest of the studied interval. Please refer to Figure R1 and R2, and  
22 relevant responses above.

23 P49 L16: "...from 29 to 35% during the 11.5 to 10.0 interval." I cannot even see a value <30% or >34%  
24 in Fig. S3, even including the envelope.

25 → We changed the sentence to be more concise:

26 → "Also plotted in Figure 84 is the boreal source fraction, defined as ratio of N-box emission to  
27 total source emissions, showing 5% increase (from 31.5 to 36.5%) during the same interval.  
28 The box model results at 9.0, 9.5, and 11.5 ka time slices are summarised in Table 2. ~~It~~  
29 shows a significant increase from ~30% at 11.5 ka to ~35% at 9.5 ka."

Ref.	N box	T box	<u>Boreal source</u> <u>fraction</u> N/(N+T+S)
(ka)	(Tg yr <sup>-1</sup> )		(%)
Brook et al., 2000	64 ± 5	123 ± 8	32 ± 3

(9.5-11.5 ka)			
Chappellaz et al., 1997 (9.5-11.5 ka)	66 ± 8	120 ± 9	33 ± 3
This study <u>(9.5 – 11.5 ka)</u> <del>(10.8 ka)</del>	<del>67 ± 3</del> <del>66 ± 4</del> <del>65 ± 2</del>	<del>118 ± 5</del> <del>120 ± 4</del> <del>122 ± 4</del>	<del>33 ± 2</del> <del>33 ± 2</del> <del>32 ± 1</del>
<u>This study</u> <u>(11.5 ka)</u>	<u>60 ± 7</u> <del>47 ± 9</del>	<u>118 ± 12</u> <del>149 ± 10</del>	<u>31 ± 4</u> <del>22 ± 5</del>
This study <del>(9.9 ka)</del> <u>(9.5 ka)</u> <del>(9.8 ka)</del>	<u>71 ± 3</u> <del>65 ± 8</del> <del>74 ± 2</del>	<u>109 ± 5</u> <del>119 ± 9</del> <del>110 ± 3</del>	<u>36 ± 2</u> <del>33 ± 5</del> <del>37 ± 1</del>
<u>This study</u> <u>(9.0 ka)</u>	<u>66 ± 4</u>	<u>112 ± 7</u>	<u>34 ± 2</u>

1

2 P49 L7-16: This entire section needs major revision. The numbers don't seem to match the  
3 presentation in the figures, the description jumps back and forth between Figures in supplements  
4 and main text, the text flow makes it hard to understand.

5 → We removed this section and replaced it with discussion using the combined IPD, following  
6 the Reviewer's suggestion above.

7 P49 L22: What conclusion?

8 → The conclusion in this sentence means the gradual increase of extratropical emission during  
9 the earlier part of the studied period. To avoid misleading, we changed the word "This  
10 conclusion" into "Our results".

11 → "This conclusion is Our results are supported by proxy-based temperature reconstructions  
12 that indicate a gradual warming in ~~northern high latitude~~ northern extratropical regions  
13 (30°N – 90°N) until ~9.6 ka, while tropical temperature remains stable (Marcott et al.,  
14 2013)."

15 P49 L30: Your 13 Tg estimate is based on IPD-1, which matches the 8.2 Tg within uncertainties. What  
16 value would you get from IPD-2?

17 → We found ~9 Tg from box model results from IPD-2 (Table S1 in previous manuscript  
18 version).

19 P51 L4: Please find a meaningful section title

20 → We removed the entire section.

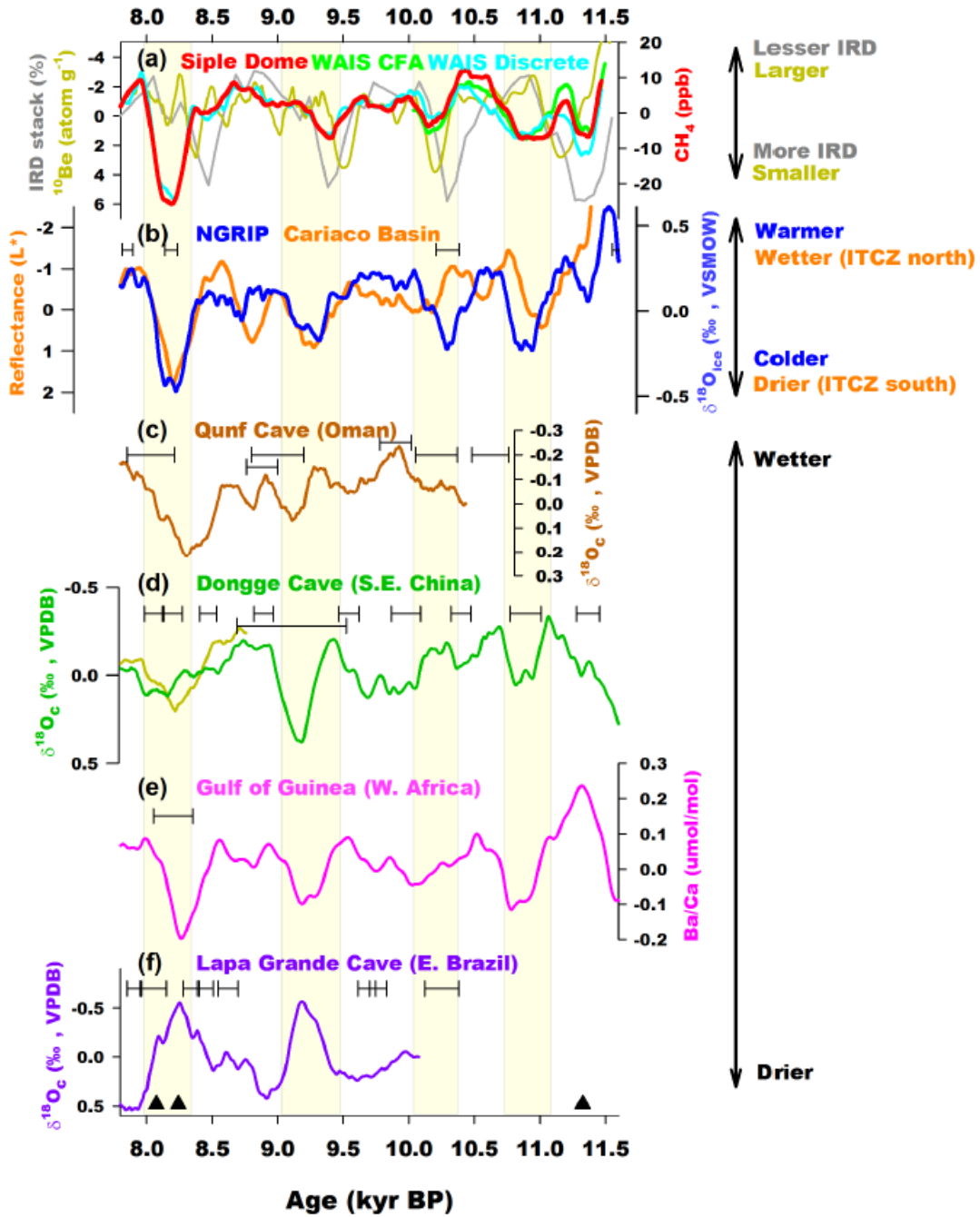
21 P51 L27ff: please generalise less and quantify more.

22 → Please refer to our response to Reviewer's comment on Conclusion.

23 P62, Figure 2: Please add next to axes what these proxies actually show, e.g. warmer, wetter, colder  
24 dryer with arrows.

1

→ We modified the figure as below:



2

3

Figure R4. Revised Figure 2 in manuscript.

4

P64, Figure 4: Please add reconstructions based on IPD-2

5

→ We replaced Figure 4 with new reconstruction based on combined IPD from IPD-1 and IPD-2.

6

Please refer to Figure R2 in our response above (Fig. 8 in revised main text).

7

P65, Figure 5: Please synchronize x-axes directions in top panels

8

→ We removed the entire section and corresponding figure.

1 P66 L2: Uncertainties or errors?

2 → Our intension was indicating uncertainty. This was revised.

3 P67ff: Please include supplements in main text

4 → We partly moved supplements in main text, but we did not include IPD-2, box model of IPD-  
5 2, and uncertainty of Styx glacier data set because these information are not essential for  
6 discussions of this manuscript.

7

8

**Anonymous Reviewer #2: Suggestions for revision or reasons for rejection (will be published if the paper is accepted for final publication)**

The manuscript presents an interesting new set of discrete CH<sub>4</sub> measurements from the Siple Dome ice core, allowing the authors to mostly discuss the early Holocene trend of atmospheric methane and to elaborate on the possible mechanisms involved to explain the trend and variability.

The analytical work is substantial and I commend the authors for this. However, like the two previous reviewers, I am puzzled by the claimed analytical error of about 2 ppb, when compared with the variability observed when performing blank tests of the system (5 to 15 ppb). The community usually attributes the blank of CH<sub>4</sub> analytical systems to degassing of the glass walls of the containers, itself depending on the variable ambient CH<sub>4</sub> concentration in the laboratory and cold room, and on the thermal history of the container. This can introduce a lot of variability, intra-day and inter-day. It is quite surprising that a small variability can be claimed by the authors at the intra-day level. I understand that the authors argue – for a good reason - on the reproducibility of duplicate measurements conducted many days apart on the Siple Dome samples, to claim that their evaluation of the different sources of errors is correct. But it remains quite puzzling from an experimental point of view... I'd suggest for the future evolution of the analytical procedure – and if not done yet – to consider performing again these blank tests while the containers are kept closed in the cold room, under zero air (or nitrogen) filling, before introduction of the ice sample. I'd suspect that this would considerably reduce the inter-day variability of the blanks.

→ We appreciate the Reviewer #2 for pinpoint comment and thoughtful suggestions. As suggested by the Reviewer #1, we modified the uncertainty estimation of our data. Taking both uncertainties caused by daily systematic offset and the others into account, we address more conservative and comprehensive analytical error. The uncertainty of systematic offset is determined daily by standard error of the mean (SEM) of the results from four bubble-free ice samples, and we used the average value of the daily SEMs for the systematic offset uncertainty ( $e_1$ ) calculation. The uncertainty of the other causes ( $e_2$ ) is estimated by pooled standard deviation (PSD) of duplicate ice measurements conducted on the same day. The  $e_2$  includes uncertainty from solubility correction and CH<sub>4</sub> inhomogeneity in ice from the same depth interval. Our final data uncertainty for the individual ice is calculated by  $((e_1)^2 + (e_2)^2)^{1/2}$ , resulting 3.8 ppb.

A correction for solubility is applied on each data point. Am I wrong or the blank tests are conducted by adding a standard gas to the blank ice? If this is the case, then the solubility effect should be accounted for - at least partly - through the blank measurements as part of the standard gas gets



into diffusive equilibrium with the blank water during the melting phase, and no (or a small) additional correction should apply.

- ➔ First, it should be noted that we modified the solubility correction method. Now we calculated the solubility effect from residual gas fraction and CH<sub>4</sub> mixing ratio of air remained in refrozen meltwater. The 2<sup>nd</sup> gas extraction tests using Styx glacier ice core, Antarctica show that CH<sub>4</sub> mixing ratio in re-trapped air is enriched by 3.11 times for glacial ice and 2.98 times for bubble-free ice. Residual gas fraction was measured from SDMA ice samples during the 10 experimental days. The average residual gas fraction is  $1.05 \pm 0.13\%$  ( $1\sigma$ ,  $n=60$ ) for SDMA ice samples and  $0.38 \pm 0.08\%$  ( $1\sigma$ ,  $n=40$ ) for bubble-free ice.
- ➔ The reviewer is right only if the bubble-free ice is a perfect “blank” ice sample that represent all of the physical- and chemical properties of glacial ice except for gas bubbles. However, our bubble-free ice shows different residual gas fraction and hence different solubility effect from glacial ice. As the bubble-free ice does not represent the solubility effect of SDMA ice, we applied the solubility correction to the bubble-free ice as well in the same manner to the SDMA ice, but using different CH<sub>4</sub> mixing ratio in re-trapped air and residual gas fraction. After corrected for the solubility effect, the offset of CH<sub>4</sub> mixing ratio between the bubble-free ice and standard air is caused by system condition change, such as leakage, contaminants, etc. Therefore, we estimate daily systematic offset with the bubble-free ice measurements. This was carried out by injecting standard air on bubble-free ice. After getting raw data, we corrected the results for re-trapped air during melting-refreeze process (solubility correction). The difference in the CH<sub>4</sub> level between the original standard air and that from the corrected bubble-free ice was used for the estimation of the daily systematic error.

Figure 1 shows at ~9.6 kyr BP a CH<sub>4</sub> spike which may not represent a true atmospheric feature when taking into account the smoothing of atmospheric variations related with gas enclosure conditions at Siple Dome. So there seems to be other sources of errors that the claimed 2 ppb analytical error do not fully cover. Or a good explanation should be brought on why such a narrow spike is observed in the Siple Dome record.

- ➔ We agreed with the Reviewer and rejected that point. However, this rejection does not change major findings in our manuscript. The figures were revised correspondingly.

The gas enclosure brings me to another concern : the authors make a big case on the interpolator

gradient. This is a tricky signal to obtain and to interpret. Notably, gas trapping conditions are key. An ideal case is to combine northern and southern records affected by similar gas trapping conditions. When combining Greenland records with the Siple Dome one, this is clearly not the case. At least the authors should consider convolving the Siple Dome signal with a log-normal distribution reflecting the gas trapping conditions at Siple Dome, before comparing with Greenland records and calculating an IPD. Or they should restrict on only using the WAIS Divide record, despite the fact that it was previously published and not resulting from the authors' work...

- The Reviewer is right. The gas age distribution of NEEM is closer to WAIS Divide than Siple Dome condition, thus Siple Dome record should be smoothed more than WAIS Divide. However, our IPD reconstructions were filtered by  $1/1000 \text{ year}^{-1}$  low-pass window, so that small changes due to different gas enclosure process were smoothed out and do not affect to our finding. The gas trapping conditions become quite important where rapid  $\text{CH}_4$  changes occur, for example, 8.2 ka cooling event and pre-boreal oscillation (PBO). As commented by the Reviewer #1, we calculated a combined IPD using both Siple Dome and WAIS Divide records.

Aside from the gas enclosure aspect, I wonder indeed if it makes sense in the end to calculate  $\text{CH}_4$  source strengths changes with a 3-box model while the source evolution is partly attributed to a shift of the ITCZ. The latter necessarily affects the inter-box exchange time as well as the pertinence of the exact latitudinal « boundaries » used between boxes. Isn't there a circular argument here ?

- We did not attribute the IPD change and box model results to ITCZ migration in the main text. We discussed only with NH extratropical temperature change and thermokarst lake emissions.

Detail :

I'm not sure that any reference to variable OH in polar regions really make sense. By far most of atmospheric  $\text{CH}_4$  is oxidized in the inter-tropical band and at relatively high altitude. The polar component does not really matter here.

- We removed the sentence that deals with polar winter, and the paragraph was modified as below:
- "The major sink of atmospheric  $\text{CH}_4$  is photochemical reactions (oxidation) with the hydroxyl radical (OH), which is mainly controlled by atmospheric temperature, humidity, and ~~concentration~~ [the mixing ratio](#) of  [\$\text{CH}\_4\$  itself](#) and non-methane volatile organic compound (NMVOC) (e.g., Levine et al., 2011 and references therein). ~~A~~The air temperature affects ~~air~~

humidity ~~thereby,~~ limiting the production of OH. ~~Oxidation of b~~Both NMVOCs and CH<sub>4</sub> ~~are competing compete~~ for OH ~~to be oxidized~~, that is, ~~an~~ increase in NMVOC emission reduces the available OH, ~~so it and~~ increases the ~~atmospheric~~ lifetime of CH<sub>4</sub> ~~in the atmosphere~~ (Valdes et al., 2005). ~~Further, since the OH is produced by photo-dissociation reaction, the CH<sub>4</sub> sink strength is affected by light availability and tropospheric ozone (e.g., Levy, 1971). Polar winters may affect the CH<sub>4</sub> sink strength by reduced OH production rate, but the seasonal scale cycles are not resolvable in ice core records due to gas dispersion in firn layers.~~ However, recent model studies suggested ~~the dominant role of source changes rather than sink in controlling atmospheric CH<sub>4</sub> during the past climate changes that CH<sub>4</sub> changes between glacial- and interglacial conditions were driven mostly by source changes, rather than sink changes~~ (Weber et al., 2010; Levine et al., 2011). ~~Therefore, the sink changes are not considered here.”~~

Apart from the points raised above, I find that the authors correctly addressed all remarks made by the two reviewers as well as the editor.

1  
2  
3  
4  
5  
6

References that are not cited in the manuscript:

Anderson, T. V.: Efficient, accurate, and non-Gaussian error propagation through nonlinear, closed-form, analytical system models, Ph. D. thesis, Brigham Young University, Provo, Utah, 78 pp., 2011.

# 1 Atmospheric methane control mechanisms during the early 2 Holocene

3 Ji-Woong Yang<sup>1</sup>, Jinho Ahn<sup>1</sup>, Edward J. Brook<sup>2</sup>, and Yeongjun Ryu<sup>1</sup>

4 <sup>1</sup>School of Earth and Environmental Sciences, Seoul National University, Seoul 08826, South Korea

5 <sup>2</sup>College of Earth, Ocean, and Atmospheric Sciences, Oregon State University, Corvallis, OR 97331, USA

6 *Correspondence to:* Jinho Ahn (jinhoahn@snu.ac.kr)

7 **Abstract.** Understanding processes controlling the atmospheric methane (CH<sub>4</sub>) mixing ratio ~~the atmospheric~~  
8 ~~methane (CH<sub>4</sub>) change~~ is crucial to predict and mitigate ~~the~~ future climate changes in this gas. ~~In spite of~~ Despite  
9 recent ~~studies using various approaches for the~~ detailed studies of the last ~1000 to 2000 years, ~~control the~~  
10 mechanisms that control atmospheric ~~of~~ CH<sub>4</sub> still remain unclear, partly because the late Holocene CH<sub>4</sub> budget  
11 ~~is~~ may be comprised of both natural and anthropogenic emissions. In contrast, the early Holocene was a period  
12 when human influence ~~should have been~~ was substantially smaller, ~~so that it allows~~ allowing us to elucidate  
13 more clearly the natural controls under interglacial conditions more clearly. Here we present new high  
14 resolution CH<sub>4</sub> records from Siple Dome, Antarctica, covering from 11.6 to 7.7 thousands of years before 1950  
15 AD (ka). We observe four ~~several~~ local CH<sub>4</sub> minima on a roughly 1000-year spacing, ~~which~~. ~~Each CH<sub>4</sub>~~  
16 ~~minimum~~ corresponds to cool periods in Greenland. We hypothesize that the cooling in Greenland forced the  
17 Intertropical Convergence Zone (ITCZ) to migrate southward, reducing rainfall in northern tropical wetlands.  
18 ~~The although there is no obvious change was observed in low latitude hydrology corresponding to abrupt CH<sub>4</sub>~~  
19 ~~reduction at ~10.3 ka.~~ inter-polar difference (IPD) of CH<sub>4</sub> shows a gradual increase from the onset of the  
20 Holocene to ~9.9~9.5 ka, which implies growth of boreal source strength following the climate ~~waring~~ warming  
21 in the northern extratropics during that period. ~~Finally, we find that amplitude of centennial to millennial scale~~  
22 ~~CH<sub>4</sub> variability of the early Holocene is larger on average than that of the earlier part of the late Holocene (3.5~~  
23 ~~1.2 ka).~~ A high resolution inter-polar difference (IPD) during the early Holocene increased from ~10.7 to 9.9 ka,  
24 and remained high until ~9.3 ka. With a simple three-box model results, our new IPD records suggest that the  
25 ratio of northern high latitude to tropical sources increased due to a boreal source expansion following the  
26 deglaciation.

## 27 1 Introduction

28 Methane (CH<sub>4</sub>) is a potent greenhouse gas whose atmospheric mixing ratio has ~~been~~ increased more than 2.5  
29 times since the Industrial Revolution (Dlugokencky et al., 2009). Although lower in abundance compared to  
30 carbon dioxide (CO<sub>2</sub>), CH<sub>4</sub> has ~28 times higher global warming potential (GWP) on ~~centennial timescales~~ a  
31 100 year time scale and even higher GWP on shorter time scales due to ~~the its short~~ shorter lifetime in the  
32 atmospheric lifetime (Stocker et al., 2013). Hence understanding the controls on atmospheric ~~the knowledge of~~  
33 ~~control mechanisms of~~ CH<sub>4</sub> is important to predict ~~foresee~~ and mitigate ~~the~~ future climatic ~~climate~~ and  
34 environmental changes.

1 Naturally, CH<sub>4</sub> is mainly produced ~~from~~by microbial decomposition by methanogens in anaerobic  
2 environments, such as waterlogged soil, wetlands, or sediments of lakes and rivers. Even though a part of CH<sub>4</sub> is  
3 oxidized, and can be emitted in the form of~~oxidized and emitted as~~ CO<sub>2</sub>, a considerable amount of CH<sub>4</sub> is still  
4 released into the atmosphere through vascular plants, diffusion and ebullition processes (e.g., Joabsson and  
5 Christensen, 2001). Other, more minor sources include ~~G~~geological CH<sub>4</sub> released from mud volcanoes and gas  
6 seepages through faults ~~is the second most important natural source~~ (e.g., Etiope et al., 2008 and references  
7 therein); pyrogenic sources such as wildfire and biomass burning (Andreae and Merlet, 2001; Ferretti et al.,  
8 2005; Hao and Ward, 1993), and microbial digestion by wild animals and termites (e.g., Sanderson, 1996).  
9 ~~Additionally, a portion of CH<sub>4</sub> is produced by termites and wild animals via microbial digestive process (e.g.,~~  
10 ~~Sanderson, 1996), and by pyrogenic sources such as wildfire and biomass burning (e.g., Daniau et al., 2012;~~  
11 ~~Andreae and Merlet, 2001; Ferretti et al., 2005; Hao and Ward, 1993).~~The oceanic CH<sub>4</sub> flux from the ocean to  
12 the atmosphere is considered as too small to create a significant change in global budget compared to the other  
13 sources (e.g., Rhee et al., 2009). The major sink of atmospheric CH<sub>4</sub> is photochemical reactions (oxidation) with  
14 the hydroxyl radical (OH), which is mainly controlled by atmospheric temperature, humidity, and ~~concentration~~  
15 the mixing ratio of CH<sub>4</sub> itself and non-methane volatile organic compound (NMVOC) (e.g., Levine et al., 2011  
16 and references therein). ~~A~~The air temperature affects ~~air~~ humidity ~~thereby~~, limiting the production of OH.  
17 Oxidation of bBoth NMVOCs and CH<sub>4</sub> ~~are competing~~ compete for OH ~~to be oxidized~~, that is, an increase in  
18 NMVOC emission reduces the available OH, ~~so it and~~ increases the atmospheric lifetime of CH<sub>4</sub> ~~in the~~  
19 atmosphere (Valdes et al., 2005). Further, since the OH is produced by photo-dissociation reaction, the CH<sub>4</sub> sink  
20 strength is affected by light availability and tropospheric ozone (e.g., Levy, 1971). ~~Polar winters may affect the~~  
21 ~~CH<sub>4</sub> sink strength by reduced OH production rate, but the seasonal scale cycles are not resolvable in ice core~~  
22 ~~records due to gas dispersion in firn layers.~~ However, recent model studies suggested the dominant role of  
23 source changes rather than sink in controlling atmospheric CH<sub>4</sub> during the past climate changes that CH<sub>4</sub>  
24 changes between glacial- and interglacial conditions were driven mostly by source changes, rather than sink  
25 changes (Weber et al., 2010; Levine et al., 2011). ~~Therefore, the sink changes are not considered here.~~

26 ~~Since the direct CH<sub>4</sub> monitoring of modern air samples only covers the late 20<sup>th</sup> and early 21<sup>st</sup> centuries~~  
27 ~~(Dlugokenky et al., 1994, 2011),~~ Polar firn and ice are the unique archives that preserves the ancient  
28 atmosphere for the research of fossil air older than the 20<sup>th</sup> century. ~~investigation further back in time requires~~  
29 ~~the unique archive of polar firn and ice that preserves the ancient atmospheric air.~~ Paleoatmospheric CH<sub>4</sub> levels  
30 have been reconstructed for the last 800 thousand of years (kyr) ka from Antarctic- and Greenland ice cores  
31 (Loulergue et al., 2008) (e.g., Spahni et al., 2005; Loulergue et al., 2008). Given the relatively long lifetime in  
32 troposphere (11.2 ± 1.3 years at present, e.g., Prather et al., 2012) compared to atmospheric mixing time, ice  
33 core CH<sub>4</sub> records represent well-mixed global signatures. ~~From the~~ The 800 ka records, it was revealed that A  
34 time series of the past CH<sub>4</sub> changes found that the shows that past CH<sub>4</sub> change generally followed the glacial-  
35 interglacial cycles, being was low with low concentrations during glacial periods and high concentrations in  
36 interglacials, as well as the shorter orbital cycles of obliquity and precession, ~~generally following the glacial-~~  
37 ~~interglacial cycles and related global ice volume changes (Lisiecki and Laymo, 2005; (e.g., Spahni et al., 2005;~~  
38 Loulergue et al., 2008). Those earlier studies have suggested that the changes in climate and hydrology in the  
39 tropics on tropical wetlands induced by the orbital changes forcing controlled the CH<sub>4</sub> emissions. The  
40 resemblance between water stable isotopes records from Greenland ice cores, a proxy for Greenland temperature

1 ~~climate change, and global CH<sub>4</sub> mixing ratios on millennial time scales is also well known. has been largely~~  
2 ~~reported.~~ This implies that local temperature change around Greenland is linked to ~~could affect~~ the major CH<sub>4</sub>  
3 sources in low latitudes (e.g., Brook et al., 1996; Chappellaz et al., 1993; Huber et al., 2006; EPICA Community  
4 Members, 2006; Grachev et al., 2007, 2009). ~~The similarity is also held in short time scale climate events.~~  
5 ~~Previous works reported that rapid CH<sub>4</sub> increases were coincident with abrupt Northern Hemispheric warming~~  
6 ~~during climate changes in Dansgaard-Oeschger (DO) events throughout during the glacial period (e.g., Brook et~~  
7 ~~al., 1996; EPICA Community Members, 2006; Grachev et al., 2007, 2009). The coincidence between abrupt~~  
8 ~~CH<sub>4</sub> and Greenland climate change was also found in 8.2k cooling event, Preboreal Oscillation (PBO), Younger~~  
9 ~~Drays (YD), and Bølling-Allerød (BA) periods (Brook et al., 2000; Kobashi et al., 2007, 2008).~~

10 Intensive precipitation changes ~~on~~ in the low latitude summer monsoon ~~area~~ regions, caused by insolation  
11 changes (e.g., Asian monsoon) have been suggested as an important CH<sub>4</sub> control during the glacial period (e.g.,  
12 Chappellaz et al., 1990). From time series analysis of past CH<sub>4</sub> records, Guo et al. (2012) found that the tropical  
13 monsoon circulations ~~are~~ is a primary control of relatively shorter (millennial) time scale variability, while long-  
14 term (multi-millennial to orbital scale) variations are dominated by solar insolation changes. ~~For shorter time~~  
15 ~~scale variability, the tropical monsoon activity and solar insolation changes were proposed as primary controls~~  
16 ~~(Guo et al., 2012).~~ It has been found that tropical monsoon activity ~~is~~ ~~is~~ were closely related to orbital-scale  
17 CH<sub>4</sub> change (e.g., Brook et al., 1996; Chappellaz et al., 1990), especially ~~reported are~~ Asian monsoon (e.g.,  
18 Loulergue et al., 2008) and South American monsoon (e.g., Cruz et al., 2005). ~~in shorter time scales,~~ However,  
19 no direct correlation between CH<sub>4</sub> and tropical monsoon signals has been reported ~~for the early Holocene,~~  
20 although ~~demonstrated were the~~ positive relationships between Greenland climate and tropical monsoons  
21 intensity (e.g., Chiang et al., 2008), ~~as well as~~ and-between Greenland climate and CH<sub>4</sub> (e.g., Spahni et al., 2005;  
22 Wang et al., 2005; Mitchell et al., 2011) have been ~~reported.~~ ~~discussed.~~ ~~Given that waterlogged wetlands are the~~  
23 ~~largest natural CH<sub>4</sub> source, this complex relationship may imply that tropical monsoons are not the sole, primary~~  
24 ~~controls; wetlands in northern high latitude and southern hemisphere might act as a secondary role.~~

25 ~~The r~~Relationship between the latitudinal shift of the ITCZ and CH<sub>4</sub> emissions varies with time scales.  
26 Landais et al. (2010) and Guo et al. (2012) suggested that ITCZ migration is not a dominant control of glacial-  
27 interglacial CH<sub>4</sub> cycle because long-term CH<sub>4</sub> trend does not follow ~~well~~ the precessional insolation change in  
28 the northern hemisphere (NH) ~~well~~. Modelling studies found the southward shift of the ITCZ coincides with  
29 reduced CH<sub>4</sub> in Last Glacial Maximum (LGM) and Heinrich Stadial (HS) events, ~~even though~~ ~~but~~ changes in  
30 wetland area and surface hydrology were ~~limited~~ ~~small~~ (Weber et al., 2010; Hopcroft et al., 2011). ~~These~~  
31 ~~authors~~ ~~They~~ instead suggested that changes in temperature and/or plant productivity affected CH<sub>4</sub> production  
32 during those events. ~~Rather,~~ ITCZ migration ~~does~~ appears to be related to ~~with~~ millennial- or sub-millennial  
33 scale CH<sub>4</sub> change, ~~however~~. Brook et al. (2000) found that sub-millennial-scale CH<sub>4</sub> minima during the last  
34 ~~deglacial-deglaciation~~ period correspond with reduced precipitation recorded in Cariaco Basin sediment data,  
35 which indicates southward displacement of ITCZ (Hughen et al., 1996). This hypothesis ~~It~~ is supported by  
36 spectral analysis of CH<sub>4</sub> during the past 800 ka record that found that ITCZ change becomes an important driver  
37 of millennial scale CH<sub>4</sub> change (Tzedakis et al., 2009; Guo et al., 2012).

38 ~~The ice core scientists started to apply high resolution CH<sub>4</sub> mixing ratio and stable isotope data to discern~~  
39 ~~governing mechanisms of Holocene CH<sub>4</sub> variation, but currently the high resolution records cover only a part of~~  
40 ~~the Holocene.~~ For the Holocene, ~~H~~high-resolution CH<sub>4</sub> records from Law Dome and West Antarctic Ice Sheet

1 (WAIS) Divide ice cores in (Antarctica) show characteristic variability ~~in-on~~ multi-decadal to centennial time  
2 scale during the late Holocene, ~~apart from long-term gradual increasing trend~~ (MacFarling-Meure et al., 2006;  
3 Mitchell et al., 2011). The high-resolution records ~~have been~~ ~~were~~ compared with various temperature- and  
4 precipitation proxies, but ~~the~~ previous works found no strong correlations that explain the observed decadal- to  
5 centennial scale variabilities. This may be because ~~Limitation was that~~ the late Holocene CH<sub>4</sub> budget ~~was may~~  
6 ~~have been~~ comprised of both natural and anthropogenic terms, making it difficult to distinguish between them.  
7 Mitchell et al. (2011) pointed out that some of the abrupt CH<sub>4</sub> decreases could have had anthropogenic causes.  
8 ~~resulted by historical events, such as Mongolian invasion, Plagues, or Spanish invasion.~~ Later, Mitchell et al.  
9 (2013) made simultaneous measurement of Antarctic (WAIS Divide) and Greenland (Greenland Ice Sheet  
10 Project 2; GISP2) ice cores to derive an IPD record, and extended their high-resolution records back to ~4 ka.  
11 They used eight-box atmospheric methane model (EBAMM) and anthropogenic- and natural emission scenarios  
12 to investigate CH<sub>4</sub> control factors. Their results showed that the late Holocene CH<sub>4</sub> evolution can be explained  
13 by a combination of natural- and anthropogenic emissions. ~~In the other hand~~ In principle, stable isotope ratios of  
14 CH<sub>4</sub> help us to distinguish the types of sources – biogenic, pyrogenic, and geologic. Sowers (2010)  
15 reconstructed the CH<sub>4</sub> mixing ratio and stable isotopic composition ~~e-ratio of CH<sub>4</sub>~~ ( $\delta^{13}\text{C-CH}_4$  and  $\delta\text{D-CH}_4$ )  
16 throughout the entire Holocene. ~~and~~ He suggested several possible control factors, such as boreal wetlands and  
17 thermokarst lakes, changing C<sub>3</sub>/C<sub>4</sub> plant ratio of CH<sub>4</sub>-emitting ecosystems, and changing composition of  
18 methanogenic communities. ~~However, but the temporal resolution of the data (~138 years in average during 7.0~~  
19 ~~–11.3 ka) was not sufficient to capture sub-millennial centennial scale variability. Currently there is no high-~~  
20 ~~resolution CH<sub>4</sub> isotope records covering the early Holocene. Former~~ Previous studies have shown the reduction  
21 of pyrogenic emission and increased agricultural emission during the last ~~millennia~~ millennium (Ferretti et al.,  
22 2005; Mischler et al., 2009). In later work using  $\delta^{13}\text{C-CH}_4$  records from North Greenland Eemian Ice Drilling  
23 (NEEM) ice core, Sapart et al. (2012) found that the centennial-scale variations during the last two millennia  
24 were caused by changes in pyrogenic- and biogenic emissions. Ruddiman et al. (2011) and Sapart et al. (2012)  
25 estimated CH<sub>4</sub> emission change due to anthropogenic land use changes, which shows a good agreement with the  
26 trends from ice core measurement ~~long-term CH<sub>4</sub> increasing trend.~~ However, ~~Since~~ there is no high-resolution  
27 reconstruction of past population and land use area, and consequently large uncertainties of CH<sub>4</sub> emission from  
28 land use change impede identification of any shorter scale changes.

29 The early Holocene is a suitable period to study natural CH<sub>4</sub> controls under Holocene interglacial climate  
30 condition. Since there was only negligible human population and relevant CH<sub>4</sub>-emitting anthropogenic activities  
31 (e.g., Goldewijk et al., 2010; Kaplan et al., 2011) during this time, the early Holocene CH<sub>4</sub> changes must have  
32 occurred mostly due to ~~the~~ natural causes. Understanding natural controls could contribute to better constraints  
33 on ~~the~~ human-induced CH<sub>4</sub> changes. However, high-resolution studies that covers the entirety ~~for the~~ early  
34 Holocene ~~have~~ ~~has~~ not been carried out extensively so far, except for ~~the~~ studies of the prominent cooling event  
35 at 8200 years BP (Spahni et al., 2003; Kobashi et al., 2007; Ahn et al., 2014). Despite Rhodes et al. (2015)  
36 reported a very high-resolution record from WAIS Divide ice core that extends from the last glacial period to  
37 the earliest Holocene (~9.8 ka), the authors do not deal with the early Holocene CH<sub>4</sub> variability. Earlier studies  
38 mainly focused on long-term change, attributing the major control to low latitude hydrology based on regional  
39 climate records that show wetter climate in tropics during the early Holocene (Blunier et al., 1995; Brook et al.,  
40 2000; Chappellaz et al., 1993, 1997). Therefore, in this study we present a new high-resolution CH<sub>4</sub> record from

1 ~~during the early Holocene and to investigate natural control mechanisms under interglacial condition. It should~~  
2 ~~be noted~~ that environmental ~~boundary~~ conditions ~~of the early Holocene~~ were not identical to those of the late  
3 Holocene. ~~The global sea level rose was rising throughout the early Holocene and there was still while~~  
4 ~~remnant ice sheets in the North America disappeared.~~ Detailed studies of CH<sub>4</sub> variability during the early  
5 Holocene period are limited, except for the prominent 8.2 ka event (Blunier et al., 1995; Brook et al., 1996;  
6 Spahni et al., 2003; Kobashi et al., 2007; Ahn et al., 2012), which is thought to be caused by abrupt fresh water  
7 input from Lakes Agassiz and Ojibway into the North Atlantic, and consequently changes in North Atlantic  
8 Deep Water (NADW) formation and meridional heat transfer (e.g., Alley and Agustsdottir, 2005). Otherwise,  
9 earlier studies mainly focused on the multi-millennial variability, attributing the major control for the Holocene  
10 CH<sub>4</sub> to low-latitude hydrology based on regional climate records that showed wet condition in tropical regions  
11 during the early Holocene (e.g., Blunier et al., 1995; Chappellaz et al., 1993, 1997; Brook et al., 2000). Climate  
12 simulation studies using the atmospheric chemistry and vegetation coupled models also confirm the previously  
13 suggested 'low-latitude control' hypothesis (Harder et al., 2007; Singarayer et al., 2011). Humans may also be  
14 an another important factor in the Holocene CH<sub>4</sub> budget. Ruddiman et al. (2008) proposed that an increase of  
15 agricultural activity (i.e. rice cultivation) was a major driver of the anomalous CH<sub>4</sub> rise after ~5 ka, based on  
16 radiocarbon dating of evidence for rice agriculture. This hypothesis was argued against later by Singarayer et al.  
17 (2011) who suggested that the insolation-induced monsoon intensification in southern hemisphere could explain  
18 the late Holocene CH<sub>4</sub> increase. On the other hand, Sowers (2010) attempted to disentangle the Holocene CH<sub>4</sub>  
19 change by taking advantage of stable isotope ratios of CH<sub>4</sub> (<sup>13</sup>C/<sup>12</sup>C and D/H) recovered from polar ice cores and  
20 suggested some possible control factors: northern emission from thermokarst lakes and wetlands, changing in  
21 C<sub>3</sub>/C<sub>4</sub> plant ratio of the CH<sub>4</sub>-emitting ecosystem, and composition of methanogenic communities. The temporal  
22 resolution of the data was not sufficient to understand the underlying mechanisms of sub-millennial scale CH<sub>4</sub>  
23 variability. Recently, emergence of high-resolution measurements permits us to study the CH<sub>4</sub> variability on  
24 multi-decadal to sub-millennial time scales, especially for the last 2000 years (Ferretti et al., 2005; MacFarling-  
25 Meure et al., 2006; Mitchell et al., 2011, 2013; Sapart et al., 2012; Rhodes et al., 2013). Mitchell et al. (2011)  
26 reported a new, decadal resolved CH<sub>4</sub> records for the last millennia from WAIS Divide, Antarctica. They  
27 tested the previous hypothesis by comparing proxies of temperature and precipitation of various regions, and  
28 found no strong correlation with CH<sub>4</sub>. Their approach was optimal for validating the hypothesis, but the  
29 limitation was that the late Holocene CH<sub>4</sub> budget may have been comprised of both natural and anthropogenic  
30 terms, making it difficult to distinguish between them. Considering together with Antarctic and Greenlandic  
31 CH<sub>4</sub> concentrations, deriving the inter-polar difference (IPD) of CH<sub>4</sub>, Mitchell et al. (2013) demonstrated that  
32 the late Holocene CH<sub>4</sub> evolution can be explained by a combined emission of natural and anthropogenic sources.  
33 Sapart et al. (2012) analysed CH<sub>4</sub> concentration simultaneously with <sup>13</sup>C/<sup>12</sup>C isotope ratio of CH<sub>4</sub> ( $\delta^{13}\text{C-CH}_4$ )  
34 using the ice core samples of North Greenland Eemian Ice Drilling (NEEM) and calculated isotopic mass  
35 balance to separate biogenic, pyrogenic and geologic emissions. Furthermore, Ruddiman et al. (2011) and  
36 Sapart et al. (2012) estimated CH<sub>4</sub> emission change due to anthropogenic land use changes, which shows a good  
37 agreement with long-term CH<sub>4</sub> increasing trend. However, there is no high-resolution reconstruction of past  
38 population and land use area, and consequently large uncertainties of CH<sub>4</sub> emission from land use change  
39 impede identification of any shorter scale changes.



1 In this paper, we present a new high-resolution CH<sub>4</sub> record during the early Holocene to study the natural  
2 control mechanisms under interglacial conditions. Since there was only negligible human population and  
3 relevant CH<sub>4</sub>-emitting anthropogenic activities (e.g., Goldewijk et al., 2010; Kaplan et al., 2011) during this  
4 time, the early Holocene CH<sub>4</sub> changes must have occurred mostly due to the natural causes. We note that  
5 environmental conditions were not identical to those of the late Holocene, given that the global sea level rise  
6 continued throughout the early Holocene as the last sections of the northern hemisphere glacial ice sheets melted.

## 7 2 Materials and Methods

8 In this study we used ice samples from ~~a~~ the Siple Dome deep ice core (SDMA) drilled from 1997 to 1999 on  
9 the Siple Coast, West Antarctica (81.65°S, 148.81°W; 621 m elevation) (Taylor et al., 2004). The SDMA  
10 samples were collected and cut at National Ice Core Laboratory (NICL, Denver, Colorado, USA) from January  
11 to February of 2013. ~~Since~~ The brittle zone of SDMA ice starts below 400 m ~~depth~~ and continues to the bottom  
12 of the core at 1004 m (Gow and Meese, 2007) and samples from this region are more likely to be fractured. ~~that~~  
13 ~~makes some part of ices fractured and/or cracked internally.~~ Hence, the samples were carefully collected from  
14 unbroken subsections ~~ices~~ during the sample preparation at NICL. The samples were packed in  
15 ~~insulated isothermal~~ foam boxes with numerous eutectic gels, and shipped to South Korea via expedited  
16 ~~airfreight. Temperature loggers were enclosed within the isothermal boxes to record the temperature change~~  
17 ~~inside during the shipping, and it showed the temperatures were maintained below -25°C. The boxes were~~  
18 ~~picked up directly just after custom clearance at the airport and then the ice samples were stored in a walk-in~~  
19 ~~freezer at Seoul National University (SNU, Seoul, South Korea) that was maintained below -20°C. We~~  
20 ~~measured 295 individual ice samples from 156 depth intervals from 518.87 to 718.83 m, covering from 8.36 to~~  
21 ~~20.25 ka after synchronizing to the Greenland Ice Core Chronology 2005 (GICC05, Rasmussen et al., 2006), of~~  
22 ~~which 256 ice samples from 120 depth intervals from 518.87 to 623.38 m are used in this study. All samples~~  
23 ~~were duplicated, so that our final CH<sub>4</sub> data were presented by averaging the results of duplicate analysis from~~  
24 ~~the same depth. and the~~ The analytical uncertainty of our data set is estimated by the uncertainty of individual  
25 ice measurement divided by square root of 2 (see below). ~~standard error of the mean of duplicate pairs.~~ We  
26 rejected data that show difference between duplicate measurements larger than 10 ppb, and 9 data points were  
27 rejected in the studied period. The results of SNU measurement (111 points) are plotted in Figure 1. The 16  
28 samples from 8 depths were used for reproducibility check on different days (Table 1). ~~We measured a total of~~  
29 ~~295 samples on 143 depth intervals from 518.87 to 623.38 m, of Siple Dome ice core, West Antarctica. Siple~~  
30 ~~Dome ice samples were cut and packed in insulated boxes and with eutectic gel packs at National Ice Core~~  
31 ~~Laboratory (NICL), and shipped to Seoul National University (SNU) via expedited air freight. Automated~~  
32 ~~temperature loggers were enclosed in the boxes to check the temperature during the shipping. The temperatures~~  
33 ~~within the boxes were kept below -20 °C and the ice samples were preserved in SNU cold storage maintained~~  
34 ~~below -20 °C. The basic principles of gas extraction and CH<sub>4</sub> analysis are described in Yang et al. (in~~  
35 ~~preparation). Briefly, the ice samples were cut by a clean band saw and trimmed outermost 2 mm to remove~~  
36 ~~possible dissolution of modern ambient atmosphere. In case of cracks, the sample was trimmed along the~~  
37 ~~fractures. The typical sample size is ~2.5 × 2.5 × 10 cm and the weight varies from 35 to 55 g depending on~~  
38 ~~sample availability.~~ The air occluded in ice was extracted by a melting and refreeze process under vacuum. Ice

1 samples were prepared in a walk-in freezer in the morning of each experiment day, and trimmed the outermost  
2 >2 mm was trimmed off to eliminate potential contamination by ambient air during the storage. Then the  
3 samples were then moved to the laboratory and placed in glass sample containers. The sample flasks/containers  
4 (sample flask hereafter) were custom-made glass flasks welded to stainless steel flanges, and attached to the  
5 vacuum line with a copper gaskets. Each day we normally analysed 3 samples in duplicate and four blank  
6 samples (bubble free ice made in the laboratory, with standard air added to the sample flask prior to air  
7 extraction). The sample flasks were partially submerged into a chilled ethanol bath while being attached to the  
8 vacuum line. during ice insert and attaching to the line for preventing temperature increase by laboratory air.  
9 After that all flasks were evacuated for at least 40 minutes, then the ice samples were melted by submerging  
10 the sample flasks in a warm water bath. Melting process was usually completed within 30 minutes. The sample  
11 flasks were then submerged in the cold ethanol bath chilled to around -82°C for more than an hour to refreeze.  
12 During the refreezing, we carried out GC pre-running (20 injections) and daily calibration of the gas  
13 chromatograph system, that normally took taking ~90 minutes. The ethanol temperature normally rose up to -  
14 55°C just after submerging the flasks, and it was chilled to below recovered to -65°C before expansion of the air  
15 in the flasks. The extracted air in the headspace was expanded into the evacuated vacuum line and sample loop  
16 of a gas chromatograph (GC) equipped with a flame ionization detector (FID) to measure CH<sub>4</sub> mixing ratio.  
17 After detecting the CH<sub>4</sub> peak in the GC chromatogram (retention time of ~1.6 minutes), the vacuum line and  
18 sample loop is evacuated again prior to the next injection. The GC linearity was tested by a series of inter-tank  
19 calibration using four working standard air cylinders (395.5, 721.3, 895.0, and 1384.9 ppb CH<sub>4</sub> in-on NOAA04  
20 scale, Dlugokencky et al., 2005). A daily GC calibration curve was determined by measurements of a working  
21 standard having the closest CH<sub>4</sub> mixing ratio of expected value from the samples; in this study, we used the  
22 721.3 ppb CH<sub>4</sub> standard for samples of the early Holocene. To account for system condition change throughout  
23 experiments (i.e., influence by water vapor), we calibrated with a standard air six times before and after  
24 sample measurements. The detailed configuration of the vacuum line and GC is described in another paper  
25 (Yang et al., in preparation).

26 Different solubilities solubility of each air component cause preferential dissolution during melting procedure.  
27 gas species cause preferential dissolution of a gas having higher solubility than others, and consequently it  
28 makes the mixing ratio of extracted air different from that trapped originally within the ice (solubility effect hear  
29 after). As the solubility of CH<sub>4</sub> is higher than the other major components of air – nitrogen (N<sub>2</sub>), oxygen (O<sub>2</sub>),  
30 Argon (Ar), the solubility effect lowers the CH<sub>4</sub> mole fraction of the extracted air is lower than originally  
31 enclosed air (solubility effect), and needs to be corrected properly. The CH<sub>4</sub> mole fraction of air enclosed in ice  
32 sample is estimated from residual gas fraction and CH<sub>4</sub> mixing ratio in air remained in refrozen meltwater  
33 (retrapped air). Residual gas fraction is a measure of how much air is retrapped during refreeze, which is defined  
34 as ratio of amount (pressure) of air extracted from the 2<sup>nd</sup> gas extraction to the 1<sup>st</sup> extraction. The 2<sup>nd</sup> gas  
35 extraction was carried out using leftover refrozen meltwater samples after the 1<sup>st</sup> extraction finished. Mean  
36 residual gas fraction is  $1.05 \pm 0.13\%$  ( $1\sigma$ ,  $n=60$ ) for SDMA ice samples and  $0.38 \pm 0.08\%$  ( $1\sigma$ ,  $n=40$ ) for  
37 bubble-free ice. The test with ice samples from Styx glacier, Antarctica revealed that CH<sub>4</sub> mixing ratio in  
38 retrapped air is enriched 3.1 times ( $n=12$ ) for glacial ice and 3.0 times ( $n=7$ ) for bubble-free ice. Then the  
39 solubility effect is corrected by using a simple mass balance calculation. Air was extracted by a traditional melt-  
40 refreeze technique, and the extracted air was expanded to gas chromatograph (GC), where CH<sub>4</sub> was separated

1 ~~and measured by a flame ionization detector (FID). The GC was calibrated daily with a standard air of 721.31~~  
2 ~~ppb CH<sub>4</sub> on the NOAA04 scale (Dlugokencky et al., 2005). The blank measurements of four bubble free blank~~  
3 ~~ice samples show a daily offset of 5–15 ppb, which is subtracted from all measurements. Preferential dissolution~~  
4 ~~of CH<sub>4</sub> into meltwater (gas solubility effect) was corrected by Henry's law, assuming that the equilibrium state~~  
5 ~~was accomplished within the sample container being a closed system. To estimate our daily blank offset, we~~  
6 ~~used four bubble free blank ices every day, instead of interpolating between days of blank analysis (Mitchell et~~  
7 ~~al., 2011).~~

8 Daily systematic offset correction was applied to account for the daily-varying system condition. To do this,  
9 we measured four bubble-free ice samples every day with SDMA ice samples. The experimental procedures for  
10 the bubble-free ice were identical to the SDMA ice. After the sample flasks are evacuated, standard air is  
11 injected into the flasks containing bubble-free ice, so that it returns similar air pressure to the typical size of  
12 SDMA ice when the extracted air inside the bubble-free ice flasks is expanded into the sample loop. The  
13 solubility correction for the bubble-free ice was done by the same formula as SDMA ice samples, but using  
14 different residual gas fraction. After corrected for solubility effect, the daily systematic offset is calculated by  
15 difference between CH<sub>4</sub> mixing ratio of the injected standard air and results from the four flasks containing  
16 bubble-free ice. The systematic offset ranges from 5 to 15 ppb during the SDMA measurement period. A daily  
17 offset is subtracted from the ice samples corrected for gas solubility effect. This is one of the major differences  
18 with OSU wet extraction system, where the systematic offset is interpolated from the results of blank tests  
19 carried out between several days (Mitchell et al., 2011).

20 The bubble-free ~~blank~~ ice was made by chilling the degassed ultrapure water (resistivity >18.2 MΩ·cm at  
21 25°C) slowly from the bottom in a closed stainless steel chamber. From gas extraction test using our bubble-free  
22 ice without injecting standard air, we observed that no significant pressure increase at the pressure gauge with a  
23 detection limit of 0.01 Torr (corresponding to less than 0.03% of sample air pressure in the extraction line) after  
24 melting-refreezing the bubble-free ice. The daily blank offset is calculated from the mean of the four blank  
25 results ranging from 5 to 15 ppb, and it reflects any daily offsets by contaminants, leaks, and any different GC  
26 conditions, instead of interpolating between days of blank analysis (Mitchell et al., 2011). The exact cause of this  
27 blank offset is currently not clear, but the four blank results agree well each other, yielding the intra day  
28 standard error of the mean of  $2.0 \pm 1.0$  ppb. This 'intra day' blank offset is much smaller than the 'inter day'  
29 offset, which implies that conditions of each sample flask are rather constant within a day, and vary  
30 systematically day by day. Since every single data point is obtained by analysis of at least in duplicate, the intra  
31 day blank offset for one depth is reduced by a factor of  $\sqrt{2}$ . This implies that offset among the flasks is not  
32 stochastic, and caused by daily systematic condition drift. The robustness of our final results was proven by re  
33 analysis of eight duplicates at adjacent depths (< 10 cm) 8 to 80 days after the first analysis. The difference of  
34 the mean of duplicates between the time intervals was 1.9 ppb on average (pooled standard deviation of 1.4 ppb).  
35 The good reproducibility of our results demonstrates that our blank correction method is reliable. The exact  
36 mechanism that draws good reproducibility is currently unknown, but it seems that the replicate measurements  
37 do not follow exactly the normal (Gaussian) distribution. Similar results were obtained from the measurements  
38 of different ice cores (see Supplement).

39 Mass dependent (gravitational) fractionation within the firn layer (Craig et al., 1988; Schwander, 1989) was  
40 corrected by ~~Our data were corrected for mass dependent (gravitational) fractionation by diffusion within the~~

1 ~~firm layer (Craig et al., 1988; Schwander, 1989). The gravitational fractionation effect was corrected using the~~  
2 ~~nitrogen isotope ratio ( $\delta^{15}\text{N}$ ) of atmospheric nitrogen ( $\text{N}_2$ ) occluded in bubbles. Siple Dome  $\delta^{15}\text{N}$  records show a~~  
3 ~~mean enrichment of  $0.23 \pm 0.01\%$  during the early Holocene (Severinghaus et al., 2009) and result in a slight~~  
4 ~~decrease of  $\text{CH}_4$  by  $1.97 \pm 0.15$  ppb, which we applied to all of our measurements.~~

5 ~~At the early stage of method development, we derive theoretically the solubility effect by using Henry's Law~~  
6 ~~in a closed and chemically equilibrated condition. After applying this theoretical solubility correction, we~~  
7 ~~observed that SDMA  $\text{CH}_4$  data measured at SNU are lower than SDMA  $\text{CH}_4$  records from OSU by  $\sim 3$  ppb in~~  
8 ~~average. Hence, we compared the theoretical solubility correction with that obtained empirically from the~~  
9 ~~second gas extraction (following the method described in Mitchell et al., 2011) and found that a correction~~  
10 ~~factor of 1.0058 from the theoretically to empirically driven solubility effect.~~

11 ~~Here we consider two types of uncertainty sources: uncertainty in (1) estimating daily systematic offset and (2)~~  
12 ~~other causes. The former indicates uncertainty of the daily systematic offset ( $e1$ ). As the daily systematic offset~~  
13 ~~is calculated from the mean of the four flasks with bubble-free ice and standard air, scattering of the bubble-free~~  
14 ~~ice samples can induce uncertainty in the systematic offset correction. The daily  $e1$  is estimated with standard~~  
15 ~~error of the mean (SEM,  $n = 4$ ), because the daily systematic offset is calculated from the mean of the four~~  
16 ~~bubble-free ice samples. The average of daily  $e1$  is 1.9 ppb. The latter ( $e2$ ) includes uncertainty due to solubility~~  
17 ~~correction and inhomogeneous distribution of  $\text{CH}_4$ . Given our solubility correction uses the mean value of~~  
18 ~~residual gas fraction and the ratio at which  $\text{CH}_4$  enriches in retrapped air, different solubility effect and/or~~  
19 ~~inhomogeneous  $\text{CH}_4$  distribution in individual ice causes offset between adjacent duplicate ice samples analysed~~  
20 ~~on the same day. As the duplicates from same depths were measured on the same day, we estimated the  $e2$  with~~  
21 ~~pooled standard deviation (PSD) between duplicate measurements from entire depths, which yields 3.3 ppb.~~  
22 ~~Taking the  $e1$  and  $e2$  into account together, the final uncertainty of individual measurement is given as 3.8 ppb~~  
23 ~~by error propagation. The uncertainty for the mean of duplicate results is obtained by dividing the individual~~  
24 ~~uncertainty by square root of 2, yielding 2.7 ppb. Further details on the correction method will be discussed in~~  
25 ~~found in our manuscript in preparation (Yang et al., in preparation). The exact cause of this blank offset is~~  
26 ~~currently not clear, but the four blank results agree well each other, yielding the intra-day standard error of the~~  
27 ~~mean of  $2.0 \pm 1.0$  ppb. This 'intra-day' blank offset is much smaller than the 'inter-day' offset, which implies~~  
28 ~~that conditions of each sample flask are rather constant within a day, and vary systematically day by day. Since~~  
29 ~~every single data point is obtained by analysis of at least in duplicate, the intra-day blank offset for one depth is~~  
30 ~~reduced by a factor of  $\sqrt{2}$ . This implies that offset among the flasks is not stochastic, and caused by daily~~  
31 ~~systematic condition drift. The robustness of our final results was proven by re-analysis of eight duplicates at~~  
32 ~~adjacent depths ( $< 10$  cm) 8 to 80 days after the first analysis. The difference of the mean of duplicates between~~  
33 ~~the time intervals was 1.9 ppb on average (pooled standard deviation of 1.4 ppb). The good reproducibility of~~  
34 ~~our results demonstrates that our blank correction method is reliable. The exact mechanism that draws good~~  
35 ~~reproducibility is currently unknown, but it seems that the replicate measurements do not follow exactly the~~  
36 ~~normal (Gaussian) distribution. Similar results were obtained from the measurements of different ice cores (see~~  
37 ~~Supplement).~~

38 ~~We made additional measurements using adjacent samples (depth difference of 10 cm) at randomly selected 8~~  
39 ~~depth intervals to examine reproducibility and long-term stability of our system. The second measurements of~~  
40 ~~duplicates were performed 8 to 80 days after the first analysis. Table 1 displays quadruplicate results at each~~

1 depth. PSD between the mean of duplicate analyses of the first and second measurements on different days  
2 yields 1.1 ppb. The good agreement between duplicate means indicates good reproducibility of our system. In  
3 the meanwhile, PSD of the quadruplicate measurements is 3.0 ppb, which is similar to PSD of duplicate samples  
4 for the entire data set (3.3 ppb). Duplicate measurements for 8 depths show  $\pm 1.0$  ppb precision (1-sigma; pooled  
5 standard deviation).

6 To check reliability of the record we compared our data set with previous SDMA measurements carried out at  
7 Oregon State University (OSU) for 8.4 to 9.1 ka period when the two records are overlapped. using the same ice  
8 core. The OSU CH<sub>4</sub> record was measured with a temporal resolution of 8 years with precision of  $\pm 2.8$  ppb  
9 (Mitchell et al., 2011; Ahn et al., 2014). Resulting The averagemean offset between the two data sets is 0.1-0.6  
10 ppb, which lies within analytical uncertainty range of data sets. both institutes. Therefore, we created a  
11 composite record by using the OSU data for 499.49 – 537.20 m interval (7.6 to 9.0 ka) because mean temporal  
12 resolution of OSU data (~22 years) is lower than SNU data (~37 years) during this period (Fig. 1). merge the two  
13 records to make the SDMA CH<sub>4</sub> composite data. Fig. 1 presents the SDMA data points during the early  
14 Holocene period (119 depths, 518.87 – 623.38 m). Our new SDMA Siple Dome CH<sub>4</sub> composite data have mean  
15 temporal resolution of ~26 years. The WAIS Divide continuous CH<sub>4</sub> records show much higher resolution (~2  
16 years), but does not cover the entire early Holocene period (Rhodes et al., 2015). is the currently third highest  
17 temporal resolution of Antarctic CH<sub>4</sub> records record is the one of the high resolution data set covering the early  
18 Holocene after the WAIS Divide continuous (~2 years, Rhodes et al., 2015) and discrete (~20 years, WAIS  
19 Divide members, 2015) records. from 11.6 to 8.5 ka, apart from the WAIS Divide records (Rhodes et al., 2015;  
20 WAIS Divide members, 2015).

### 3. Result and Discussion

#### 3.1 Millennial scale variability

~~To extract millennial scale variability, w~~We carried out spectral analysis of SDMA composite record using the REDFIT program (Schulze and Mudelsee, 2002). ~~Ma~~nd moderate (over 90% significance level) ~~powers~~ spectral power was ~~were~~ found at ~1340, 401, 309, and 96-year periods. Given the ~42 years of gas age distribution of SDMA (Ahn et al., 2014), it would not be reliable to study centennial scale variability. Therefore, ~~we~~ ~~Thus we produced annual da~~smoothed the data by a 250-year running average to remove centennial- to multi-centennial scale components and then detrended by a high-pass filter with a cut off period of 1800 years to isolate millennial scale variability. ~~by interpolation and then calculated 250 year running means to smooth high frequency components having shorter period than 309 year. Then t~~The smoothed time series was then filtered with a high pass window (cut off period of 1800 years). We applied a 250 year running average and high pass filter (cut off period of 1800 years) to Siple Dome CH<sub>4</sub> composite to study millennial scale variability throughout the early Holocene. For comparison, the same signal-processing scheme was applied to WAIS Divide time series and we observed that Siple Dome and WAIS Divide CH<sub>4</sub> anomalies share similar millennial scale variability, confirming the reliability of both our data and observed millennial scale changes (Fig. 2).

##### 3.1.1 Low latitude hydrology

The high-pass filtered CH<sub>4</sub> time series anomalies demonstrate millennial scale minima at ~8.2, 9.3, 10.2 and 10.9 ka, which occurred ~~withi~~n nearly 1000-year spacing. The REDFIT results for 7.6 to 11.2 ka interval that excludes PBO shows moderate (80% significance level) powers at ~731 and 430 (860)-year periods. Each minimum ~~was~~ accompanied by depletion of water stable isotope ratio ( $\delta^{18}\text{O}_{\text{ice}}$ ) from North Greenland Ice Core Project (NGRIP) ice core, which implies climate cooling in Greenland. A close relationship between CH<sub>4</sub> and Greenland  $\delta^{18}\text{O}_{\text{ice}}$  has been previously reported in glacial-interglacial cycles and Dansgaard-Oeschger (DO) events during the last glacial period (e.g., Brook et al., 1996, 2000; Blunier and Brook, 2001; Chappellaz et al., 1993, 2013; EPICA Community Members, 2006). However, it has not been confirmed ~~fora~~t interglacial climate conditions during the Holocene. Mitchell et al. (2011) found no significant correlation with Greenland climate in multi-decadal scale during the late pre-industrial Holocene (LPIH), possibly because LPIH CH<sub>4</sub> budget is also affected substantially by anthropogenic emissions (e.g., Ferretti et al., 2005; Mischler et al., 2009; Mitchell et al., 2013; Sapart et al., 2012). In contrast, we observe a ~~moderate~~significant positive correlation ( $r = 0.57-0.66$ ,  $p \equiv 0.06-0.0013$ ) between the millennial-scale change of Siple Dome CH<sub>4</sub> and NGRIP  $\delta^{18}\text{O}_{\text{ice}}$  during the early Holocene, ~~which~~. The correlation coefficient between the smoothed- and filtered time series of SDMA CH<sub>4</sub> (before synchronization to GICC05) and NGRIP  $\delta^{18}\text{O}_{\text{ice}}$  was calculated for the 7.8 - 11.5 ka by interpolating to the original ages of SDMA CH<sub>4</sub> composite, with a reduced degree of freedom.

The gas chronology of SDMA was developed based on CH<sub>4</sub> and  $\delta^{18}\text{O}$  of air ( $\delta^{18}\text{O}_{\text{atm}}$ ) correlation (Severinghaus et al., 2009). In this study, we improved the chronology by synchronization of the previous chronology to The gas age scale, which was previously constrained (Brook et al., 2005), The previous SDMA gas chronology (Brook et al., 2005; Severinghaus et al., 2009) was synchronized to the Greenland Ice Core Chronology 2005 (GICC05) GICC05 age scale by setting 3 age tie-points with stable water isotope ( $\delta^{18}\text{O}$ )

1 record from the North Greenland Ice Core Project (NGRIP) ice cores during the abrupt climate change events of  
2 the Preboreal Oscillation (PBO) and the 8.2 ka event, given that both events have been proved to be  
3 synchronous with CH<sub>4</sub> change (Kobashi et al., 2007, 2008). Ages between tie-points were inferred by linear  
4 interpolation of the age offset of nearest tie-points. ~~The synchronization between the tie points was done by~~  
5 ~~linear interpolation of age differences between the synchronized and the previous ones,~~ which range from -114  
6 to 28 years. After synchronizing to the GICC05 scale, the correlation coefficient between SDMA CH<sub>4</sub>  
7 composite and the NGRIP  $\delta^{18}\text{O}_{\text{ice}}$  increases to  $r = 0.74$  ( $p < 0.01$ ). It implies that natural CH<sub>4</sub> budget is closely  
8 connected with Greenland climate on millennial timescales, even though this conclusion is less robust as there is  
9 no age tie-points between the 8.2 ka episode and PBO (Fig. S1 3), the Preboreal oscillation. (Fig. S1). The  
10 positive correlation implies that the natural CH<sub>4</sub> budget is connected with Greenland climate on millennial  
11 timescales.

12 The uncertainty of the modified chronology was examined by comparing with a tentative age scale  
13 determined by CH<sub>4</sub> correlation with NEEM CH<sub>4</sub> discrete measurement data. NEEM CH<sub>4</sub> data follow  
14 GICC05modelext-NEEM-1 scale (Rasmussen et al., 2013). The detailed method for CH<sub>4</sub> correlation is  
15 described in Section 3.2. The age difference between the two chronologies is plotted in Figure 4, showing the  
16 maximum age difference of 105 years. In addition, we include the maximum layer counting uncertainty of 99  
17 years (Rasmussen et al., 2006) and delta-age uncertainty of 30 years (Rasmussen et al., 2013) during the early  
18 Holocene. Therefore, error propagation of the above three errors indicate that the maximum error of SDMA gas  
19 age used in this study is ~147 years.

20 According to atmospheric modelling studies, abrupt cooling in the North Atlantic regions can alter  
21 atmospheric circulation and to cause southward migration of the mean latitudinal position of the ~~Intertropical~~  
22 ~~Convergence Zone (ITCZ)~~ (e.g., Chiang and Bitz, 2005; Broccoli et al., 2006; Cvijanovic and Chiang, 2012).  
23 Climate proxies demonstrate the climatic teleconnection between northern North Atlantic and low latitude  
24 regions. ~~The climatic teleconnection between northern North Atlantic and low latitude regions is shown by~~  
25 ~~climate proxies. The southward displacement of ITCZ leads further weakening of Asian and Indian summer~~  
26 ~~monsoons and probably reduces CH<sub>4</sub> emission from northern tropical wetlands.~~ Sediment reflectance record  
27 from Cariaco Basin shows increased rainfall and humidity – which is due to southward displacement of ITCZ –  
28 corresponding to the 8.2, 9.3, and 10.9 ka abrupt cooling event, ~~each abrupt cooling event,~~ as revealed in  
29 previous studies for the different time periods (Peterson et al., 2000; Haug et al., 2001; Fleitmann et al., 2007;  
30 Deplazes et al., 2013). The southward displacement of the ITCZ leads further weakening of Asian and Indian  
31 summer monsoons and probably reduces CH<sub>4</sub> emission from northern tropical wetlands. ~~Moreover, The~~ <sup>18</sup>O  
32 enrichments in ~~of~~ speleothems from ~~in~~ Dongge Cave (China), Qunf Cave (Oman), and Hoti Cave (Oman, not  
33 shown, Neff et al., 2001) ~~Asian (Dongge) and Indian (Hoti and Qunf) cave stalagmites~~ occurred at similar  
34 timing with abrupt cooling in Greenland at 8.2, 9.3, and 10.9 ka, which indicates s the reduction of monsoonal  
35 rainfall in ~~at~~ northern tropical wetlands. The speleothem records from Chinese and Oman caves seem to lag by  
36 ~100 – 200 years after the CH<sub>4</sub> change at ~9.3 ka, but this lies within chronological uncertainties of ~200 – 400  
37 years at around ~9.0 ka (Dykoski et al., 2005; Fleitmann et al., 2007). Moreover, sediment Ba/Ca ratio from  
38 Gulf of Guinea demonstrates concurrent decrease of West African monsoon (Weldeab et al., 2007). ~~The record~~  
39 ~~indicates that precipitation over the major wetland area was reduced and in turn it would lower the wetland CH<sub>4</sub>~~

1 ~~emissions in NH. In contrast~~the meanwhile, an inverse relationship is observed from the Eastern Brazilian  
2 speleothem data (Lapa Grande Cave, Strikis et al., 2011) that ~~demonstrates~~suggest an ~~the~~ increase in ~~of~~  
3 precipitation at the time of abrupt CH<sub>4</sub> decreases. ~~occurred as a result of southward migration of ITCZ.~~ Rhodes  
4 et al. (2015) pointed out that strong southward migration of the ITCZ could induce an abrupt CH<sub>4</sub> increase from  
5 southern hemisphere (SH) during the HS 1, 2, 4, and 5 events. Sperlich et al. (2015) also ~~suggested~~found that a  
6 sharp CH<sub>4</sub> peak at Greenland Interstadial 21.2 (~85 ka) was ~~caused~~occurred by emission from Asian and  
7 Amazon ~~South American~~ wetlands. However, considering the orbital parameters that indicate maximum  
8 summer insolation in NH while minimum in SH during the early Holocene, it can be inferred that contribution  
9 of SH wetland emission was relatively weak and overcompensated by reduction of NH emission.

10 The possibility that the observed CH<sub>4</sub> minima were caused by reduction of northern extra-tropical sources is  
11 not supported by previous modelling ~~studies~~study. Zürcher et al. (2013) found that abrupt cooling in Greenland  
12 and northern high latitudes by large freshwater input to the North Atlantic causes boreal peatland CH<sub>4</sub> emission  
13 to decrease substantially, which can ~~explain~~explains ~23% of abrupt CH<sub>4</sub> decrease (~80 ppb) during the 8.2 ka  
14 event. ~~If we assume linear scaling of the model response, it implies that boreal peatland source change only~~  
15 ~~accounts for ~23% of total CH<sub>4</sub> change during the rest of CH<sub>4</sub> decrease events.~~ Given the meltwater pulses  
16 during the early Holocene before the 8.2 ka event ~~are~~were probably much weaker ~~more than 10 times weaker~~  
17 (Teller and Leverington, 2004) than that corresponding to the 8.2 ka event, ~~we consider~~we suggest that  
18 boreal emission change is not the major cause of the CH<sub>4</sub> local minima.

19 Previously, Björck et al. (2001) found ~~that~~the climate cooling in the northern Atlantic and Santa Barbara  
20 Basin occurred ~~associated with a change in~~with solar-forcing ~~change~~ at ~10.3 ka. However, ~~in the proxy data,~~  
21 ~~there is~~ the proxy data in Figure 2 show no clear indication of southward migration of ~~the~~ ITCZ ~~position~~ and  
22 ~~reduction of~~ changes in Asian, Indian, African, and South American summer monsoon intensity ~~corresponding~~  
23 ~~associated with~~ to the ~10.2 ka cooling and CH<sub>4</sub> decrease. (Fig. 2b-f). ~~Furthermore,~~ Moreover, speleothem  $\delta^{18}\text{O}$   
24 records from Mawmluh Cave (not shown) show no weakening of the Indian monsoon (Berkelhammer et al.,  
25 2012), and there was no distinct change in  $\Delta_{\text{ELAND}}$  at that time, a proxy of global terrestrial respiratory  
26 fractionation of atmospheric O<sub>2</sub> at this time, which is affected by low latitude surface hydrology (Severinghaus  
27 et al., 2009). These evidences suggest that ~~This paleoproxy record suggests that changes in precipitation and~~  
28 ~~surface hydrology in the northern tropics may have not changed significantly during around the 10.2 ka.~~ Instead,  
29 there are two small decreases at ~9.9 and ~10.6 ka ~~as shown in Dongge cave deposit record (Fig. 2d).~~, but it is  
30 ~~difficult to tell, given dating uncertainties, if these events correlate with the 10.2 ka cooling.~~ These episodes are  
31 ~~not likely associated with the CH<sub>4</sub> minimum at 10.2 ka because the timing differences between the CH<sub>4</sub>~~  
32 ~~minimum and reductions of Asian summer monsoon intensity are beyond the chronological uncertainty.~~ The age  
33 uncertainty of Dongge Cave deposits is  $\pm 77$  years (2-sigma error; Dykoski et al., 2005), and that the 2-sigma  
34 estimated error of SDMA CH<sub>4</sub> gas age scale in this study is estimated to be ~147 years, less than ~150 years  
35 (see Supplement and see above S3), the Siple Dome age uncertainty is likely less than ~100 years (see above and  
36 Fig. S1). ~~The climate teleconnection between North Atlantic and tropical hydrology at 10.2 ka might not have~~  
37 ~~been~~ was not sufficiently strong enough to change the low latitude climate. Weak cooling around the North  
38 Atlantic region can be a candidate, given that NGRIP  $\delta^{18}\text{O}_{\text{ice}}$  records demonstrate smaller amplitude negative  
39 anomaly during ~10.2 ka event than those of 8.2 and 9.3 ka, but this ~~The amplitude of  $\delta^{18}\text{O}_{\text{ice}}$  changes at 10.2~~  
40 ~~ka of the high pass filtered GRIP and GISP2 records does show smaller variability than those at 8.2 and 9.3 ka~~



1 ~~cooling events, but larger than the variability at 10.9 ka (Fig. 5S2). Hence, the “weak cooling” speculation is not~~  
2 ~~fully supported by the other Greenland ice core records. However, this is not supported by other Greenland ice~~  
3 ~~core records such as Greenland Ice Core Project (GRIP) and Greenland Ice Sheet Project 2 (GISP2), because~~  
4 ~~the high pass filtered GRIP and GISP2  $\delta^{18}\text{O}_{\text{ice}}$  records show even smaller variability at ~10.9 ka (Fig. S2).~~  
5 Although there appears to have been no strong change in low latitude hydrology at 10.2 ka, the amplitude of  
6  $\text{CH}_4$  decrease at 10.2 ka is similar order to the other millennial events. ~~Given that no clear reduction weak~~  
7 ~~reduction of the Asian, Indian, and African monsoon intensity is observed, This it is possible that may imply the~~  
8  ~~$\text{CH}_4$  reduction decrease at 10.2 ka was controlled by other processes, outside of the northern tropics, than the~~  
9 ~~monsoon circulation change, the Asian monsoon intensity change. If the climate proxy from Dongge cave~~  
10 ~~reflects rather regional climate changes, monsoonal rainfalls and surface hydrology of other regions could be~~  
11 ~~responsible for  $\text{CH}_4$  decrease. The speleothem  $\delta^{18}\text{O}$  records from Mawmluh Cave show no weakening of the~~  
12 ~~Indian monsoon (Berkelhammer et al., 2012), moreover, there was no distinct change in  $\Delta_{\text{GLAND}}$ , a proxy of~~  
13 ~~global terrestrial respiratory fractionation of atmospheric oxygen, which is affected by low latitude surface~~  
14 ~~hydrology (Severinghaus et al., 2009). This paleo proxy record suggests that changes in precipitation and~~  
15 ~~surface hydrology in the northern tropics may have not changed significantly during around the 10.2 ka.~~

### 16 **3.1.2 External forcing**

17 ~~There should be an ultimate cause of the  $\text{CH}_4$  and climate change in the early Holocene. Previous studies~~  
18 ~~works have suggested an important role of solar forcing during the Holocene (e.g., Björck et al., 2001; Bond et~~  
19 ~~al., 1997, 2001). Bond et al. (1997) reported four large ice-rafted debris (IRD) drifts occurred at ~8.1, 9.4, 10.3~~  
20 ~~and 11.1 ka caused by surface cooling of North Atlantic Ocean. They found that the ocean surface cooling and~~  
21 ~~the IRD events are closely related to cooling over the Greenland. Figure 2 shows that each IRD event (maxima~~  
22 ~~in hematite stained grain) occurred concurrently with minima of NGRIP  $\delta^{18}\text{O}_{\text{ice}}$  record within age uncertainty.~~  
23 ~~We postulate that Then the Greenland cooling leads to southward shift of the ITCZ and in turn it changes~~  
24 ~~wetland  $\text{CH}_4$  emission in low latitudes. Bond et al. (2001) found that IRD maxima during the Holocene coincide~~  
25 ~~with solar activity minima. The authors and suggested that solar forcing could affect the climate change around~~  
26 ~~the North Atlantic Ocean (and Greenland), through amplification by changes in sea ice and/or deep water~~  
27 ~~formation. A close interplay between solar activity and monsoon intensity is confirmed by has been observed in~~  
28 ~~previous studies using the Chinese and Oman speleothem records during the Holocene (Neff et al., 2001; Wang~~  
29 ~~et al., 2005; Gupta et al., 2005), even on multi-decadal time scales (Agnihotri et al., 2002). However, the forcing~~  
30 ~~mechanism of solar activity on the North Atlantic and global climate is not well understood. Jiang et al. (2015)~~  
31 ~~found positive correlations between North Atlantic SST and solar forcings inferred from paleo-proxies ( $^{14}\text{C}$  and~~  
32  ~~$^{10}\text{Be}$ ) for the last 4000 years, while although the correlation disappears during the mid- and early Holocene.~~  
33 ~~They hypothesized that climate sensitivity to solar forcing is high for cooler climate. As evidenced above, The~~  
34 ~~above evidence suggests that the early Holocene  $\text{CH}_4$  minima may be linked to anomalies in were likely~~  
35 ~~triggered by anomalous low solar activity, but future study is needed to make it more conclusive.~~

36 Figure 2(a) shows a possible cause of the observed millennial scale climatic changes and abrupt cooling  
37 recorded in Greenland ice cores. Four large ice rafted debris (IRD) drift deposits occurred during the early  
38 Holocene at ~8.5, 9.3, 10.3 and 11.3 ka (Bond et al., 2001). This record lacks a large IRD deposit that

1 corresponds to 8.2 ka cooling (Bond et al., 2001). Later study found that increase of hematite stained glass  
2 (HSG) at the timing of 8.5 ka should be revised to 8.2 ka based on quartz to plagioclase ratio analysis (Moros et  
3 al., 2004). Additionally, Bond et al. (2001) found that 1500 year cycle of IRD in the North Atlantic are  
4 concurrent with the global climate cooling and the negative solar activity inferred by ice core  $^{10}\text{Be}$  and  $\Delta^{14}\text{C}$   
5 records. From this evidence the authors speculated that the solar influence should be amplified by changes of  
6 sea ice and/or in deep water formation in the North Atlantic. However, the forcing mechanism of solar activity  
7 on the North Atlantic and global climate is not well understood during the early Holocene. Renssen et al. (2006)  
8 suggested that low solar activity (in terms of total solar irradiance) can induce sea ice expansion around the  
9 Nordic Seas and weakening of deep water formation and cooling in North Atlantic region. Nevertheless, the  
10 anti-correlation between solar forcing and sea ice expansion (and hence deep water formation weakening) is not  
11 strong during the early Holocene due to relatively warm climate conditions. Jiang et al. (2015) also found a  
12 negative correlation between North Atlantic SST and solar forcing proxies ( $^{14}\text{C}$  and  $^{10}\text{Be}$ ), which is statistically  
13 significant for the last 4000 years, while the correlation disappeared during the mid- and early Holocene. They  
14 hypothesized that climate sensitivity to solar forcing is high for cooler climate. Meanwhile, a shifting to an El  
15 Niño-like SST state condition was suggested as another mechanism that changes tropical rainfall patterns  
16 (Marchitto et al., 2010). According to modern atmospheric observations, El Niño conditions leads to drying  
17 conditions in low latitude wetlands in Africa, Asia, and the Americas (e.g., Dai and Wigley, 2000; Lyon and  
18 Barnston, 2005; Hodson et al., 2011), which reduces tropical  $\text{CH}_4$  emissions. Thus, we could speculate that both  
19 the ITCZ migration and El Niño-like SST change affected the tropical surface hydrology and  $\text{CH}_4$  emission.  
20 According to Holocene ENSO activity reconstructions by Moy et al. (2002), no ENSO event was recorded  
21 during the early Holocene until around 7 ka, except weak ENSO events during 10.4 – 10.1 ka, where abrupt we  
22 observe a  $\text{CH}_4$  drop apparently unrelated to monsoon proxies. decrease is observed without significant changes  
23 in ITCZ and NH monsoon intensities. Mitchell et al. (2011) observed a significant positive correlation between  
24  $\text{CH}_4$  and Pacific Decadal Oscillation (PDO) variability during the late Holocene. It has been reported that PDO  
25 modulates the wet/dry impact of ENSO depending on phase relationship between ENSO and PDO (e.g., Wang  
26 et al., 2014 and references therein). The-Using a Holocene PDO reconstruction from sediment grain size  
27 analysis by Kirby et al. (2010) shows PDO-related drying intervals in North America during 9.5 – 9.1, 8.9 – 8.6,  
28 and 8.3 – 7.8 ka, which overlap the  $\text{CH}_4$  minima at 8.2 and 9.3 ka present in this study.

29 Marchitto et al. (2010) suggested that negative solar forcing induces so called “El Niño like” conditions;  
30 warming in East Tropical Pacific and weakened Asian and Indian summer monsoons. A close interplay between  
31 solar activity and monsoon intensity is confirmed by previous studies in Chinese and Oman speleothem records  
32 (Neff et al., 2001; Wang et al., 2005; Gupta et al., 2005), even on multi-decadal time scales (Agnihotri et al.,  
33 2002). Marchitto et al. (2010) also suggested a connection between “El Niño like” climate and IRD events  
34 (except for 8.2 ka event), through reorganization of ocean currents around the North Atlantic due to intensified  
35 El Niño Southern Oscillation (ENSO) driven by the solar forcing so that it may have driven more IRD episodes  
36 (Emile-Geay et al., 2007). According to modern climate conditions it has been found that the El Niño state  
37 generally induces wetter conditions in tropical land area and vice versa (e.g., Dai and Wigley, 2000; Lyon and  
38 Barnston, 2005; Hodson et al., 2011). However, since there is no ENSO and PDO index reconstructions back to  
39 the early Holocene at present, with different climate boundary conditions, we cannot test this hypothesis.

## 3.2 Latitudinal source distribution Inter-polar difference of CH<sub>4</sub> during the early Holocene

### 3.2.1 Inter-polar difference of CH<sub>4</sub> and source distribution model

We calculated the inter-polar difference (IPD) of CH<sub>4</sub> to trace the latitudinal source distribution change during the early Holocene. The currently available high-resolution CH<sub>4</sub> records covering the early Holocene are SDMA discrete (this study), WAIS Divide discrete (WAIS Divide project members, 2015), WAIS Divide continuous (Rhodes et al., 2015), NEEM discrete (Chappellaz et al., 2013) and NEEM continuous data (Chappellaz et al., 2013). Among the Antarctic records, we consider WAIS continuous records most reliable from ~9.9 to 11.5 ka interval. For the rest of the studied period, SDMA discrete records are better constrained than WAIS discrete data, because SDMA records have better analytical precision, as well as comparison with OSU measurements reveals a minimal offset for the early Holocene interval. Before IPD calculation, WAIS continuous data were calibrated to SDMA data, given the discrete measurements generally have better accuracy than continuous ones. ~~are more~~ Regarding the Greenland side, we use NEEM discrete records because not only there are discrepancies between continuous- and discrete data in some intervals, but also because NEEM discrete records were measured by similar wet extraction technique at OSU (Chappellaz et al., 2013). ~~we use NEEM discrete records because there are discrepancies between continuous and discrete data in some intervals, but also because the NEEM continuous record is not exactly "continuous". Hence, here we regard the NEEM discrete, Siple Dome discrete, and WAIS Divide continuous data as more reliable ones than the others to reconstruct IPD during the early Holocene. In this study, the IPD was calculated by using our Siple Dome CH<sub>4</sub> record and a NEEM high resolution discrete CH<sub>4</sub> record (Chappellaz et al., 2013).~~

Precise synchronization is crucial for direct comparison between data sets which have high frequency variations. For synchronizing between Antarctic (Siple Dome and WAIS Divide continuous) and NEEM records, ~~the~~ the NEEM CH<sub>4</sub> record (~11 years resolution on average) is chosen as reference, ~~because the mean time resolution is higher than our data set.~~ Synchronization was done by two steps: First, we made initial synchronization between the Antarctic and NEEM data by setting ~~7~~ match points at the midpoint of abrupt CH<sub>4</sub> change, and then we linearly interpolated the age offset of each match point for the rest of data points. Then we applied a Monte Carlo simulation to find a maximum correlation. Both data sets were resampled every 30 years, and each point was randomly ~~perturbed~~ ~~disturbed~~ (assuming a normal distribution with 1 sigma of 30 years). By doing so 1000 different time series were created, and ~~one~~ the set having a maximum correlation with NEEM data was chosen. Criteria for "best fit" is correlation coefficient of 0.8 with NEEM original age scale, so that a maximum correlation less than 0.8 was discarded. This procedure was repeated to make 20 sets of maximum correlation time series, and the mean ages of 20 replicate simulations were set to synchronized age scale. ~~Temporal uncertainty (synchronizing error) was determined for each point as 1 standard deviation of 20 replicates and CH<sub>4</sub> uncertainty includes analytical error of the both records.~~ The uncertainty range of IPD was calculated from synchronization uncertainty and CH<sub>4</sub> data uncertainty. To estimate synchronization uncertainty, we created 20 IPDs from the 20 sets of maximum correlation time series, and the standard deviation of the 20 records was taken as synchronization uncertainty for each of the data points. The CH<sub>4</sub> data uncertainty was estimated with the stated uncertainty of each data set (4.3 ppb for NEEM discrete and ~~2.7 ppb~~ 1.4 ppb for SDMA / 1.5 ppb for WAIS continuous, 1 sigma). To check the sensitivity of the uncertainties, we carried out Monte Carlo simulations. We produced 1000 different sets of IPD, which vary randomly with Gaussian

1 propagation in their ages and CH<sub>4</sub> concentration uncertainties. Each IPD was annually interpolated and  
2 smoothed by a 1/1000 year<sup>-1</sup> low-pass filter. The cutoff frequency of 1000 years was chosen to examine multi-  
3 centennial to millennial scale change, because ~~Since the IPD calculation is very sensitive to high frequency~~  
4 ~~variability of CH<sub>4</sub> records from both poles. To report 95% confidence interval, we multiplied the standard~~  
5 ~~deviation by 1.96 and enveloped the IPD, and it is difficult to reconstruct reliable IPD in short time scales, all~~  
6 ~~IPD records in this study were filtered by a 1000-year low-pass window to discuss multi-centennial to millennial~~  
7 ~~scale change. As discrete measurements are regarded as more accurate than continuous ones in absolute sense,~~  
8 ~~WAIS continuous data were calibrated against to Siple Dome data instead of WAIS discrete record, because~~  
9 ~~Siple Dome records were more rigorously tested for its reproducibility, and also compared with OSU~~  
10 ~~measurements that shows small offset during the early Holocene interval.~~

11 Figure 6 displays the IPDs calculated from various pairs of data set with 95% significant interval. The two  
12 IPD records derived from most reliable data sets ~~The IPDs from those three data sets are plotted in red grey~~  
13 ~~(NEEM discrete – Siple Dome, IPD-1 hereafter) and green (NEEM discrete – WAIS continuous, IPD-2~~  
14 ~~hereafter) in Figure 3. Resulting Both IPD-1 and IPD-2 show a long-term increase from 11.5 to 9.9 ka, which~~  
15 ~~indicates that boreal source contribution enhanced. However, IPD-1 shows a sharper increase during the PBO~~  
16 ~~followed by decrease until ~10.7 ka, and in the latter case both IPDs differ beyond 95% envelope (from 10.4 to~~  
17 ~~10.8 ka). Although these differences are significant, and are probably due to small errors in the time scale and~~  
18 ~~absolute concentrations differences, for example, due to uncertainties in blank corrections or solubility~~  
19 ~~corrections, or core quality, they do not affect our basic interpretation of the trends. Instead, we combined the~~  
20 ~~two IPDs to resolve this. Given the IPD-2 is better constrained than IPD-1, we use IPD-2 curve from 9.9 to 11.5~~  
21 ~~ka interval and IPD-1 for the rest of the studied period (Fig. 6). The combined IPD shows ~13 ppb increase from~~  
22 ~~11.5 to 9.5 ka. It displays similar trend with the NH extratropical (30° - 90°N) temperature reconstruction~~  
23 ~~(Marcott et al., 2013) and the modelled CH<sub>4</sub> emission from boreal thermokarst lakes (Walter et al., 2014),~~  
24 ~~indicating that NH extratropical source strength increased during this period. This is because Siple Dome~~  
25 ~~discrete data are higher than WAIS continuous data during this interval. Similarly, the small peak of IPD-1 at~~  
26 ~~~11.1 ka that is not seen in IPD-2 may be caused by offset between Siple and WAIS data during 11.0 to 11.3 ka.~~

27 Fig. 3 shows our IPD results with 95% significance envelope. Our IPD agrees with the previous low-  
28 resolution estimates for the earlier part of the Holocene (9.5–11.5 ka) (Chappellaz et al., 1997; Brook et al.,  
29 2000). Our results show an increase from ~10.7 ka to ~9.9 ka, which was not previously reported. Considering  
30 the long-term decreasing trend of CH<sub>4</sub> mixing ratio in both poles during the early Holocene, the increasing IPD  
31 implies that the amount of boreal emission reduction should have been less than that of low-latitude  
32 emissions. Given the new high-resolution CH<sub>4</sub> records from both poles and IPD, By using our new IPDs and the  
33 reliable highly resolved CH<sub>4</sub> records (NEEM discrete – SDMA discrete / WAIS continuous), we ran  
34 the source strength of low- and high-latitude sources, we employed a simple 3-box CH<sub>4</sub> source distribution  
35 model used in previous studies (Chappellaz et al., 1997; Brook et al., 2000), to quantify how much the boreal  
36 and tropical source strengths were changed. Here we used the same box model employed in Chappellaz et al.  
37 (1997) and Brook et al. (2000). Briefly, the model contains 3 boxes; northern high-extra-tropical latitude (30°N  
38 – 90°N, N-box), tropical (30°S – 30°N, T-box), and southern high-extra-tropical latitude boxes (30°S – 90°S, S-  
39 box). CH<sub>4</sub> concentrations-mixing ratios in 3 boxes (in Tg box<sup>-1</sup>) were determined from CH<sub>4</sub> mixing ratio of  
40 Antarctica and Greenland. ~~To calculate the N-box CH<sub>4</sub>, we subtracted the 7% of IPD from Greenland CH<sub>4</sub>~~

1 concentration, assuming the difference between Greenland and the mean latitude of N-box is  $\sim 7\%$  of IPD  
2 (~~Chappellaz et al., 1997~~). The mean  $\text{CH}_4$  mole fraction of N-box ( $30^\circ\text{N} - 90^\circ\text{N}$ ) is not identical to that of  
3 Greenland ice core record, given the latitudinal  $\text{CH}_4$  distribution (e.g., Fung et al., 1991). To derive the N-box  
4  $\text{CH}_4$ , we followed the assumption of Chappellaz et al. (1997), where the authors assumed that difference  
5 between Greenland and the mean N-box  $\text{CH}_4$  is  $7\%$  of IPD. Hence here the N-box  $\text{CH}_4$  is calculated by  
6 subtracting  $7\%$  of IPD from the Greenland mixing ratio. T-box ~~concentration~~-mixing ratio is inferred by  
7 assuming that the S-box emission is constant of  $15 \text{ Tg yr}^{-1}$  (Fung et al., 1991). Emission from each box ( $\text{Tg yr}^{-1}$ )  
8 is then estimated by using the ~~concentration~~-mixing ratios of the boxes, lifetime of  $\text{CH}_4$  in each box, and  
9 transport times among the boxes. Following Chappellaz et al. (1997), we assume the lifetime of 18.7, 8.1, and  
10 26.8 years in N, T, and S-box, respectively, and transport time of 9 months. The modelled emission changes in  
11 NH extratropical and tropical boxes from IPD 1 are plotted in Figure 8.4 (see Fig. S3 for results from IPD 2).  
12 The model results reveals that decreasing tropical sources decrease (accounting for the largest portion in  $\text{CH}_4$   
13 budget), while enhancing NH extratropical emissions increase. The T-box emission is reduced from  $\sim 118 \text{ Tg yr}^{-1}$   
14 to  $\sim 109 \text{ Tg yr}^{-1}$ , and the N-box source strength increases from  $\sim 60 \text{ Tg yr}^{-1}$  to  $\sim 71 \text{ Tg yr}^{-1}$  during the 11.5 – 9.5  
15 ka interval (Fig. 8). The tropical emission was elevated by  $\sim 98 \text{ Tg yr}^{-1}$  from the onset of the Holocene to its  
16 maximum at 10.6 ka, followed by  $\sim 15 \text{ Tg yr}^{-1}$  reduction to  $\sim 111 \text{ Tg yr}^{-1}$  at 9.5 ka. Tropical emission decrease is  
17 also observed in IPD 2 from 134 to 115  $\text{Tg yr}^{-1}$  during the 11.5–10.0 ka, but this change is not significant in 95%  
18 confidence range (Fig. S3 and Table S2). The long-term decreasing trend decrease of tropical emission follows  
19 the NH summer insolation change. This covariation may reflect the insolation-driven changes in emissions on  
20 multi-millennial timescale (e.g., Louergue et al., 2008; Guo et al., 2012).  $\text{CH}_4$  flux from NH extratropical box  
21 increased from  $\sim 57 \text{ Tg yr}^{-1}$  (11.5 ka) to  $\sim 70 \text{ Tg yr}^{-1}$  (9.5 ka), showing a local minimum of  $\sim 63 \text{ Tg yr}^{-1}$  at 10.7 ka.  
22 Also plotted in Figure 8.4 is the boreal source fraction, defined as ratio of N-box emission to total source  
23 emissions, showing 5% increase (from 31.5 to 36.5%) during the same interval. The box model results at 9.0,  
24 9.5, and 11.5 ka time slices are summarised in Table 2. It shows a significant increase from  $\sim 30\%$  at 11.5 ka to  
25  $\sim 35\%$  at 9.5 ka. The box model results from IPD 2 demonstrate increase of NH extratropical emission from 60  
26 to  $71 \text{ Tg yr}^{-1}$ , and hence increase of the boreal source fraction from 29 to 35% during the 11.5 to 10.0 ka interval.  
27 The results of our model are consistent with previous estimates by Chappellaz et al. (1997) and Brook et al.  
28 (2000). Although the early studies reported average value for the 11.5–9.5 ka interval, our IPD records show  
29 similar value before the IPD starts to rise at  $\sim 10.7$  ka (Fig. 4 and Table 1). After that, our results show an  
30 increase of boreal emission by  $9 \text{ Tg yr}^{-1}$  and a decrease in tropical emission. Boreal source fraction, a ratio of  
31 boreal emission to total emission, reveals an increase by  $5\%$ . This result supports our interpretation that the  
32 boreal sources were less reduced than those in low latitudes. This conclusion is Our results are supported by  
33 proxy-based temperature reconstructions that indicate a gradual warming in northern high latitude–northern  
34 extratropical regions ( $30^\circ\text{N} - 90^\circ\text{N}$ ) until  $\sim 9.6$  ka, while tropical temperature remains stable (Marcott et al.,  
35 2013). The climate warming in northern high latitudes caused ice sheet retreat (e.g., Dyke, 2004) and may have  
36 enhanced  $\text{CH}_4$  emission from boreal permafrost by forming new wetlands in permafrost regions mid to high  
37 latitudes (e.g., Gorham et al., 2007; Yu et al., 2013) and accelerating microbial decomposition of organic  
38 materials (e.g., Christensen et al., 2004; Schuur et al., 2015). Thermokarst lakes created by thawing ice wedges  
39 and ground ices in Alaskan- and Siberian permafrost are has been suggested as a source of  $\text{CH}_4$  (e.g., Walter et  
40 al., 2006, 2007; Brosius et al., 2012). The modelled enhancement of NH extratropical emission of  $\sim 11$ – $13 \text{ Tg yr}^{-1}$

1 is similar to ~~greater than~~ the CH<sub>4</sub> release of 8.2 Tg yr<sup>-1</sup> from thermokarst lake thawing, which is estimated based  
2 on present-day observations (Walter et al., 2014). Since most thermokarst lakes are located in NH high latitude  
3 regions (e.g., Walter et al., 2006, 2014), it may ~~support the box model results. indicate that other sources, such~~  
4 ~~as northern peatlands or mid latitude wetlands, should contribute to increasing NH extratropical emission. Our~~  
5 ~~results are consistent with previous findings based on~~ CH<sub>4</sub> stable isotope analysis. Fischer et al. (2008) found  
6 ~~that increase of boreal source contribution is required to explain the more depleted δ<sup>13</sup>C-CH<sub>4</sub> during Preboreal~~  
7 ~~period Holocene than the Younger Dryas interval. Sowers (2010) extended the CH<sub>4</sub> isotopic ratio into the entire~~  
8 ~~Holocene and showed that displayed~~ a gradual decrease of δ<sup>13</sup>C-CH<sub>4</sub> by ~2‰ from 10.5 to 4 ka, which was  
9 ~~attributed to progressive expansion of NH high latitude sources.~~

10 Indeed, the increased boreal CH<sub>4</sub> emission of 9 Tg yr<sup>-1</sup> is in similar order of the CH<sub>4</sub> release of 8.2 Tg yr<sup>-1</sup>  
11 from thermokarst lake reported by Walter Anthony et al. (2014). However, it should be noted that the CH<sub>4</sub>  
12 release estimates from the thermokarst lakes are based on present-day CH<sub>4</sub> flux measurements in Siberian and  
13 Alaskan lakes and that 9 Tg yr<sup>-1</sup> is a small change in the budget that could be driven by conventional northern  
14 CH<sub>4</sub> emission. A recent study also argued a possibility of underestimation of such CH<sub>4</sub> emission measurements  
15 (Wik et al., 2016). We could not estimate the IPD for the later part of the record (7.7–8.8 ka) due to a lack of  
16 high resolution CH<sub>4</sub> from Greenland ice cores. However, since the first generation lakes produce CH<sub>4</sub> more  
17 actively than later generation lakes formed after drainage (Brosius et al., 2012), it is unlikely that thermokarst  
18 lake CH<sub>4</sub> emission would remain higher after 9.0 ka. Future study should include extending high resolution CH<sub>4</sub>  
19 record from Greenland, as well as CH<sub>4</sub> isotope ratio data for the younger time period.

### 20 3.2.2 IPD during the Pre-Boreal Oscillation (PBO)

21 We also observed a high IPD at the earliest part of the Holocene, where CH<sub>4</sub> records from both  
22 ~~hemispheres poles show a large variability. This could be due to mismatching of synchronized time scales and~~  
23 ~~different surface conditions of drilling site and hence signal attenuation process within firn. A sensitivity test on~~  
24 ~~synchronizing error has been carried out by shifting the reference age scale (in this study, NEEM chronology)~~  
25 ~~15 years back and forth given that the initial age match points were resampled every 30 years. The IPDs~~  
26 ~~calculated with shifted age scales (plus 15 years, control, and minus 15 years) are plotted in Fig. S3, showing a~~  
27 ~~consistent high IPD values during ~11.0 to 11.2 ka interval, while for the earlier part IPD seems to be highly~~  
28 ~~sensitive to synchronization. Nevertheless, this might be a result of different gas enclosing processes within firn~~  
29 ~~layers in both ice cores. As the width at half height of the gas age distribution at NEEM site was reported as ~32~~  
30 ~~years (Buizert et al., 2012), which is ~23 % narrower than that of Siple Dome (Ahn et al. 2014). It means that~~  
31 ~~the NEEM signal has been less attenuated than Siple Dome one, which could result in higher (lower) IPD at the~~  
32 ~~period where rapid CH<sub>4</sub> increase (decrease) is observed. Indeed, the discrete and continuous CH<sub>4</sub> record from~~  
33 ~~WAIS Divide, which has a mean accumulation rate similar to NEEM (Buizert et al., 2013), shows ~10 to 20 ppb~~  
34 ~~higher amplitude variability.~~

35 Our new CH<sub>4</sub> data confirms the abrupt doubling at the Younger Dryas termination. Previous studies using  
36 ~~stable isotopes of CH<sub>4</sub> have shown contradictory results. Previous studies that, using the stable isotopic~~  
37 ~~composition of C and H in CH<sub>4</sub> that aimed to disentangle the cause of abrupt CH<sub>4</sub> increase during the earliest~~  
38 ~~period of the Holocene have shown contradictory results. Schaefer et al. (2006) calculated isotopic (δ<sup>13</sup>C-CH<sub>4</sub>)~~  
39 ~~mass balance model to discern major source term that caused a slight enrichment in <sup>13</sup>C during the Younger~~  
40 ~~Dryas termination, suggesting tropical wetland emission as a dominant source. The authors also proposed~~

1 biomass burning, geologic CH<sub>4</sub> and enhanced sink process at marine boundary layer as alternatives, but less  
2 probable scenarios. On the other hand, Fischer et al. (2008) argued nearly constant biomass burning emission of  
3 ~45 Tg yr<sup>-1</sup> throughout the last glacial termination with a slight increase in PB, and also showed that the boreal  
4 sources were expanded during the YD-PB transition. However, Möller et al. (2013) pointed out the possibility of  
5 changing isotopic signature of each source itself, and they found that less pyrogenic emission is required for  
6 LGM condition if they increased the δ<sup>13</sup>C-CH<sub>4</sub> signatures of tropical wetland and of biomass burning. The triple  
7 isotopic mass balance model using δ<sup>13</sup>C-CH<sub>4</sub>, δD-CH<sub>4</sub> and Δ<sup>14</sup>C-CH<sub>4</sub>, Melton et al. (2012) suggested the  
8 biomass burning and thermokarst lakes are the most important additional sources. The enhanced biomass  
9 burning agrees with global charcoal influx, an independent proxy for wildfire, which shows intensified wildfire  
10 in northern tropical regions (Daniau et al., 2012). However, it is unlikely that the increased pyrogenic emission  
11 in tropics leads to higher IPD. Brosius et al. (2012), using an isotopic mass balance model including thermokarst  
12 lake sources, suggested another scenario that the enhanced boreal wetland emission contributed largely for the  
13 CH<sub>4</sub> overshoot. In the meanwhile, the boreal emission hypothesis was refuted by a recent study of <sup>14</sup>C-CH<sub>4</sub>  
14 change during the YD termination that revealed the major carbon source for abrupt CH<sub>4</sub> doubling was not the  
15 permafrost-origin old carbon (e.g., Petrenko et al., 2009, 2015). Therefore, the cause of the high IPD at the start  
16 of the Holocene still remains elusive.)

### 17 3.3. Comparison with late Holocene variability

18 We compared amplitude of CH<sub>4</sub> variability between the early and the late Holocene in multi-centennial to  
19 millennial time scales. Figure 5 shows amplitude spectrum and root mean square (RMS) amplitude for the early  
20 Holocene and the late Holocene, respectively. The amplitude of the early Holocene CH<sub>4</sub> change is ~10 ppb and  
21 does not change greater except for PBO and the 8.2 ka event, while the late Holocene spectrum shows smaller  
22 amplitude than early Holocene for shorter term change and larger for longer term fluctuation. Late Pre-  
23 Industrial Holocene (LPIH) CH<sub>4</sub> amplitude is elevated to early Holocene level from ~0 C.E. (~2.0 ka), and  
24 increases up to higher from ~1450 C.E. (~0.5 ka).

25 The reason of low amplitude variability during 3.5 to 1.2 ka, or why the early Holocene CH<sub>4</sub> variability is  
26 larger than this period, is probably related to different orbital configuration in both time periods. Previous  
27 studies found covariation between CH<sub>4</sub> amplitude and NH summer insolation change, reflecting that mean  
28 temperature of the warmest seasons is an important factor of CH<sub>4</sub> emission, during the interstadial conditions  
29 (Flückiger et al., 2004; Baumgartner et al., 2014). Combined with elevated summer insolation in Northern  
30 Hemisphere (NH) and with climate warming in NH extratropics, the amplified variability of the early Holocene  
31 may suggest that CH<sub>4</sub> control by NH wetlands was likely stronger than the late Holocene period. Meanwhile,  
32 lower summer insolation during the late Holocene might induce diminished CH<sub>4</sub> amplitude. This evidence  
33 indicates the natural forcing in centennial to millennial time scales is reduced in the late Holocene, given that  
34 the atmospheric CH<sub>4</sub> budget during 3.5-1.2 ka (604.9 ppb) is similar to that during 9.0-7.6 ka (628.6 ppb), and  
35 that anthropogenic emission is greater in later Holocene than the early Holocene. Abrupt increase of CH<sub>4</sub>  
36 amplitude since ~800 C.E. (1.2 ka) is likely driven by increasing anthropogenic contribution, which is consistent  
37 with anthropogenic emission scenario based on past population and agricultural activity (Mitchell et al., 2013).  
38 Also superimposed are short term cooling events during Little Ice Age, making CH<sub>4</sub> variability greater.

#### 4. Conclusion and summary

~~In this study we~~ We reconstructed a new high resolution CH<sub>4</sub> record during the early Holocene from Siple Dome ice core, Antarctica, to study millennial CH<sub>4</sub> variability and its natural controls under Holocene interglacial condition. The new Siple Dome record agrees well with previous records measured at OSU within analytical uncertainty, showing a mean difference of 0.1 ppb. By combining the two data sets, we present a SDMA CH<sub>4</sub> composite record covering from ~7.7 to 11.6 ka. ~~the early Holocene CH<sub>4</sub> time series in high resolution to discuss natural processes that control the millennial scale CH<sub>4</sub> variations in the past atmosphere. Since the new SDMA data agree well with previous measurements at OSU, we made SDMA CH<sub>4</sub> composite data covering ~7.7 to 11.6 ka. We observed~~ Our results show a series of the four millennial scale CH<sub>4</sub> minima having 10–20 ppb of amplitude with 300–400 years duration. It is found that these CH<sub>4</sub> minima were accompanied with Greenland cooling, changes in ITCZ position and reduced Asian and Indian monsoon intensities. The observed evidences suggest that low latitude hydro climate changes were closely related to millennial scale CH<sub>4</sub> minima. ~~and the evidence suggests that the low latitude source changes were the major causes of the early Holocene CH<sub>4</sub> minima. Further, this study presented the millennial scale change of IPD, which was calculated from high resolution discrete data set of NEEM and SDMA, and a continuous record of WAIS Divide. Here we reported that the IPD increased by ~13 ppb increase from the onset of the Holocene to ~9.9 ka~9.5 ka following the temperature rise in NH extra-tropical regions. The three-box model demonstrates that elevated emission from NH extratropics and reduction of tropical sources NH extratropical emissions elevated by ~11 Tg yr<sup>-1</sup>, while tropical emission was reduced by ~9 Tg yr<sup>-1</sup>, resulting the increased contribution of the NH extra-tropical sources by ~5%. Finally, we observed that RMS amplitude of earlier part of the late Holocene is smaller than that of the early Holocene, which may be attributed to different orbital paramet~~ However, the North Atlantic induced changes in low latitude hydrology cannot fully explain the CH<sub>4</sub> minimum at ~10.2 ka. High resolution IPD and 3 box source distribution model results indicate that fraction of boreal sources increased by 5 % during the early Holocene, which indicates that fraction of boreal sources increased from ~10.7 ka and remained high until ~9.3 ka. To summarize, the millennial scale variability of CH<sub>4</sub> during the early Holocene was primarily controlled by low latitude climatic and surface hydrological conditions, while relative boreal source contribution increased during 10.7–9.3 ka by newly developed high latitude sources following terrestrial deglaciation. Further, our observations imply that ~20–40 ppb of CH<sub>4</sub> change could be induced naturally by low latitude hydroclimate changes.

*Acknowledgements.* Financial support was provided by the Basic Science Research Program through the National Research Foundation of Korea (NRF) (NRF-2015R1A2A2A01003888) and Korea Polar Research Institution (KOPRI) research grant (PD12010 and PE15010). This work was also supported by the US National Science Foundation Grant PLR 1043518. We appreciate all the efforts of sample cutting and shipping of the Siple Dome ice core by Brian Bencivengo, Richard Nunn, and Geoffrey Hargreaves of National Ice Core Laboratory, Denver, Colorado. We sincerely thank to Yoo-Hyeon Jin, Jinhwa Shin, and Hun-Gyu Lee for their laboratory assistance and helpful discussions. Thanks should go to Heejo Lee for her help in preparing English manuscript. We are grateful to Mark Twickler and the NICL Science Management Office for providing the Siple Dome ice core samples, the collection of which was supported by the US National Science Foundation.



1 [Data availability](#)

2 [The early Holocene Siple Dome CH<sub>4</sub> data will be available on NOAA Paleoclimatology database and](#)  
3 [PANGAEA data repository.](#)

4 **References**

5 Agnihotri, R., Dutta, K., Bhushan, R., and Somayajulu, B. L. K.: Evidence for solar forcing on the Indian  
6 monsoon during the last millennium, *Earth Planet. Sci. Lett.*, 198, 521-527, 2002.

7 Ahn, J., Brook, E. J., and Buizert, C.: Response of atmospheric CO<sub>2</sub> to the abrupt cooling event 8200 years ago,  
8 *Geophys. Res. Lett.*, 41, 604-609, 2014.

9 ~~Alley, R. B., and Agustsdottir, A. M.: The 8k event: cause and consequences of a major Holocene abrupt~~  
10 ~~climate change, *Quaternary Sci. Rev.*, 24, 1123-1149, 2005.~~

11 [Andreae, M. O., and Merlet, P.: Emission of trace gases and aerosols from biomass burning, \*Global\*](#)  
12 [\*Biogeochem. Cycles\*, 15, 955-966, 2001.](#)

13 [Baumgartner, M., Kindler, P., Eicher, O., Floch, G., Schilt, A., Schwander, J., Spahni, R., Capron, E.,](#)  
14 [Chappellaz, J., Leuenberger, M., Fischer, H., and Stocker, T. F.: NGRIP CH<sub>4</sub> concentration from 120 to 10](#)  
15 [kyr before present and its relation to a  \$\delta^{15}\text{N}\$  temperature reconstruction from the same ice core, \*Clim. Past\*, 10,](#)  
16 [903-920, 2014.](#)

17 [Berger, A., and Loutre, M. F.: Insolation values for the climate of the last 10 million years, \*Quat. Sci. Rev.\*, 10,](#)  
18 [297-317, 1991.](#)

19 Berkelhammer, M., Sinha, A., Stott, L., Cheng, H., Pausata, F., and Yoshimura, K.: An abrupt shift in the Indian  
20 Monsoon 4000 years ago, *Geophys. Monogr. Ser.*, 198, 75-87, 2012.

21 [Björck, S., Muscheler, R., Kromer, B., Andresen, C. S., Heinemeier, J., Johnsen, S. J., Conley, D., Koç, N.,](#)  
22 [Spurk, M., and Veski, S.: High-resolution analyses of an early Holocene climate event may imply decreased](#)  
23 [solar forcing as an important climate trigger, \*Geology\*, 29, 1107-1110, 2001.](#)

24 Blunier, T., Chappellaz, J., Schwander, J., Stauffer, B., and Raynaud, D.: Variations in atmospheric methane  
25 concentration during the Holocene epoch, *Nature*, 374, 46-49, 1995.

26 Blunier, T., and Brook, E. J.: Timing of millennial-scale climate change in Antarctica and Greenland during the  
27 last glacial period, *Science*, 291, 109-112, 2001.

28 Broccoli, A. J., Dahl, K. A., and Stouffer, R. J.: Response of the ITCZ to northern hemisphere cooling, *Geophys.*  
29 *Res. Lett.*, 33, L01702, 2006.

30 Bond, G., Kromer, B., Beer, J., Muscheler, R., Evans, M. N., Showers, W., Hoffmann, S., Lotti-Bond, R.,  
31 Hajdas, I., and Bonani, G.: Persistent solar influence on north Atlantic climate during the Holocene, *Science*,  
32 294, 2130-2136, 2001.

33 Brook, E. J., Sowers, T., and Orchard, J.: Rapid variations in atmospheric methane concentration during the  
34 past 110,000 years, *Science*, 273, 1087-1091, 1996.

35 Brook, E. J., Harder, S., Severinghaus, J. P., Steig, E. J., and Sucher, C. M.: On the origin and timing of rapid  
36 changes in atmospheric methane during the last glacial period, *Global Biogeochem. Cy.*, 14, 559-572, 2000.

1 Brook, E. J., White, J. W. C., Schilla, A. S. M., Bender, M. L., Barnett, B., Severinghaus, J. P., Taylor, K. C.,  
2 Alley, R. B., and Steig, E. J.: Timing of millennial-scale climate change at Siple Dome, West Antarctica,  
3 during the last glacial period, *Quat. Sci. Rev.*, 24, 1333-1343, 2005.

4 Brosius, L. S., Walter Anthony, K. M., Grosse, G., Chanton, J. P., Farquharson, L. M., Overduin, P. P., and  
5 Meyer, H.: Using the deuterium isotope composition of permafrost meltwater to constrain thermokarst lake  
6 contributions to atmospheric CH<sub>4</sub> during the last deglaciation, *J. Geophys. Res.*, 117, G01022, 2012.

7 ~~Buizert, C., Martinerie, P., Petrenko, V. V., Severinghaus, J. P., Trudinger, C. M., Witrant, E., Rosen, J. L., Orsi,  
8 A. J., Rubino, M., Etheridge, D. M., Steele, L. P., Hogan, C., Laube, J. C., Sturges, W. T., Levchenko, V.  
9 A., Smith, A. M., Levin, I., Conway, T. J., Dlugokencky, E. J., Lang, P. M., Kawamura, K., Jenk, T. M.,  
10 White, J. W. C., Sowers, T., Schwander, J., and Blunier, T.: Gas transport in firn: multiple tracer  
11 characterisation and model intercomparison for NEEM, Northern Greenland, *Atmos. Chem. Phys.*, 12, 4259-  
12 4277, 2012.~~

13 ~~Buizert, C., Sowers, T., and Blunier, T.: Assessment of diffusive isotopic fractionation in polar firn, and  
14 application to ice core trace gas records, *Earth Planet. Sci. Lett.*, 361, 110-119, 2013.~~

15 ~~Buizert, C., Cuffey, K. M., Severinghaus, J. P., Baggenstos, D., Fudge, T. J., Steig, E. J., Markle, B. R.,  
16 Winstrup, M., Rhodes, R. H., Brook, E. J., Sowers, T. A., Clow, G. D., Cheng, H., Edwards, R. L., Sigl, M.,  
17 McConnell, J. R., and Taylor, K. C.: The WAIS Divide deep ice core WD2014 chronology—Part 1: methane  
18 synchronization (68–31 ka BP) and the gas age–ice age difference, *Clim. Past*, 11, 153–173, 2015.~~

19 ~~Chappellaz, J.,~~

20 Chappellaz, J., Blunier, T., Raynaud, D., Barnola, J. M., Schwander, J., and Stauffer, B.: Synchronous changes  
21 in atmospheric CH<sub>4</sub> and Greenland climate between 40 and 8 kyr BP, *Nature*, 366, 443-445, 1993.

22 Chappellaz, J., Blunier, T., Kints, S., Dällenbach, A., Barnola, J. M., Schwander, J., Raynaud, D., and Stauffer,  
23 B.: Changes in the atmospheric CH<sub>4</sub> gradient between Greenland and Antarctica during the Holocene, *J.*  
24 *Geophys. Res.*, 102, 15987-15997, 1997.

25 Chappellaz, J., Stowasser, C., Blunier, T., Baslev-Clausen, D., Brook, E. J., Dallmayr, R., Faïn, X., Lee, J. E.,  
26 Mitchell, L. E., Pascual, O., Romanini, D., Rosen, J., and Schüpbach, S.: High-resolution glacial and  
27 deglacial record of atmospheric methane by continuous-flow and laser spectrometer analysis along the NEEM  
28 ice core, *Clim. Past*, 9, 2579-2593, 2013.

29 Chiang, J. C. H., and Bitz, C. M.: Influence of high latitude ice core on the marine intertropical convergence  
30 zone, *Clim. Dynam.*, 25, 477-496, 2005.

31 Chiang, J. C. H., Cheng, W., and Bitz, C. M.: Fast teleconnections to the tropical Atlantic sector from Atlantic  
32 thermohaline adjustment, *Geophys. Res. Lett.*, 35, L07704, 2008.

33 Christensen, T. R., Johansson, T., Jonas Åkerman, H., Mastepanov, M., Malmer, N., Friberg, T., Crill, P., and  
34 Svensson, B. H.: Thawing sub-arctic permafrost: effects on vegetation and methane emissions, *Geophys. Res.*  
35 *Lett.*, 31, L04501.

36 Cvijanovic, I., and Chiang, J. C. H.: Global energy budget changes to high latitude North Atlantic cooling and  
37 the tropical ITCZ response, *Clim. Dynam.*, 40, 1435-1452, 2013.

38 [Craig, H., Horibe, Y., and Sowers, T.: Gravitational separation of gases and isotopes in polar ice caps, \*Science\*,](#)  
39 [242, 1675-1678, 1988.](#)

- 1 [Cruz, F. W., Burns, S. J., Karmann, I., Sharp, W. D., Vuille, M., Cardoso, A. O., Ferrari, J. A., Silva Dias, P. L.,](#)  
2 [and Viana, O.: Insolation-driven changes in atmospheric circulation over the past 116,000 years in subtropical](#)  
3 [Brazil, \*Nature\*, 63-66, 2005.](#)
- 4 Dai, A., and Wigley, T. M. L.: Global patterns of ENSO-induced precipitation, *Geophys. Res. Lett.*, 27, 1283-  
5 1286, 2000.
- 6 ~~Daniau, A. L., Bartlein, P. J., Harrison, S. P., Prentice, I. C., Brewer, S., Friedlingstein, P., Harrison Prentice,~~  
7 ~~T. I., Inoue, J., Izumi, K., Marlon, J. R., Mooney, S., Power, M. J., Stevenson, J., Tinner, W., Andric, M.,~~  
8 ~~Atanassova, J., Behling, H., Black, M., Blarquez, O., Brown, K. J., Carcaillet, C., Colhoun, E. A.,~~  
9 ~~Colombaroli, D., Davis, B. A. S., D'Costa, D., Dodson, J., Dupont, L., Eshetu, Z., Gavin, D. G., Genries, A.,~~  
10 ~~Haberle, S., Hallett, D. J., Hope, G., Horn, S. P., Kassa, T. G., Katamura, F., Kennedy, L. M., Kershaw, P.,~~  
11 ~~Krivonogov, S., Long, C., Magri, D., Marinova, E., McKenzie, G. M., Moreno, P. I., Moss, P., Neumann, F.~~  
12 ~~H., Norstrom, E., Paitre, C., Rius, D., Roberts, N., Robinson, G. S., Sasaki, N., Scott, L., Takahara, H.,~~  
13 ~~Terwilliger, V., Thevenon, F., Turner, R., Valsecchi, V. G., Vanniere, B., Walsh, M., Williams, N., and~~  
14 ~~Zhang, Y.: Predictability of biomass burning in response to climate changes, *Global Biogeochem. Cy.*, 26,~~  
15 ~~GB4007, 2012.~~
- 16 Deplazes, G., Luckge, A., Peterson, L. C., Timmermann, A., Hamann, Y., Hughen, K. A., Rohl, U., Laj, C.,  
17 Cane, M. A., Sigman, D. M., and Haug, G. H.: Links between tropical rainfall and North Atlantic climate  
18 during the last glacial period, *Nat. Geosci.*, 6, 213-217, 2013.
- 19 Dlugokencky, E. J., Steele, L. P., Lang, P. M., and Masarie, K. A.: The growth rate and distribution of  
20 atmospheric methane, *J. Geophys. Res.*, 99, 17021-17043, 1994.
- 21 Dlugokencky, E. J., Myers, R. C., Lang, P. M., Masarie, K. A., Crotwell, A. M., Thoning, K. W., Hall, B. D.,  
22 Elkins, J. W., and Steele, L. P.: Conversion of NOAA atmospheric dry air CH<sub>4</sub> mole fractions to a  
23 gravimetrically prepared standard scale. *J. Geophys. Res.*, 110, 2005.
- 24 Dlugokencky, E. J., Bruhwiler, L., White, J. W. C., Emmons, L. K., Novelli, P. C., Montzka, S. A., Masarie, K.  
25 A., Lang, P. M., Crotwell, A. M., Miller, J. B., and Gatti, L. V.: Observational constraints on recent increases  
26 in the atmospheric CH<sub>4</sub> burden, *Geophys. Res. Lett.*, 36, L18803, 2009.
- 27 Dlugokencky, E. J., Nisbet, E. J., Fisher, R., and Lowry, D.: Global atmospheric methane: Budget, changes, and  
28 dangers, *Philosophical Transactions of the Royal Society A*, 369, 2058-2072, 2011.
- 29 ~~Dyke, A. S., Moore, A., and Robertson, L.: Deglaciation of North America, *Geol. Surv. Of Can., Ottawa, Ont.,*~~  
30 ~~Open File Rep. 1574, 2003.~~
- 31 Dyke, A. S.: An outline of North American deglaciation with emphasis on central and northern Canada, in:  
32 Quaternary Glaciations - Extent and Chronology Part II: North America, Volume 2, edited by: Ehlers J. and  
33 Gibbard, P. L., Elsevier, Amsterdam, 373-424, 2004.
- 34 Dykoski, C. A., Edwards, R. L., Cheng, H., Yuan, D., Cai, Y., Zhang, M., Lin, Y., Qing, J., An, Z., and  
35 Revenaugh, J.: A high-resolution, absolute-dated Holocene and deglacial Asian monsoon record from Dongge  
36 Cave, China, *Earth Planet. Sci. Rev.*, 233, 71-86, 2005.
- 37 ~~Emile-Geay, J., Cane, M., Seager, R., Kaplan, A., and Almasi, P.: El Niño as a mediator of the solar influence~~  
38 ~~on climate, *Paleoceanography*, 22, PA3210, 2007.~~
- 39 EPICA, [C. M. EPICA Community Members](#): One-to-one coupling of glacial climate variability in Greenland  
40 and Antarctica, *Nature*, 444, 195-198, 2006.

1 Etiope, G., Lassey, K. R., Klusman, R. W., and Boschi, E.: Reappraisal of the fossil methane budget and related  
2 emission from geologic sources, *Geophys. Res. Lett.*, 35, L09307, 2008.

3 Ferretti, D., Miller, J. B., White, J. W. C., Etheridge, D. M., Lassey, K. R., Lowe, D. C., MacFarling-Meure, C.  
4 M., Dreier, M. F., Trudinger, C. M., van Ommen, T. D., and Langenfelds, R. L.: Unexpected changes to the  
5 global methane budget over the past 2000 years, *Science*, 309, 1714-1717, 2005.

6 Finkel, R. C., and Nishizumi, K.: Beryllium 10 concentrations in the Greenland Ice Sheet Project 2 ice core  
7 from 3-40 ka, *J. Geophys. Res.*, 102, 26699-26706, 1997.

8 Fischer, H., Behrens, M., Bock, M., Richter, U., Schmitt, J., Loulergue, L., Chappellaz, J., Spahni, R., Blunier,  
9 T., Leuenberger, M., and Stocker, T. F.: Changing boreal methane sources and constant biomass burning  
10 during the last termination, *Nature*, 452, 864-867, 2008.

11 Fleitmann, D., Burns, S. J., Mangini, A., Mudelsee, M., Kramers, J., Villa, I., Neff, U., Al-Subbary, A. A.,  
12 Buettner, A., Hippler, D., and Matter, A.: Holocene ITCZ and Indian monsoon dynamics recorded in  
13 stalagmites from Oman and Yemen (Socotra), *Quaternary Sci. Rev.*, 26, 170-188, 2007.

14 [Flückiger, J., Blunier, T., Stauffer, B., Chappellaz, J., Spahni, R., Kawamura, K., Schwander, J., Stocker, T. F.,  
15 and Dahl-Jensen, D.: N<sub>2</sub>O and CH<sub>4</sub> variations during the last glacial epoch: Insight into global processes,  
16 \*Global Biogeochem. Cycles\*, 18, GB1020, 2004.](#)

17 Fung, I., John, J., Lerner, J., Matthews, E., Prather, M., Steele, L. P., and Fraser, P. J.: Three-dimensional model  
18 synthesis of the global methane cycle, *J. Geophys. Res.*, 96, 13033-13065, 1991.

19 Goldewijk, K. K., Beusen, A., and Janssen, P.: Long-term dynamic modelling of global population and built-up  
20 area in a spatially explicit way: HYDE 3.1, *The Holocene*, 1-9, 2010.

21 Gorham, E., Lehman, C., Dyke, A., Janssens, J., and Dyke, L.: Temporal and spatial aspects of peatland  
22 initiation following deglaciation in North America, *Quaternary Sci. Rev.*, 26, 300-311, 2007.

23 [Gow, A. J., and Meese, D.: Physical properties, crystalline textures and c-axis fabrics of the Siple Dome  
24 \(Antarctica\) ice core, \*J. Glaciol.\*, 53, 573-584, 2007.](#)

25 [Grachev, A. M., Brook, E. J., and Severinghaus, J. P.: Abrupt changes in atmospheric methane at the MIS 5b-5a  
26 transition, \*Geophys. Res. Lett.\*, 34, L20703, 2007.](#)

27 Grachev, A. M., Brook, E. J., Severinghaus, J. P., and Piasias, N. G.: Relative timing and variability of  
28 atmospheric methane and GISP2 oxygen isotopes between 68 and 86 ka, *Global Biogeochem. Cy.*, 23,  
29 GB2009, 2009.

30 Guillevic, M., Bazin, L., Landais, A., Stowasser, C., Masson-Delmotte, V., Blunier, T., Eynaud, F., Falourd, S.,  
31 Michel, E., Minster, B., Popp, T., Prié, F., and Vinther, B. M.: Evidence for a three-phase sequence during  
32 Heinrich Stadial 4 using a multi-proxy approach based on Greenland ice core records, *Clim. Past*, 10, 2115-  
33 2133, 2014.

34 Guo, Z., Zhou, X., and Wu, H.: Glacial-interglacial water cycle, global monsoon and atmospheric methane  
35 changes, *Clim. Dynam.*, 39, 1073-1092, 2012.

36 Gupta, A. K., Das, M., and Anderson, D. M.: Solar forcing on the Indian summer monsoon during the Holocene,  
37 *Geophys. Res. Lett.*, 32, L17703, 2005.

38 [Hao, W. M., and Ward, D. E.: Methane production from global biomass burning, \*J. Geophys. Res.\*, 98, 20657-  
39 20661, 1993.](#)

1 ~~Harder, S. L., Shindell, D. T., Schmidt, G. A., and Brook, E. J.: A global climate model study of CH<sub>4</sub> emissions~~  
2 ~~during the Holocene and glacial-interglacial transitions constrained by ice core data, *Global Biogeochem. Cy.*,~~  
3 ~~21, GB1011, 2007.~~

4 Haug, G. H., Hughen, K. A., Sigman, D. M., Peterson, L. C., and Röhl, U.: Southward migration of the  
5 intertropical convergence zone through the Holocene, *Science*, 293, 1304-1308, 2001.

6 Hodson, E. L., Poulter, B., Zimmermann, N. E., Prigent, C., and Kaplan, J. O.: The El Niño-Southern  
7 Oscillation and wetland methane interannual variability, *Geophys. Res. Lett.*, 38, L08810, 2011.

8 [Hopcroft, P. O., Valdes, P. J., and Beerling, D. J.: Simulating idealized Dansgaard-Oeschger events and their](#)  
9 [potential impacts on the global methane cycle, \*Quat. Sci. Rev.\*, 30, 3258-3268, 2011.](#)

10 ~~Hoek, W. Z.: Vegetation response to the ~14.7 and ~11.5 ka cal. BP climate transitions: is vegetation lagging~~  
11 ~~climate?, *Global Planet. Change*, 30, 103-115, 2001.~~

12 [Hughen, K. A., Overpeck, J. T., Peterson, L. C., and Trumbore, S.: Rapid climate changes in the tropical](#)  
13 [Atlantic region during the last deglaciation, \*Nature\*, 380, 51-54, 1996.](#)

14 Jiang, H., Muscheler, R., Björck, S., Seidenkrantz, M. S., Olsen, J., Sha, L., Sjolte, J., Eriksson, J., Ran, L.,  
15 Knudsen, K. L., and Knudsen, M. F.: Solar forcing of Holocene summer sea-surface temperatures in the  
16 northern North Atlantic, *Geology*, 43, 2015.

17 Joabsson, A., and Christensen, T. R.: Methane emissions from wetlands and their relationship with vascular  
18 plants: an Arctic example, *Global Change Biol.*, 7, 919-932, 2001.

19 [Kaplan, J. O., Krumhardt, K. M., Ellis, E. C., Ruddiman, W. F., Lemmen, C., and Goldewijk, K. K.: Holocene](#)  
20 [carbon emissions as a result of anthropogenic land cover change, \*The Holocene\*, 21, 775-791, 2011.](#)

21 [Kirby, M. E., Lund, S. P., Patterson, W. P., Anderson, M. A., Bird, B. W., Ivanovici, L., Monarrez, P., and](#)  
22 [Nielsen, S.: A Holocene record of Pacific Decadal Oscillation \(PDO\)-related hydrologic variability in](#)  
23 [Southern California \(Lake Elsinore, CA\), \*J. Paleolimnol.\*, 44, 819-839, 2010.](#)

24 Kobashi, T., Severinghaus, J. P., Brook, E. J., Barnola, J. -M., and Grachev, A. M.: Precise timing and  
25 characterization of abrupt climate change 8200 years ago from air trapped in polar ice, *Quaternary Sci. Rev.*,  
26 26, 1212-1222, 2007.

27 Kobashi, T., Severinghaus, J. P., and Barnola, J. -M.:  $4 \pm 1.5$  °C abrupt warming 11270 yr ago identified from  
28 trapped air in Greenland ice, *Earth Planet. Sci. Lett.*, 268, 397-407, 2008.

29 [Landais, A., Dreyfus, G., Capron, E., Masson-Delmotte, V., Sanchez-Goñi, M. F., Desprat, S., Hoffmann, G.,](#)  
30 [Jouzel, J., Leuenberger, M., and Johnsen, S.: What drives the millennial and orbital variations of  \$\delta^{18}\text{O}\_{\text{am}}\$ ?](#)  
31 [Quat. Sci. Rev., 29, 235-246, 2010.](#)

32 Levine, J. G., Wolff, E. W., Jones, A. E., Sime, L. C., Valdes, P. J., Archibald, A. T., Carver, G. D., Warwick, N.  
33 J., and Pyle, J. A.: Reconciling the changes in atmospheric methane sources and sinks between the Last  
34 Glacial Maximum and the pre-industrial era, *Geophys. Res. Lett.*, 38, L23804, 2011.

35 Levy II, H.: Normal atmosphere: large radical and formaldehyde concentrations predicted, *Science*, 173, 141-  
36 143, 1971.

37 ~~Lisiecki, L. E., and Raymo, M. E.: A Pliocene-Pleistocene stack of 57 globally distributed benthic  $\delta^{18}\text{O}$  records,~~  
38 ~~*Paleoceanography*, 20, PA1003, 2005.~~

1 Louergue, L., Schilt, A., Sphani, R., Masson-Delmotte, V., Blunier, T., Lemieux, B., Barnola, J. -M., Raynaud,  
2 D., Stocker, T. F., and Chappellaz, J.: Orbital and millennial-scale features of atmospheric CH<sub>4</sub> over the past  
3 800,000 years, *Nature*, 453, 383-386, 2008.

4 Lyon, B., and Barnston, A. G.: ENSO and the spatial extent of interannual precipitation extremes in tropical  
5 land areas, *J. Clim.*, 18, 5095-5109, 2005.

6 MacDonald, G. M., Beilman, D. W., Kremenetski, K. V., Sheng, Y., Smith, L. C., and Velichko, A. A.: Rapid  
7 early development of circumarctic peatlands and atmospheric CH<sub>4</sub> and CO<sub>2</sub> variations, *Science*, 314, 285-288,  
8 2006.

9 MacFarling-Meure, C., Etheridge, D., Trudinger, C., Steele, P., Langenfelds, R., van Ommen, T., Smith, A., and  
10 Elkins, J.: Law Dome CO<sub>2</sub>, CH<sub>4</sub> and N<sub>2</sub>O ice core records extended to 2000 years BP, *Geophys. Res. Lett.*, 33,  
11 L14810, 2006.

12 ~~Mantua, N. J., and Hare, S. R.: The Pacific Decadal Oscillation, *J. Oceanography*, 58, 35-44, 2002.~~

13 Marchitto, T. M., Muscheler, R., Ortiz, J. D., Carriquiry, J. D., and van Geen, A.: Dynamical response of the  
14 tropical Pacific Ocean to solar forcing during the early Holocene, *Science*, 330, 1378-1381, 2010.

15 Marcott, S. A., Shakun, J. D., Clark, P. U., and Mix, A. C.: A reconstruction of regional and global temperature  
16 for the past 11300 years, *Science*, 339, 1198-1201, 2013.

17 ~~Melton, J. R., Schaefer, H., and Whiticar, M. J.: Enrichment in <sup>13</sup>C of atmospheric CH<sub>4</sub> during the Younger  
18 Dryas termination, *Clim. Past*, 8, 1177-1197, 2012.~~

19 [Mischler, J. A., Sowers, T. A., Alley, R. B., Battle, M., McConnell, J. R., Mitchell, L., Popp, T., Sofen, E., and  
20 Spencer, M. K.: Carbon and hydrogen isotopic composition of methane over the last 1000 years, \*Global  
21 Biogeochem. Cycles\*, 23, GB4024, 2009.](#)

22 Mitchell, L. E., Brook, E. J., Sowers, T., McConnell, J. R., and Taylor, K.: Multidecadal variability of  
23 atmospheric methane, 1000–1800 C.E., *J. Geophys. Res.*, 116, G02007, 2011.

24 Mitchell, L. E., Brook, E. J., Lee, J. E., Buizert, C., and Sowers, T.: Constraints on the Late Holocene  
25 anthropogenic contribution to the atmospheric methane budget, *Science*, 342, 964-966, 2013.

26 [Moy, C.M., Seltzer, G. O., Rodbell, D. T., and Anderson, D. M.: Variability of El Niño/Southern Oscillation  
27 activity at millennial timescales during the Holocene epoch, \*Nature\*, 420, 162-165, 2002.](#)

28 ~~Moros, M., Emeis, K. C., Risebrobakken, B., Snowball, I., Kuijpers, A., McManus, J., and Jansen, E.: Sea  
29 surface temperatures and ice rafting in the Holocene north Atlantic: climate influences on northern Europe  
30 and Greenland, *Quaternary Sci. Rev.*, 23, 2113-2126, 2004.~~

31 Neff, U., Burns, S. J., Mangini, A., Mudelsee, M., Fleitmann, D., and Matter, A.: Strong coherence between  
32 solar variability and the monsoon in Oman between 9 and 6 kyr ago, *Nature*, 411, 290-293 2001.

33 Petrenko, V. V., Smith, A. M., Brook, E. J., Lowe, D., Riedel, K., Brailsford, G., Hua, Q., Schaefer, H., Reeh,  
34 N., Weiss, R. F., Etheridge, D., and Severinghaus, J. P.: 14CH<sub>4</sub> measurements in Greenland ice: investigating  
35 last glacial termination CH<sub>4</sub> sources, *Science*, 324, 506-508, 2009.

36 [Prather, M. J., Holmes, C. D., and Hsu, J.: Reactive greenhouse gas scenarios: Systematic exploration of  
37 uncertainties and the role of atmospheric chemistry, \*Geophys. Res. Lett.\*, 39, L0980, 2012.](#)

38 ~~Petrenko, V. V., Severinghaus, J. P., Smith, A. M., Riedel, K., Brook, E. J., Schaefer, H., Baggenstos, D., Harth,  
39 C., Hua, Q., Buizert, C., Schilt, A., Fain, X., Mitchell, L. E., Bauska, T., and Orsi, A.: Ice core measurements~~

~~of  $^{14}\text{C}$  show no evidence of methane release from methane hydrates or old permafrost carbon during a large warming event 11,600 years ago. In EGU General Assembly Conference Abstracts, 17, 6712, 2015.~~

Rasmussen, S. O., Andersen, K. K., Svensson, A. M., Steffensen, J. P., Vinther, B. M., Clausen, H. B., Siggaard-Andersen, M. -L., Johnsen, S. J., Larsen, L. B., Dahl-Jensen, D., Bigler, M., Rothlisberger, R., Fischer, H., Goto-Azuma, K., Hansson, M. E., and Ruth, U.: A new Greenland ice core chronology for the last glacial termination, *J. Geophys. Res.*, 111, D06102, 2006.

[Rasmussen, S. O., Abbott, P. M., Blunier, T., Bourne, A. J., Brook, E., Buchardt, S. L., Buizert, C., Chappellaz, J., Clausen, H. B., Cook, E., Dahl-Jensen, D., Davies, S. M., Guillevic, M., Kipstuhl, S., Laepple, T., Seierstad, I. K., Severinghaus, J. P., Steffensen, J. P., Stowasser, C., Svensson, A., Vallelonga, P., Vinther, B. M., Wilhelms, F., and Winstrup, M.: A first chronology for the North Greenland Eemian Ice Drilling \(NEEM\) ice core, \*Clim. Past\*, 9, 2713-2730, 2013.](#)

Renssen, H., Goosse, H., and Muscheler, R.: Coupled climate model simulation of Holocene cooling events: oceanic feedback amplifies solar forcing, *Clim. Past*, 2, 79-90, 2006.

Rhee, T. S., Kettle, A. J., and Andreae, M. O.: Methane and nitrous oxide emissions from the ocean: A reassessment using basin-wide observations in the Atlantic, *J. Geophys. Res.*, 114, D12304, 2009.

[Rhodes, R. H., Brook, E. J., Chiang, J. C. H., Blunier, T., Maselli, O. J., McConnell, J. R., Romanini, D., and Severinghaus, J. P.: Enhanced tropical methane production in response to iceberg discharge in the North Atlantic, \*Science\*, 348, 1016-1019, 2015.](#)

~~Ruddiman, W. F., Guo, Z., Zhou, X., Wu, H., and Yu, Y.: Early rice farming and anomalous methane trends, *Quaternary Sci. Rev.*, 27, 1291-1295, 2008.~~

[Ruddiman, W. F., Kutzbach, J. E., and Vavrus, S. J.: Can natural or anthropogenic explanations of late-Holocene  \$\text{CO}\_2\$  and  \$\text{CH}\_4\$  increases be falsified?, \*The Holocene\*, 21, 865-879, 2011.](#)

Sanderson, M. G.: Biomass of termites and their emissions of methane and carbon dioxide: A global database, *Global Biogeochem. Cy.*, 10, 543-558, 1996.

Sapart, C. J., Monteil, G., Prokopiou, M., van de Wal, R. S. W., Kaplan, J. O., Sperlich, P., Krumhardt, K. M., van der Veen, C., Houweling, S., Krol, M. C., Blunier, T., Sowers, T., Martinerie, P., Witrant, E., Dahl-Jensen, D., and Röckmann, T.: Natural and anthropogenic variations in methane sources during the past two millennia, *Nature*, 490, 85-88, 2012.

~~Schaefer, H., Whiticar, M. J., Brook, E. J., Petrenko, V. V., Ferretti, D. F., and Severinghaus, J. P.: Ice records of  $\delta^{13}\text{C}$  for atmospheric  $\text{CH}_4$  across the Younger Dryas-Preboreal transition, *Science*, 313, 1109-1112, 2006.~~

Schuur, E. A. G., McGuire, A. D., Schadel, C., Grosse, G., Harden, J. W., Hayes, D. J., Hugelius, G., Koven, C. D., Kuhry, P., Lawrence, D. M., Natali, S. M., Olefeldt, D., Romanovsky, V. E., Schaefer, K., Turetsky, M. R., Treat, C. C., and Vonk, J. E.: Climate change and the permafrost carbon feedback, *Nature*, 520, 171-179.

Severinghaus, J. P., Beaudette, R., Headly, M. A., Taylor, K., and Brook, E. J.: Oxygen-18 of  $\text{O}_2$  records the impact of abrupt climate change on the terrestrial biosphere, *Science*, 324, 1431-1434, 2009.

Singarayer, J. S., Valdes, P. J., Friedlingstein, P., Nelson, S., and Beerling, D. J.: Late Holocene methane rise caused by orbitally controlled increase in tropical sources, *Nature*, 470, 82-86, 2011.

Sowers, T.: [Atmospheric methane isotope records covering the Holocene period, \*Quat. Sci. Rev.\*, 29, 213-221.](#) ~~Late Quaternary atmospheric  $\text{CH}_4$  isotope record suggests marine clathrate are stable, *Science*, 311, 838-840, 2010.~~

- 1 Spahni, R., Schwander, J., Flückiger, J., Stauffer, B., Chappellaz, J. and Raynaud, D.: The attenuation of fast  
2 atmospheric CH<sub>4</sub> variations recorded in polar ice cores, *Geophys. Res. Lett.*, 30, 1571, 2003.
- 3 Spahni, R., Chappellaz, J., Stocker, T. F., Loulergue, L., Hausammann, G., Kawamura, K., Flückiger, J.,  
4 Schwander, J., Raynaud, D., Masson-Delmotte, V., and Jouzel, J.: Atmospheric methane and nitrous oxide of  
5 late Pleistocene from Antarctic ice cores, *Science*, 310, 1317-1321, 2005.
- 6 [Sperlich, P., Schaefer, H., Mikaloff Fletcher, S. E., Guillevic, M., Lassey, K., Sapart, C. J., Röckmann, T., and  
7 Blunier, T.: Carbon isotope ratios suggest no additional methane from boreal wetlands during the rapid  
8 Greenland Interstadial 21.2, \*Global Biogeochem. Cycles\*, 29, 1962-1976, 2015.](#)
- 9 [Stocker, T. F., Qin, D., Plattner, G.-K., Tignor, M., Allen, S. K., Boschung, J., Nauels, A., Xia, Y., Bex, V., and  
10 Midgley, P. M. \(Eds.\): IPCC, 2013: Climate Change 2013: The Physical Science Basis, Contribution of  
11 Working Group I to the Fifth Assessment Report of the Intergovernmental Panel on Climate Change,  
12 Cambridge University Press, Cambridge, United Kingdom and New York, NY, USA, 1535 pp., 2013.](#)
- 13 ~~Stocker, T. F., Dahe, Q., and Plattner, G.-K.: Climate Change 2013: The Physical Science Basis. Contribution  
14 of Working Group I to the Fifth Assessment Report of the Intergovernmental Panel on Climate Change,  
15 Summary for Policymakers (IPCC, 2013), 2013.~~
- 16 ~~Stuiver, M., and Grootes, P. M.: GISP2 oxygen isotope ratios, *Quaternary Research*, 53, 277-284, 2000.~~
- 17 [Taylor, K. C., Alley, R. B., Meese, D. A., Spencer, M. K., Brook, E. J., Dunbar, N. W., Finkel, R. C., Gow, A. J.,  
18 Kurbatov, A. V., Lamorey, G. W., Mayewski, P. A., Meyerson, E. A., Nishiizumi, K., and Zielinski, G. A.:  
19 Dating the Siple Dome \(Antarctica\) ice core by manual and computer interpretation of annual layering, \*J.  
20 Glaciol.\*, 50, 453-461, 2004.](#)
- 21 [Tzedakis, P. C., Pälike, H., Roucoux, K. H., and de Abreu, L.: Atmospheric methane, southern European  
22 vegetation and low-mid latitude links on orbital and millennial timescales, \*Earth Planet. Sci. Lett.\*, 277, 307-  
23 317, 2009.](#)
- 24 Valdes, P. J., Beerling, D. J., and Johnson, C. E.: The ice age methane budget, *Geophys. Res. Lett.*, 32, L02704,  
25 2005.
- 26 Wang, Y., Cheng, H., Edwards, R. L., He, Y., Kong, X., An, Z., Wu, J., Kelly, M. J., Dykoski, C. A., and Li, X.:  
27 The Holocene Asian monsoon: links to solar changes and north Atlantic climate, *Science*, 308, 854-857, 2005.
- 28 ~~WAIS Divide Project Members: Onset of deglacial warming in West Antarctica driven by local orbital forcing,  
29 *Nature*, 500, 440-446, 2013.~~
- 30 WAIS Divide Project Members: Precise inter-polar phasing of abrupt climate change during the last ice age,  
31 *Nature*, 520, 661-665, 2015.
- 32 Walter, K. M., Zimov, S. A., Chanton, J. P., Verbyla, D., and Chapin III, F. S.: Methane bubbling from Siberian  
33 thaw lakes as a positive feedback to climate warming, *Nature*, 443, 71-75, 2006.
- 34 Walter, K. M., Edwards, M. E., Grosse, G., Zimov, S. A., and Chapin III, F. S.: Thermokarst lakes as a source  
35 of atmospheric CH<sub>4</sub> during the last deglaciation, *Science*, 318, 633-636, 2007.
- 36 Walter Anthony, K. M., Zimov, S. A., Grosse, G., Jones, M. C., Anthony, P. M., Chapin III, F. S., Finlay, J. C.,  
37 Mack, M. C., Davydov, S., Frenzel, P., and Frohling, S.: A shift of thermokarst lakes from carbon sources to  
38 sinks during the Holocene epoch, *Nature*, 511, 452-456, 2014.



1 Weber, S. L., Drury, A. J., Toonen, W. H. J., and van Weele, M.: Wetland methane emissions during the Last  
2 Glacial Maximum estimated from PMIP2 simulations: Climate, vegetation, and geographic controls, *J.*  
3 *Geophys. Res.*, 115, D06111, 2010.

4 ~~Wik, M., Thornton, B. F., Bastviken, D., Uhlback, J., and Crill, P. M.: Biased sampling of methane release from~~  
5 ~~northern lakes: A problem for extrapolation, *Geophys. Res. Lett.*, 43, 2016.~~

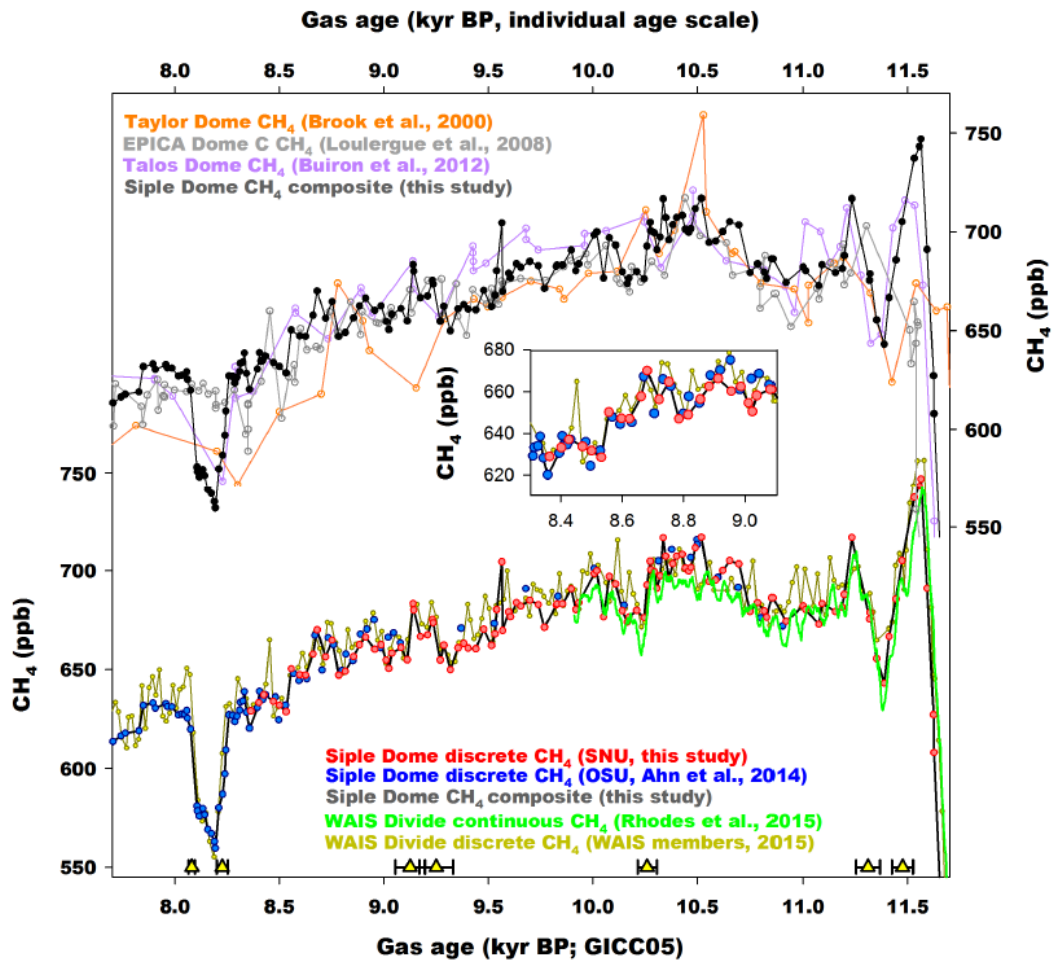
6 ~~Williams, J. W., D. M. Post, L. C. Cwynar, A. F. Lotter and A. J. Levesque (2002), Rapid and widespread~~  
7 ~~vegetation responses to past climate change in the North Atlantic region, *Geology*, 30, 971-974.~~

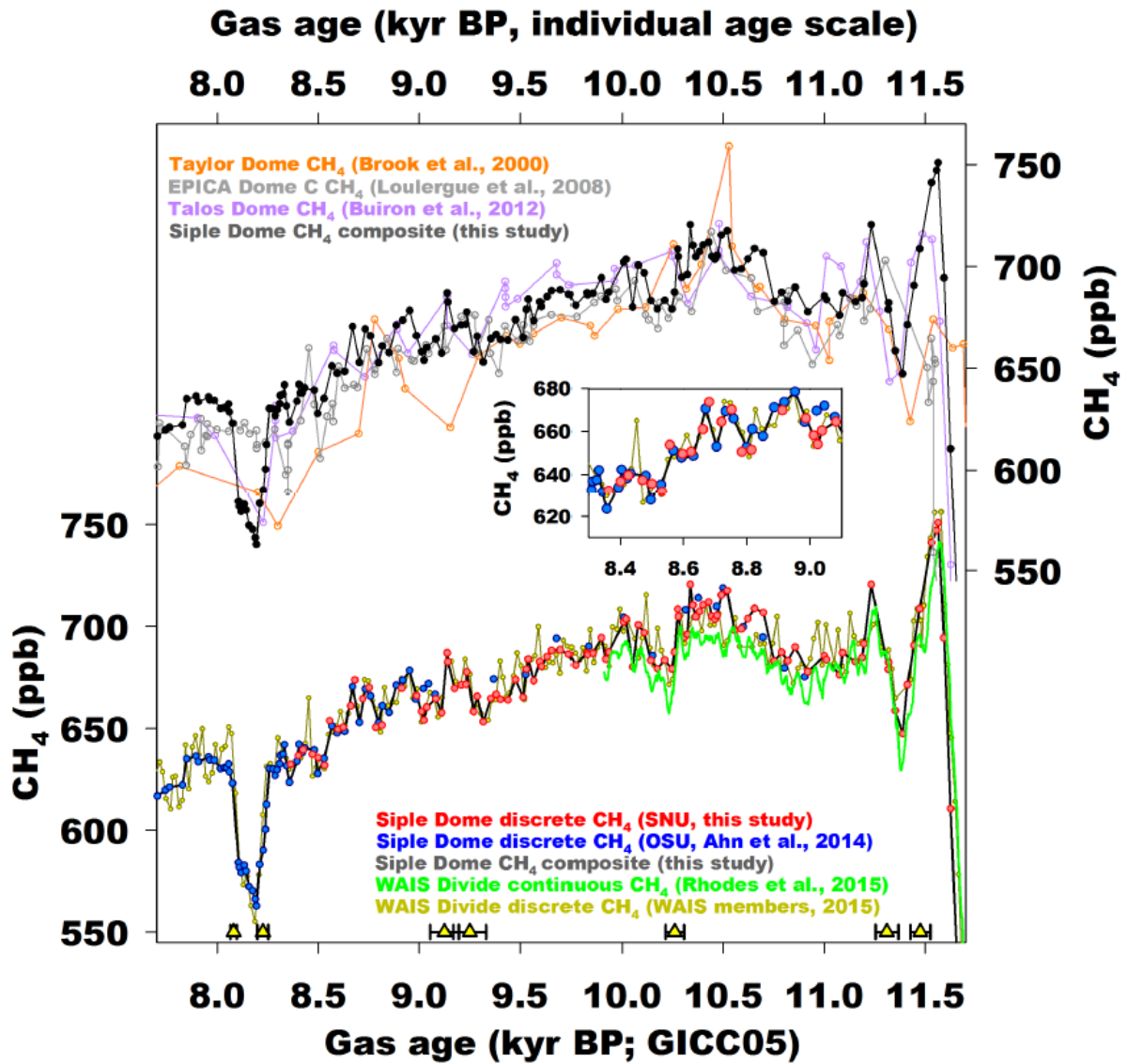
8 ~~Yiou, F., Raisbeck, G. M., Baumgartner, S., Beer, J., Hammer, C., Johnsen, S., Jouzel, J., Kubik, P. W.,~~  
9 ~~Lestringuez, J., Stievenard, M., Suter, M., and Yiou, P.: Beryllium-10 in the Greenland Ice Core Project ice~~  
10 ~~core at Summit, Greenland, *J. Geophys. Res.*, 102, 26783-26794, 1997.~~

11 ~~Yu, Z.: Rapid response of forested vegetation to multiple climatic oscillations during the last deglaciation in the~~  
12 ~~northeastern United States, *Quaternary Res.*, 67, 297-303, 2007.~~

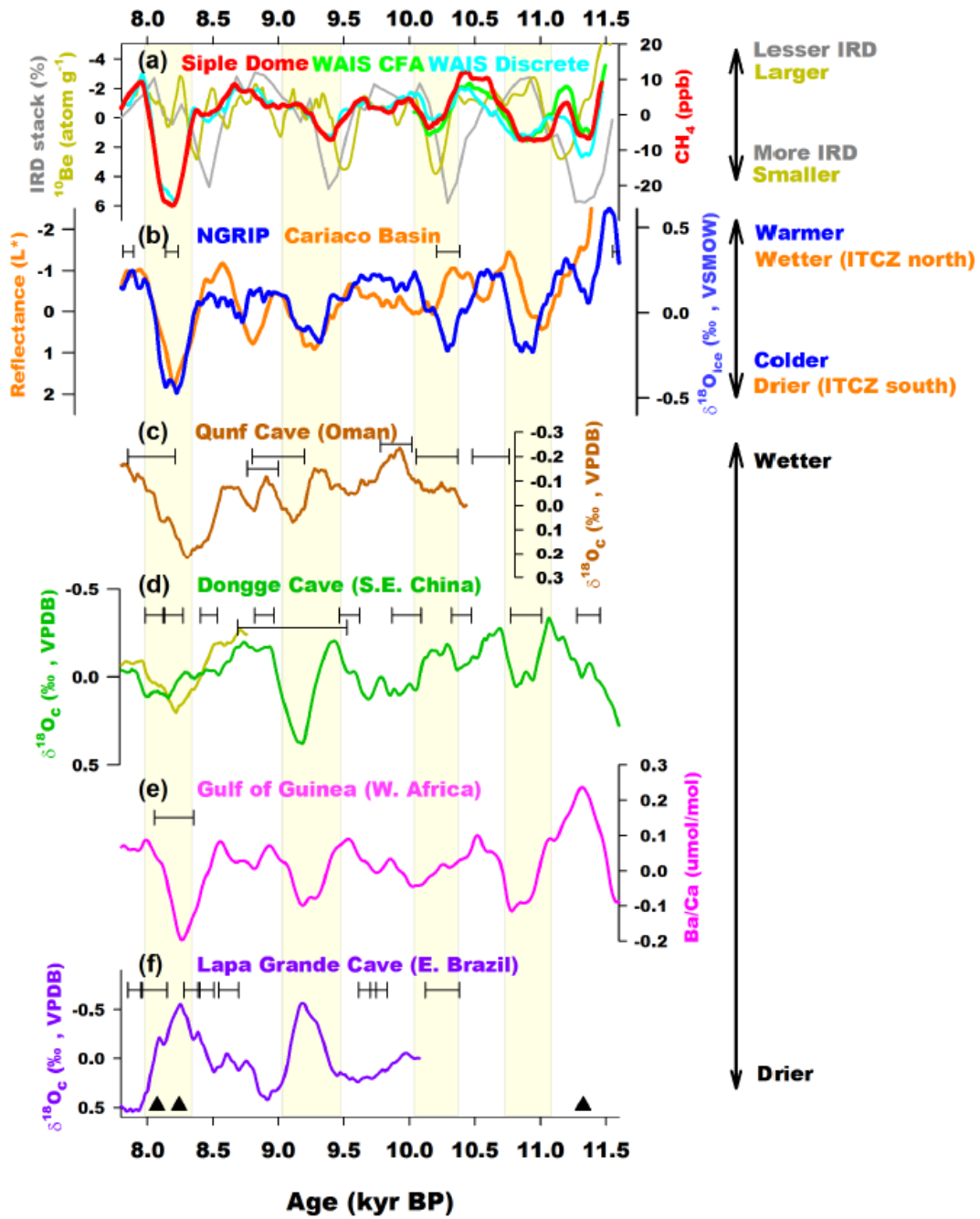
13 Yu, Z., Loisel, J., Turetsky, M. R., Cai, S., Zhao, Y., Frohling, S., MacDonald, G. M., and Bubier, J. L.:  
14 Evidence for elevated emissions from high-latitude wetlands contributing to high atmospheric CH<sub>4</sub>  
15 concentration in the early Holocene, *Global Biogeochem. Cy.*, 27, 1-10, 2013.

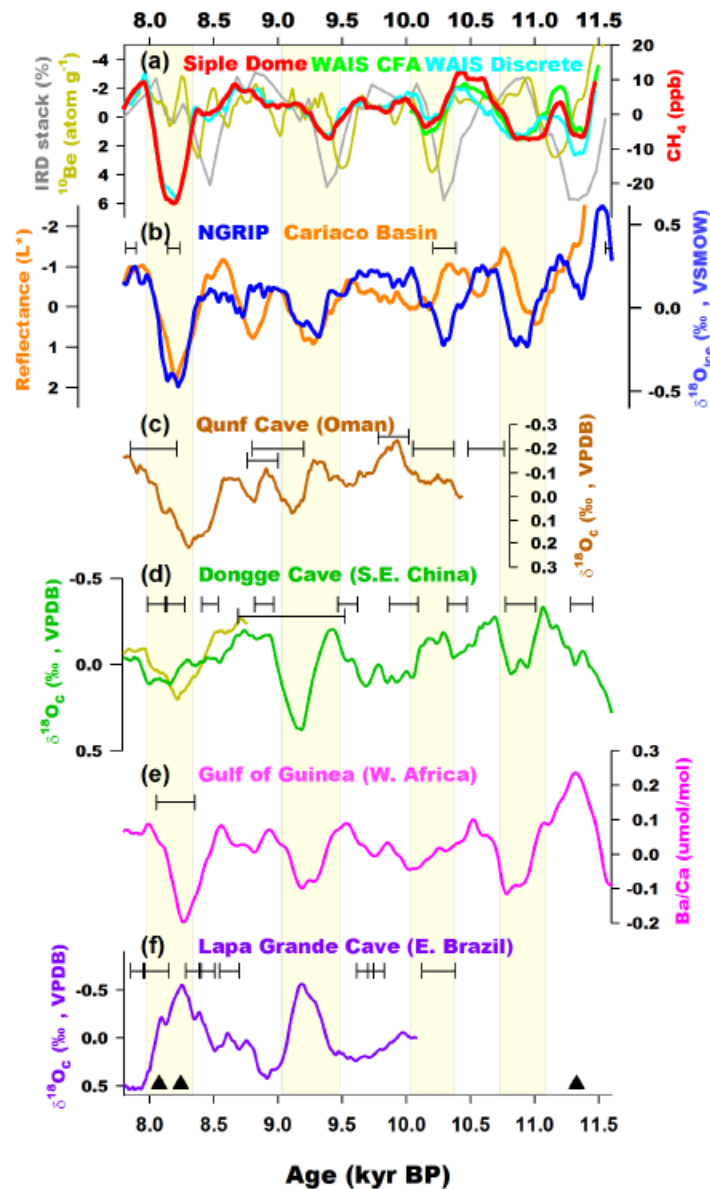
16  
17  
18  
19  
20  
21  
22  
23  
24  
25  
26  
27





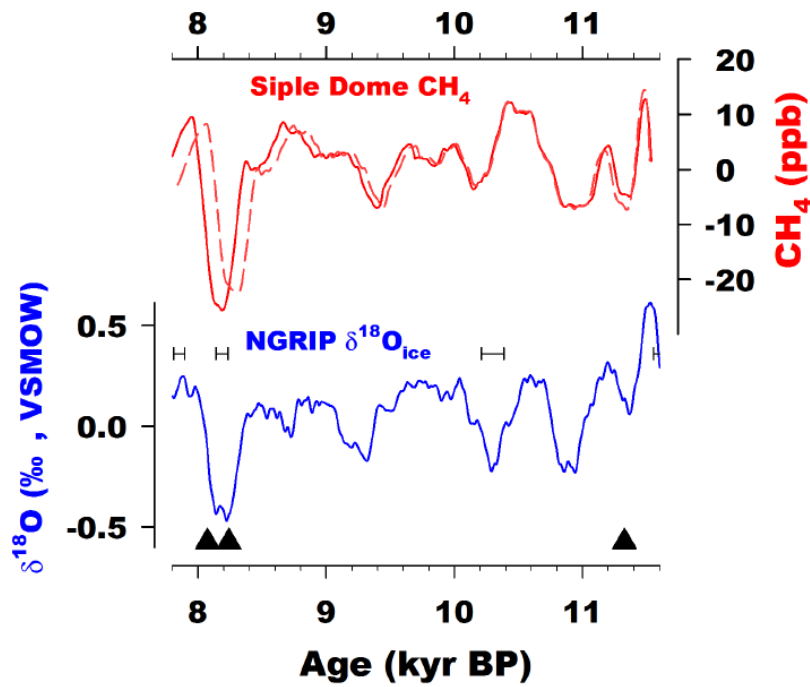
1  
2 Figure 1. [Atmospheric CH<sub>4</sub> concentration reconstructions during the early Holocene. Top: new high-resolution Siple](#)  
3 [Dome composite \(black, this study and Ahn et al., 2014\) compared with previous records from Taylor Dome \(orange,](#)  
4 [Brook et al., 2000\), EPICA Dome C \(grey, Loulergue et al., 2008\), and Talos Dome \(purple, Buiron et al., 2012\).](#)  
5 [Bottom: Siple Dome CH<sub>4</sub> records measured in at OSU \(blue, Ahn et al., 2014\) and SNU \(red, this study\). Siple Dome](#)  
6 [composite \(black line\) is plotted with WAIS Divide discrete \(dark yellow, WAIS Divide project members, 2015\) and](#)  
7 [continuous measurement records \(green, Rhodes et al., 2015\). Inset: Enlarged plot showing overlapped interval](#)  
8 [between OSU and SNU Siple Dome data.](#)  
9





1  
2 **Figure 2. Millennial scale climate variability.** All proxies presented here were smoothed by 250-year running average  
3 **and detrended by high-pass filter with 1/1800-year window.** (a) Siple Dome  $\text{CH}_4$  (red, this study), Greenland  $^{10}\text{Be}$   
4 **(dark yellow, Finkel and Nishizumii, 1997), North Atlantic IRD stack (grey, Bond et al., 2001). Also shown are WAIS**  
5 **Divide  $\text{CH}_4$  data by discrete (cyan, denoted “WAIS Discrete”, WAIS Divide project members, 2015) and continuous**  
6 **(yellow green, denoted “WAIS CFA”, Rhodes et al., 2015) technique.** (b) NGRIP stable water isotope ratio (blue,  
7 **Rasmussen et al., 2006) and Cariaco Basin reflectance (orange, Deplazes et al., 2013).** (c) Qunf Cave speleothem  
8 **oxygen isotope (Fleitmann et al., 2007).** (d) Dongge Cave speleothem oxygen isotope (green, Dykoski et al., 2005; dark  
9 **yellow, Wang et al., 2005).** (e) Gulf of Guinea planktonic Ba/Ca ratio (Weldeab et al., 2007). (f) Lapa Grande Cave  
10 **speleothem oxygen isotope (purple, Strikis et al., 2011). Black solid triangles are age tie-points used to adjust Siple**  
11 **Dome and WAIS Divide  $\text{CH}_4$  data to GICC05 scale. Millennial-scale variability of  $\text{CH}_4$  and other climate proxies. All**  
12 **climate proxies are smoothed with 250-year window after filtered in 1/1800 year high-pass window.** (a) Millennial-  
13 **scale Siple Dome  $\text{CH}_4$  anomaly (red) is plotted with North Atlantic IRD stack (grey, Bond et al., 2001) and Greenland**  
14 **composite  $^{10}\text{Be}$  concentration from GRIP and GISP2 (olive yellow, Finkel and Nishizumii, 1997; Yiou et al., 1997).-**  
15 **GRIP and GISP2 ice core chronologies are synchronized to GICC05 scale by visual matching between  $\delta^{18}\text{O}_{\text{ice}}$  time-**

1 series. WAIS Divide  $\text{CH}_4$  anomalies are shown in green (Rhodes et al., 2015) and cyan (WAIS Divide Project  
 2 Members, 2015). (b) NGRIP  $\delta^{18}\text{O}_{\text{ice}}$  on GICC05 time scale (dark blue, Rasmussen et al., 2006) and Cariaco basin  
 3 sediment reflectance (orange, Deplazes et al., 2013). Black error bars indicate maximum age uncertainty of GICC05  
 4 scale as stated in Rasmussen et al. (2006). (e) Oman speleothem records from Qunf (purple, Fleitmann et al., 2007)  
 5 and Hoti cave (grey, Neff et al., 2001) on their own chronology. (d) Siple Dome AELAND (red, Severinghaus et al., 2009)  
 6 and Dongge Cave speleothem  $\delta^{18}\text{O}$  composite (green) from Dykoski et al. (2005) and Wang et al. (2005).



8  
 9 Figure 4.3. Upper: Comparison between Siple Dome  $\text{CH}_4$  anomalies plotted with gas age adjusted to GICC05 (red,  
 10 solid) and previous gas age (red, dashed; Brook et al., 2005). Lower: NGRIP  $\delta^{18}\text{O}$  anomaly in GICC05 scale. The  
 11 horizontal error bars denote the age uncertainty of GICC05 chronology (Rasmussen et al., 2006), and the black  
 12 triangles are age tie points used to adjusting the Siple Dome age scale to GICC05 scale.

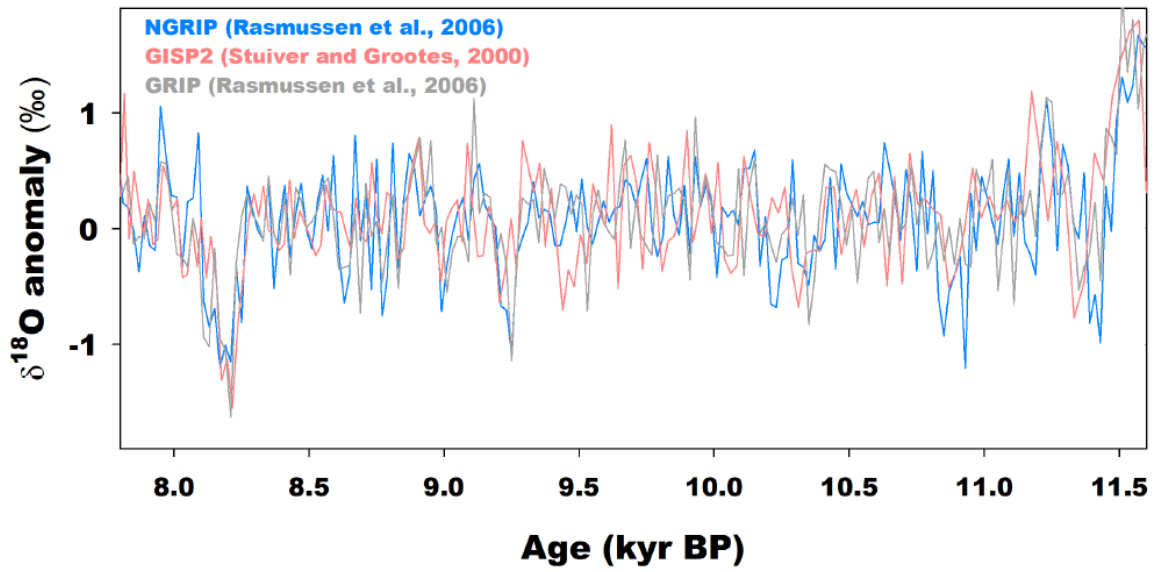
13



1  
2  
3  
4  
5  
6

Figure 4. Age difference between the new gas age scale adjusted to GICC05 by Monte Carlo matching with NEEM discrete CH<sub>4</sub> (Chappellaz et al., 2013) and the original gas age based on CH<sub>4</sub> and  $\delta^{18}\text{O}_{\text{atm}}$  correlation (Severinghaus et al., 2009).

1



2

3

4

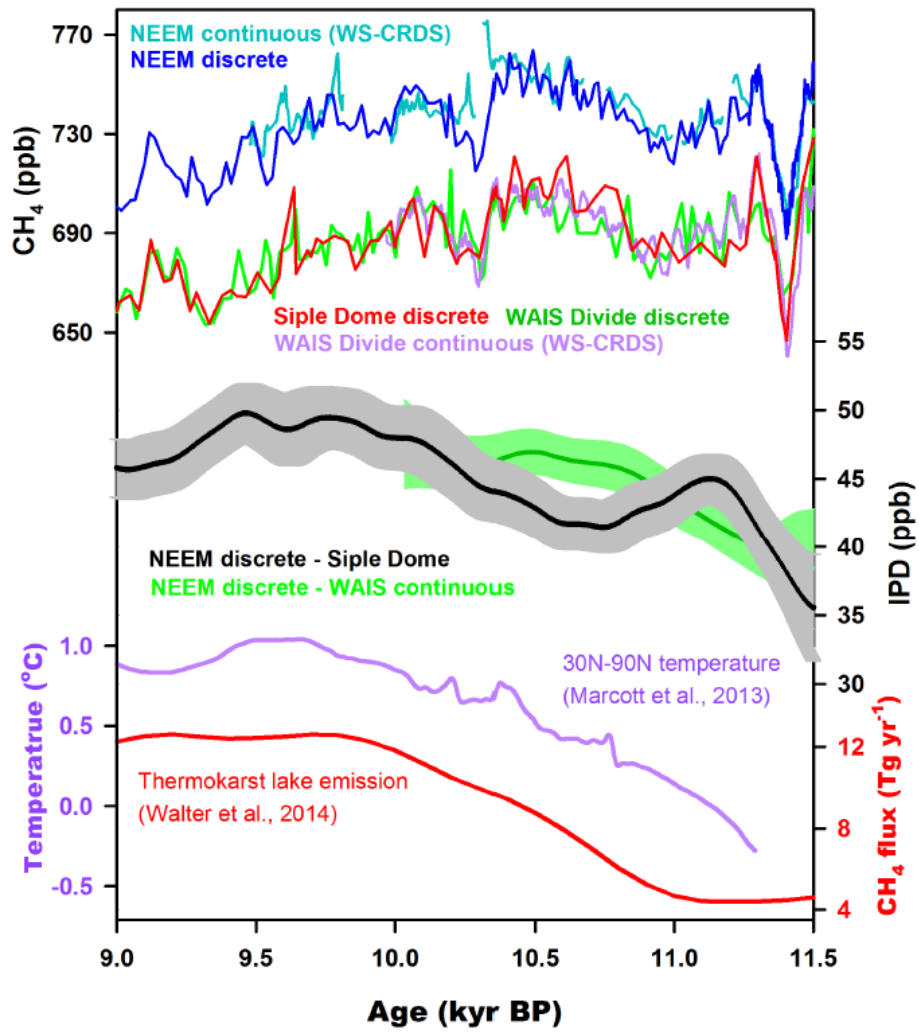
5

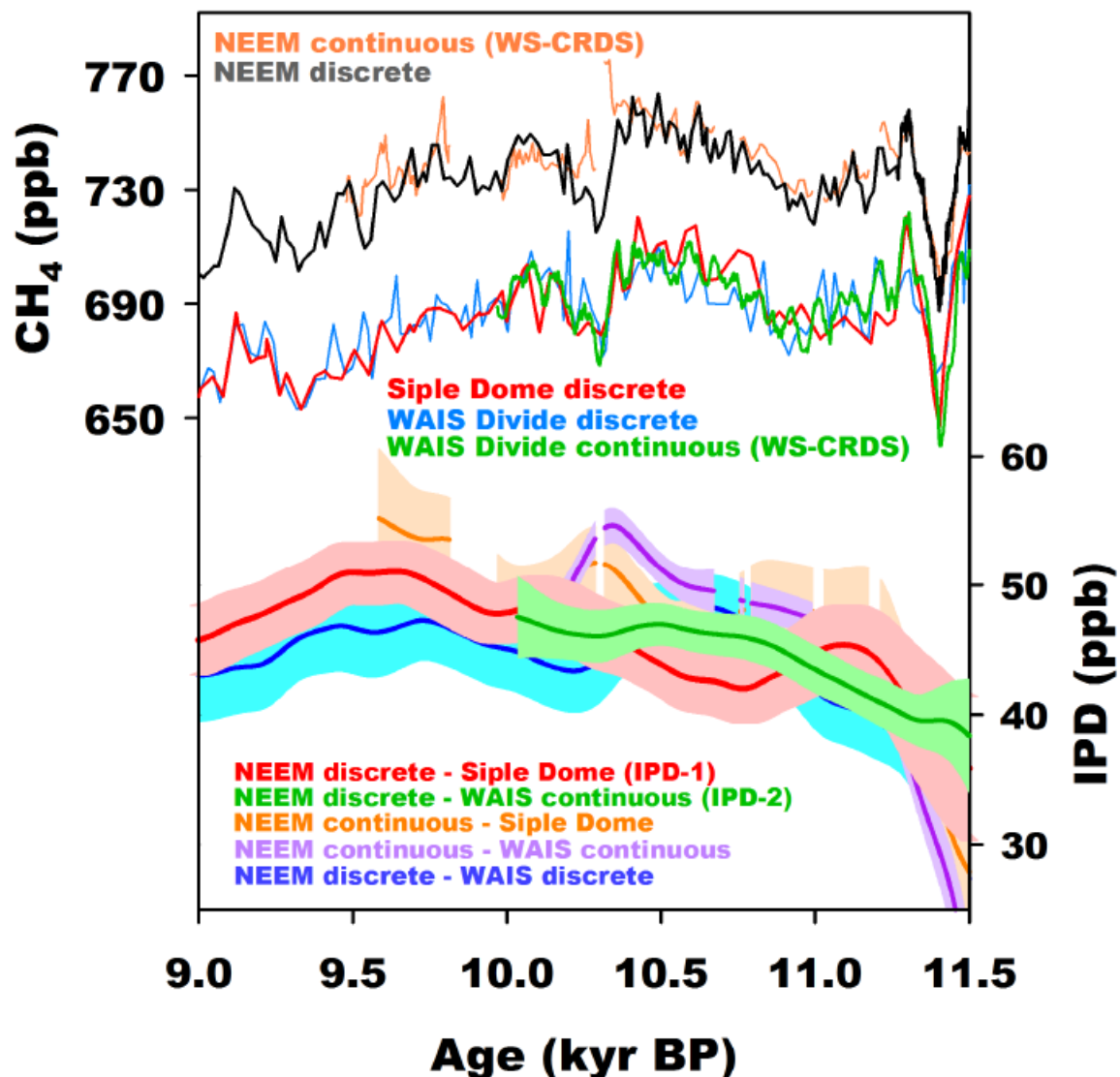
6

7

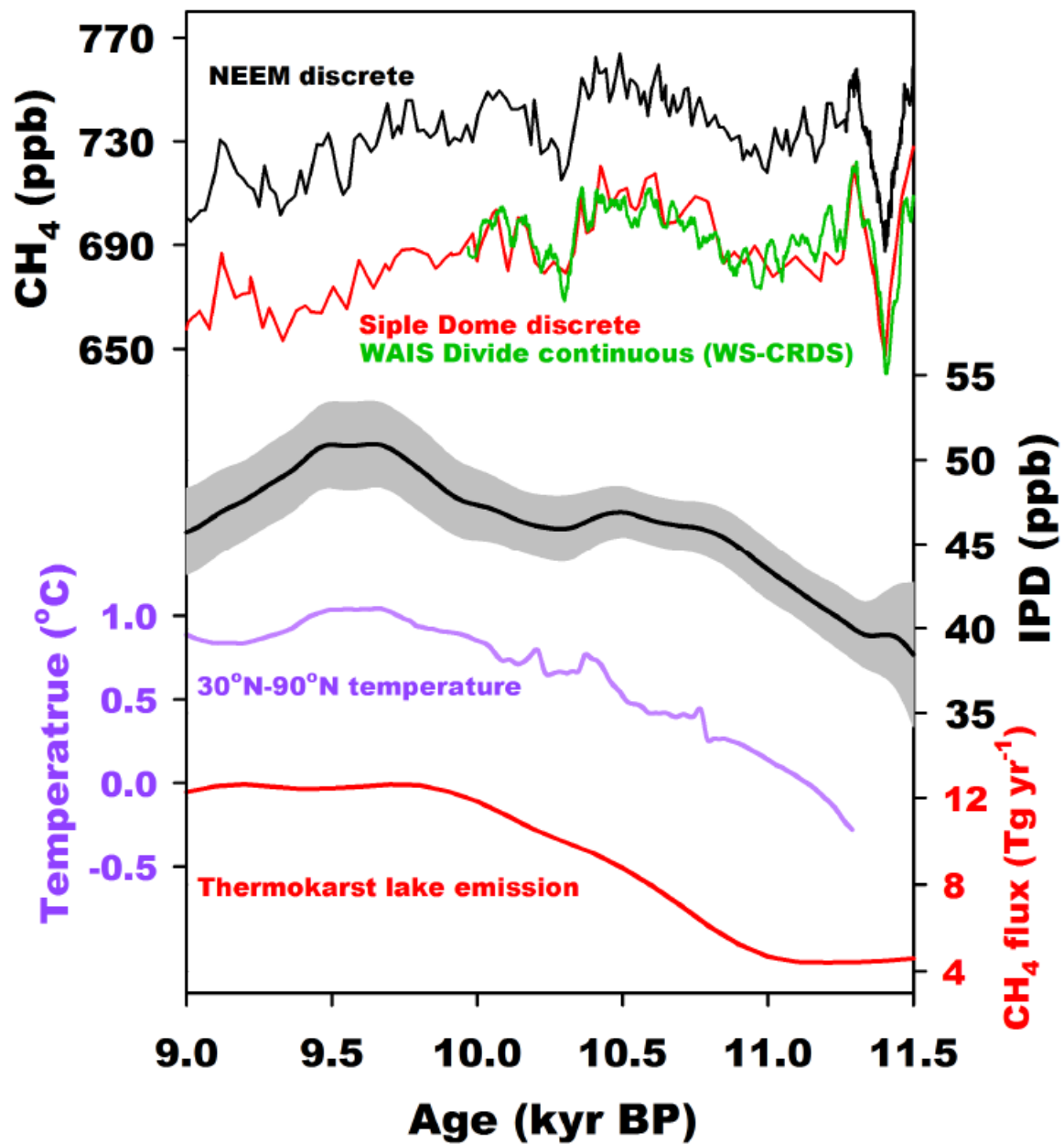
Figure 5. Comparison of Greenland oxygen isotope ratios from NGRIP (blue, Rasmussen et al., 2006), GRIP (grey, Rasmussen et al., 2006) and GISP2 (red, Stuiver and Grootes, 2000). All time series were high-pass filtered with 1/1800-year window. Note that the cooling amplitude at 10.3 ka is smaller than 8.2 and 9.3 ka events in NGRIP records, but this is not clear in GRIP and GISP2 ice cores.



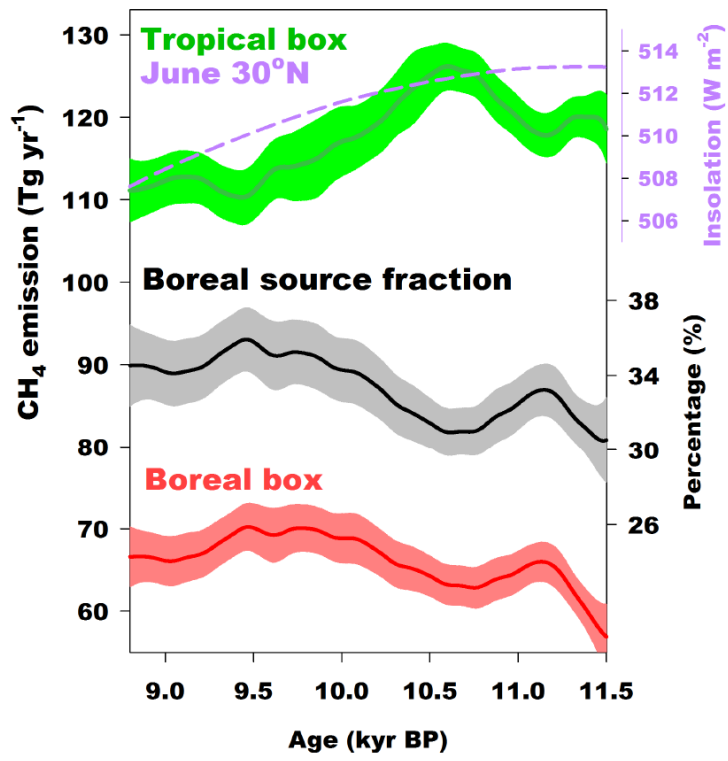


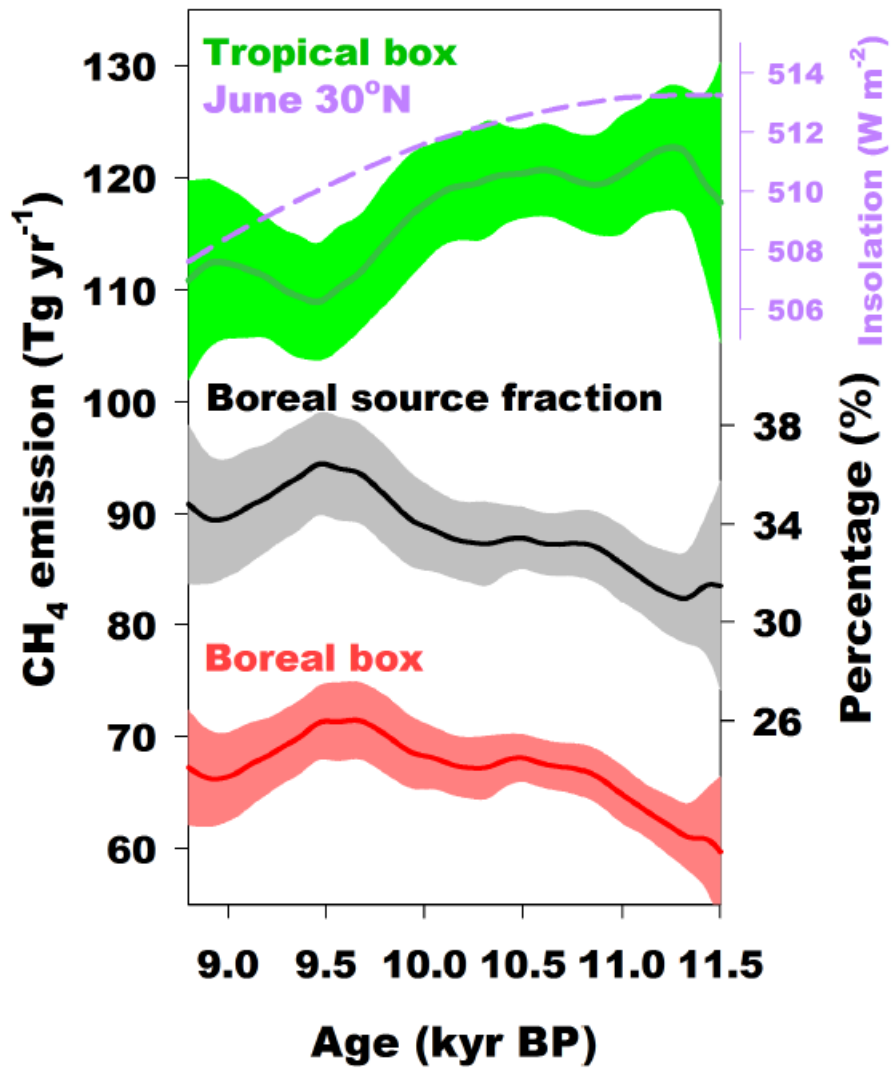


1  
2 Figure 63. CH<sub>4</sub> inter-polar difference (IPD) and high latitude CH<sub>4</sub> sources. Top: High-resolution CH<sub>4</sub> discrete  
3 measurements from NEEM discrete (blackblue, Chappellaz et al., 2013), NEEM continuous (orangeturquoise,  
4 Chappellaz et al., 2013), WAIS Divide discrete (light blueyellow-green, WAIS Divide project members, 2015), WAIS  
5 Divide continuous (greenpurple, Rhodes et al., 2015), and Siple Dome (red, this study) ice core records. Middle: IPD  
6 (light grey) and 500 Bottom: 1000-year low-pass filtered IPD reconstructions by using various pairs of Greenland-  
7 and Antarctic records. IPD-1 (black) and IPD-2 (green) with 95 % significance interval (shaded), in which the IPD-  
8 1 and IPD-2 are shown in red and green, respectively. The shaded area indicate 95% significance interval. Bottom:  
9 Previous estimates are marked in green and orange (Brook et al., 2000; Chappellaz et al., 2013). Proxy-based  
10 temperature reconstruction for 30°N-90°N and 30°S-30°N latitude (blue, Marcott et al., 2013). CH<sub>4</sub> flux estimate  
11 from Siberian and Alaskan thermokarst lakes (red, Walter Anthony et al., 2014).



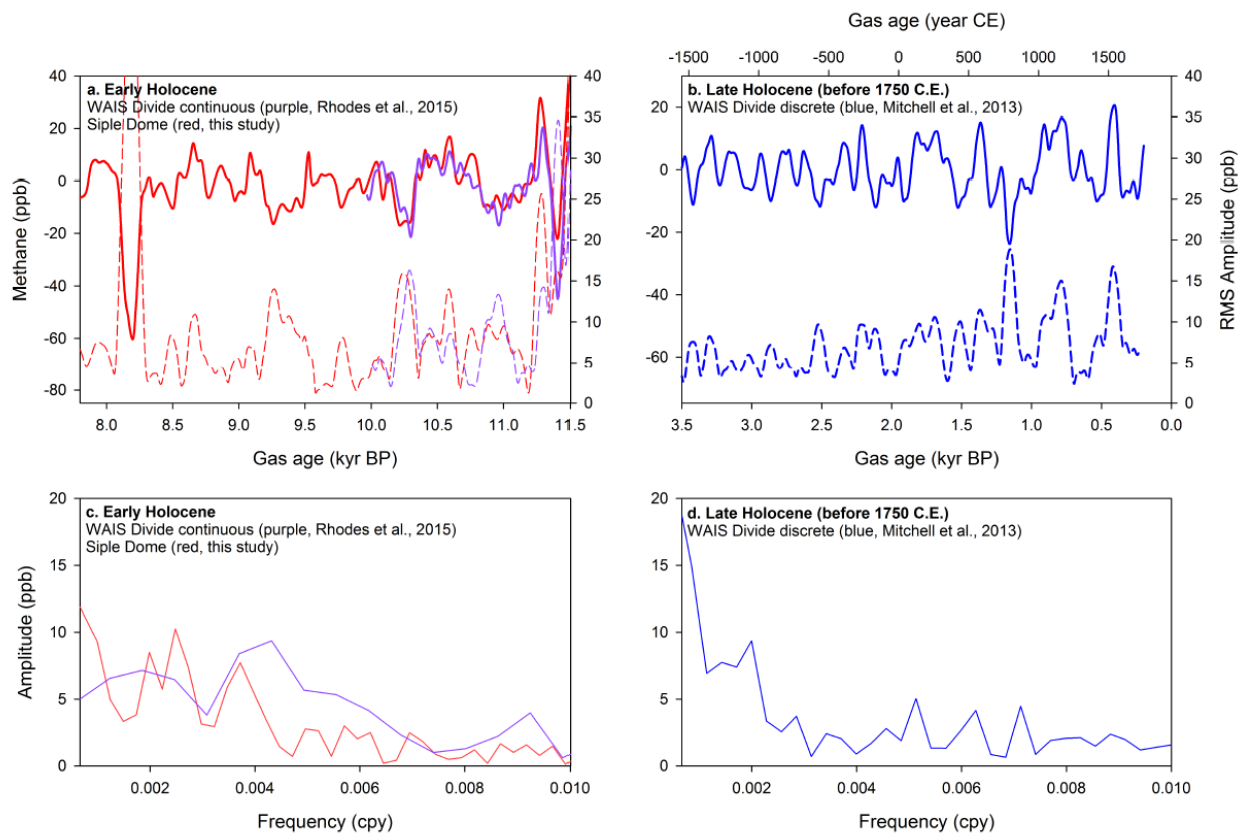
1  
 2 [Figure 7. CH<sub>4</sub> inter-polar difference \(IPD\) and high latitude CH<sub>4</sub> sources. Top: High-resolution CH<sub>4</sub> discrete](#)  
 3 [measurements from NEEM discrete \(black, Chappellaz et al., 2013\), WAIS Divide continuous \(green, Rhodes et al.,](#)  
 4 [2015\), and Siple Dome \(red, this study\) ice core records. Middle: 1000-year low-pass filtered combined IPD with 95%](#)  
 5 [significance interval \(shaded\). Bottom: Previous estimates are marked in green and orange \(Brook et al., 2000;](#)  
 6 [Chappellaz et al., 2013\). Proxy-based temperature reconstruction for 30°N-90°N \(purple, Marcott et al., 2013\). CH<sub>4</sub>](#)  
 7 [flux estimate from Siberian- and Alaskan thermokarst lakes \(red, Walter-Anthony et al., 2014\).](#)  
 8





1  
2  
3  
4  
5  
6  
7  
8

Figure 4.8. 3-box source distribution model results of tropical (green) and boreal (red) boxes. Black line shows the boreal to total source fraction (see text). Purple dashed line plotted with tropical emission is summer insolation in 30°N (Berger and Loutre, 1991).



1  
2 **Figure 5. Upper: Detrended (75 to 1800-year band-pass filtered) CH<sub>4</sub> for the early (a) and late (b) Holocene from**  
3 **Siple Dome (red, this study), WAIS divide continuous (purple, Rhodes et al., 2015), and WAIS divide discrete (blue,**  
4 **Mitchell et al., 2013) data. Dashed lines are root mean square (RMS) amplitude running averaged by 75-year window.**  
5 **Lower: Amplitude spectrum of Early (c) and Late (d) Holocene CH<sub>4</sub> records. Note that CH<sub>4</sub> data before 1750 C.E.**  
6 **are used for the preindustrial late Holocene.**

7

1 Table 1. Summary of results of replicate analysis from 8 depth intervals. Depth difference between the first- and  
 2 second replicate samples is 10 cm.

3

	1 <sup>st</sup> measurements					2 <sup>nd</sup> measurements				
Depth	Dup.1	Dup.2	Mean	1sigma	Date	Dup.1	Dup.2	Mean	1sigma	Date
(m)	(ppb)	(ppb)	(ppb)	(ppb)	(dd/mm/yy)	(ppb)	(ppb)	(ppb)	(ppb)	(dd/mm/yy)
523.150	634.8	634.7	634.7	0.1	27-1-14	637.5	634.3	635.9	1.6	24-2-14
530.950	669.0	665.8	667.4	1.6	03-2-14	669.4	670.7	670.0	0.7	24-2-14
558.295	682.5	678.2	680.3	2.2	14-3-14	687.5	678.3	682.9	4.6	02-4-14
559.850	689.8	680.3	685.0	4.7	03-2-14	683.8	690.0	686.9	3.1	26-3-14
561.150	687.8	689.2	688.5	0.7	14-3-14	684.0	690.4	687.2	3.2	02-4-14
562.407	687.2	685.5	686.4	0.8	26-3-14	689.4	686.4	687.9	1.5	02-4-14
575.913	679.2	679.2	679.2	0.0	07-2-14	686.7	678.9	682.8	3.9	28-3-14

4

5

1 **Table 2. Results of the 3-box source distribution model from the combined IPD showing emissions of ~~results of~~ tropical**  
 2 **(green, T) and boreal (red, N) boxes and boreal source fraction ( $N/(T+N+S)$ ) at specific time slices. Also shown are**  
 3 **previous estimates for comparison. ~~compared with previous results.~~ Errors denote 95% confidence interval. The**  
 4 **uncertainty for 9.5 – 11.5 ka period is the average of 95% confidence interval of the low-pass filtered reconstruction of**  
 5 **each box emission.**  
 6

Ref.	N box	T box	<u>Boreal source fraction</u> $N/(N+T+S)$
(ka)	(Tg yr <sup>-1</sup> )		(%)
Brook et al., 2000 (9.5-11.5 ka)	64 ± 5	123 ± 8	32 ± 3
Chappellaz et al., 1997 (9.5-11.5 ka)	66 ± 8	120 ± 9	33 ± 3
This study <u>(9.5 – 11.5 ka)</u> ( <del>10.8 ka</del> )	<u>67 ± 3</u> <del>66 ± 4</del> <del>65 ± 2</del>	<u>118 ± 5</u> <del>120 ± 4</del> <del>122 ± 4</del>	<u>33 ± 2</u> <del>33 ± 2</del> <del>32 ± 1</del>
<u>This study</u> <u>(11.5 ka)</u>	<u>60 ± 7</u> <del>47 ± 9</del>	<u>118 ± 12</u> <del>149 ± 10</del>	<u>31 ± 4</u> <del>22 ± 5</del>
This study <del>(9.9 ka)</del> <u>(9.5 ka)</u> <del>(9.8 ka)</del>	<u>71 ± 3</u> <del>65 ± 8</del> <del>74 ± 2</del>	<u>109 ± 5</u> <del>119 ± 9</del> <del>110 ± 3</del>	<u>36 ± 2</u> <del>33 ± 5</del> <del>37 ± 1</del>
<u>This study</u> <u>(9.0 ka)</u>	<u>66 ± 4</u>	<u>112 ± 7</u>	<u>34 ± 2</u>

7

8

---



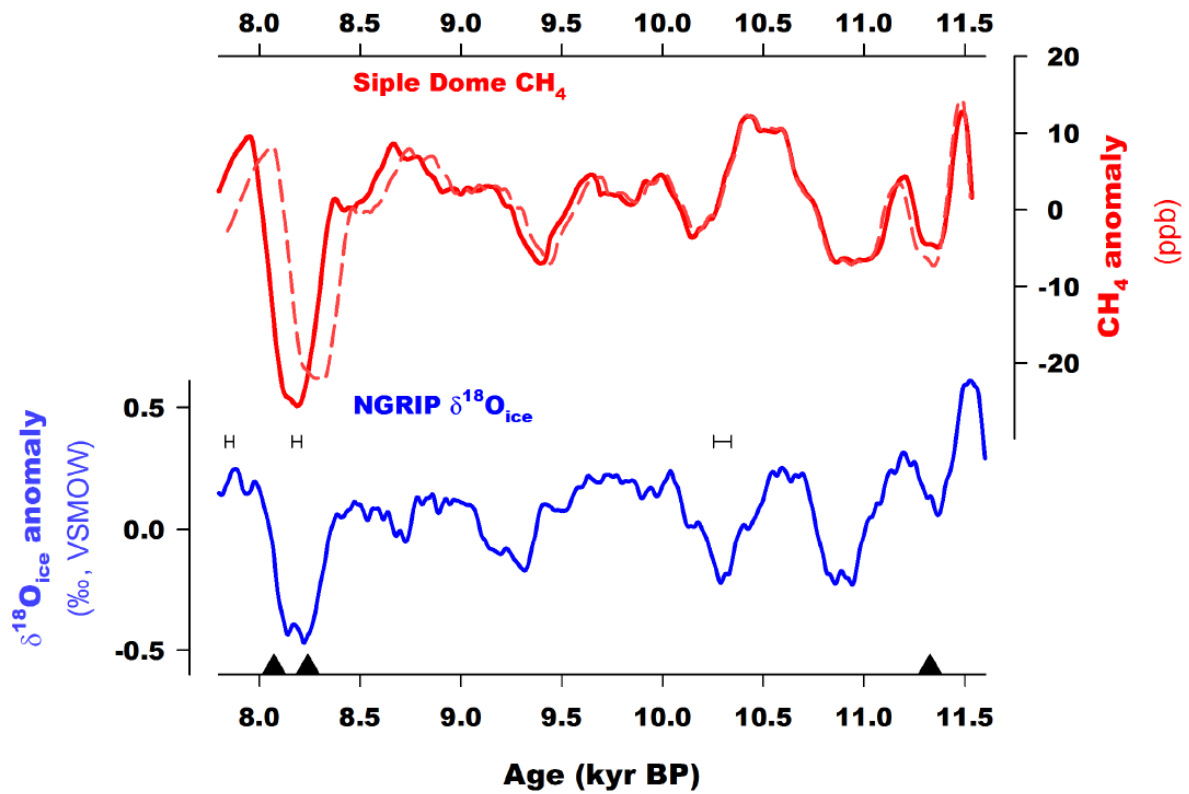
## Supplementary text

### Reproducibility test from Styx Glacier ice core

~~Here we present results of reproducibility test by using different ice core samples in the same manner as used for Siple Dome ices, to demonstrate the reliability of our analytical system. The ice core was drilled at Styx glacier (73° 51.10'S, 163° 41.22'E, 1623 m a.s.l) in 2014-2015 austral summer, and mean snow accumulation rate was estimated as 0.13 Mg m<sup>-2</sup> yr<sup>-1</sup> (Han et al., 2015). The replicate measurements were carried out at randomly chosen 7 depths with time interval of 51 to 226 days. Depth difference between the replicate pairs is less than 10 cm. Results show the mean absolute difference between the original and replicate measurements of 1.9, which is as good as the Siple Dome results. The daily blank offset (see the main text) ranges from ~6 to 19 ppb, and the intra-day blank offset is 2.4 ppb (standard error of the mean, n = 4). Again, these results reveal the robustness of our blank correction methods.~~

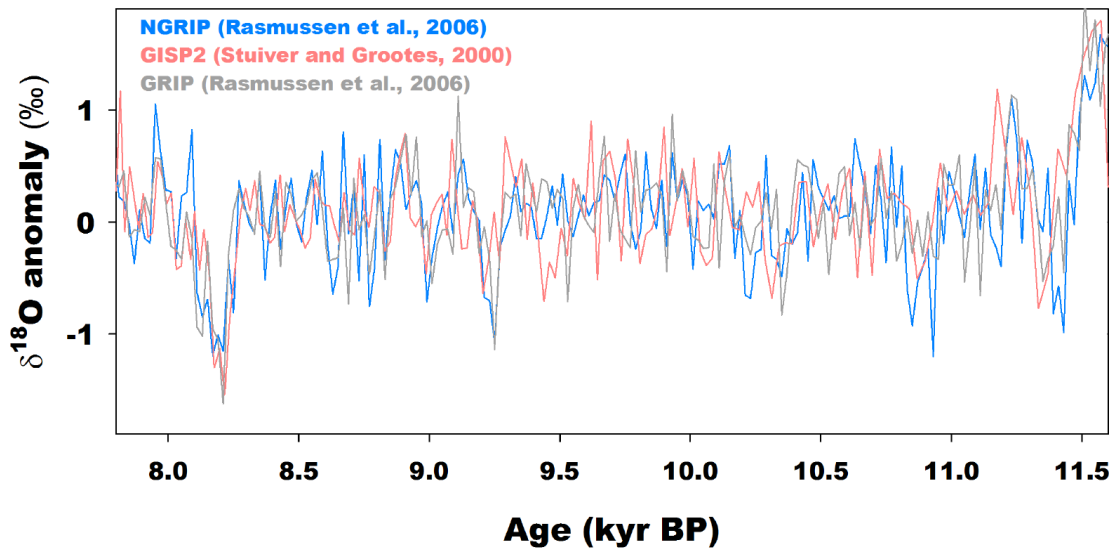
### Maximum SDMA gas age uncertainty

~~In this paper we used a modified gas age scale from the previous one based on  $\delta^{15}\text{N}$  measurements (Severinghaus et al., 2009) by setting 3 age tie points and interpolating the age offset between the tie points (Fig. S1). To estimate gas age uncertainty, we compared the SDMA-modified gas age (this study) to the new gas age determined by  $\text{CH}_4$  correlation with NEEM discrete  $\text{CH}_4$  data measured at OSU (Chappellaz et al., 2013). Figure S3 shows the offset between the two age scales, which it should be moved to adjust the NEEM  $\text{CH}_4$  in GICC05modelext NEEM-1 age. In addition, we take into account the maximum layer counting uncertainty of 99 years (Rasmussen et al., 2006) and delta age uncertainty of 30 years (Rasmussen et al., 2013) during the early Holocene. Error propagation gives us the maximum uncertainty of the early Holocene SDMA gas age of ~147.4 years.~~



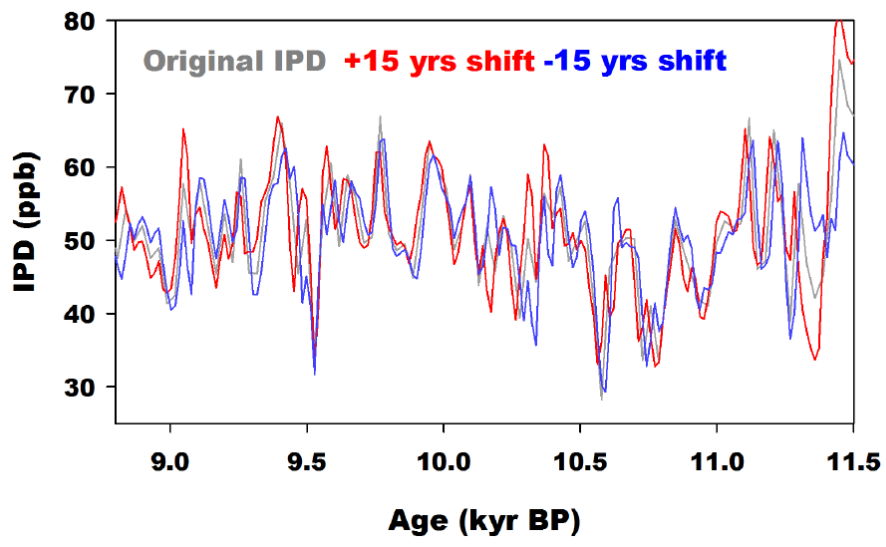
1  
 2 **Figure S1. Upper: Comparison between Siple Dome CH<sub>4</sub> anomalies plotted with gas age adjusted to GICC05 (red,**  
 3 **solid) and previous gas age (red, dashed; Brook et al., 2005). Lower: NGRIP δ<sup>18</sup>O anomaly in GICC05 scale. The**  
 4 **horizontal error bars denote the age uncertainty of GICC05 chronology (Rasmussen et al., 2006), and the black**  
 5 **triangles are age tie points used to adjusting the Siple Dome age scale to GICC05 scale.**

6  
 7  
 8  
 9  
 10  
 11  
 12  
 13  
 14  
 15

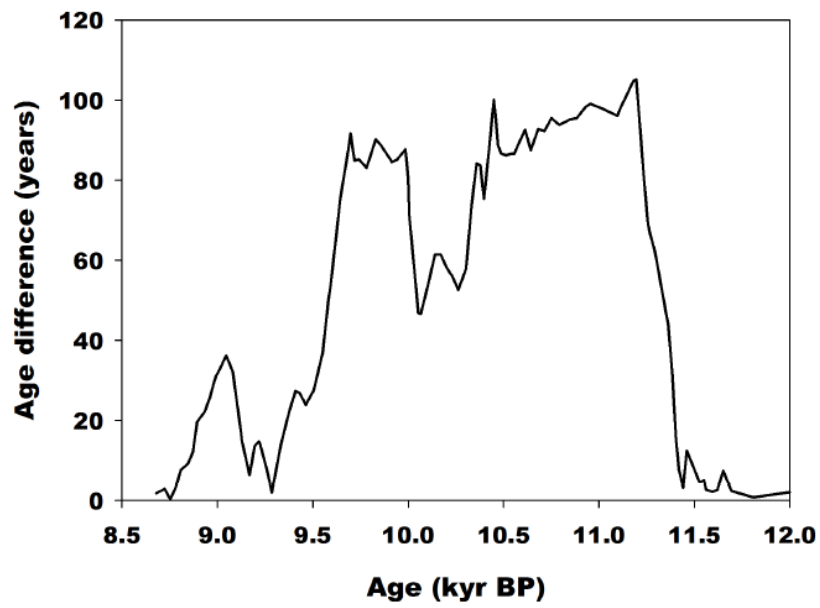


1  
2  
3  
4  
5  
6  
7  
8  
9  
10  
11  
12  
13  
14  
15  
16  
17  
18

Figure S1. Comparison of Greenland oxygen isotope ratios from NGRIP (blue, Rasmussen et al., 2006), GRIP (grey, Rasmussen et al., 2006) and GISP2 (red, Stuiver and Grootes, 2000). All time series were high pass filtered with 1/1800-year window. Note that the cooling amplitude at 10.3 ka is smaller than 8.2 and 9.3 ka events in NGRIP records, but this is not clear in GRIP and GISP2 ice cores.



- 1
- 2
- 3



1  
2  
3  
4  
5

Figure S4. Age difference between the new gas age scale adjusted to GICC05 by Monte Carlo matching with NEEM discrete CH<sub>4</sub> (Chappellaz et al., 2013) and the original gas age based on  $\delta^{15}\text{N}$  records (Severinghaus et al., 2009).

---

Table S1. 3-box source distribution model results of tropical (green, T) and boreal (red, N) boxes and boreal source fraction obtained from IPD-2. Errors denote 95% confidence interval.

<u>Ref.</u>	<u>N-box</u>	<u>T-box</u>	<u>Boreal source fraction</u>
<u>(ka)</u>	<u>(Tg yr<sup>-1</sup>)</u>		<u>(%)</u>
<u>This study</u> <u>(11.5 ka)</u>	<u>60 ± 7</u>	<u>134 ± 16</u>	<u>29 ± 4</u>
<u>This study</u> <u>(10.0 ka)</u>	<u>71 ± 7</u>	<u>115 ± 11</u>	<u>35 ± 4</u>

---

1 **Reference**

2 Han, Y., Jun, S. J., Miyahara, M., Lee, H. G., Ahn, J., Chung, J. W., Hur, S. D., and Hong, S. B.: Shallow ice  
3 core drilling on Styx glacier, northern Victoria Land, Antarctica in the 2014-2015 summer, J. Geol. Soc. Korea,  
4 51, 343-355, 2015 (in Korean with English abstract).

5 Rasmussen, S. O., Abbott, P. M., Blunier, T., Bourne, A. J., Brook, E., Buchardt, S. L., Buizert, C., Chappellaz,  
6 J., Clausen, H. B., Cook, E., Dahl-Jensen, D., Davies, S. M., Guillevic, M., Kipstuhl, S., Laepple, T., Seierstad, I.  
7 K., Severinghaus, J. P., Steffensen, J. P., Stowasser, C., Svensson, A., Vallelonga, P., Vinther, B. M., Wilhelms-  
8 F., and Winstrup, M.: A first chronology for the North Greenland Eemian Ice Drilling (NEEM) ice core, Clim.  
9 Past, 9, 2713-2730, 2013.

10 Stuiver, M., and Grootes, P. M.: GISP2 oxygen isotope ratios, Quaternary Research, 53, 277-284, 2000.

11

12

13

14